Studies on the Synthesis of Bacterial Cellulose and its Utilization in Value-Added Chemical Transformation and Biomedical Applications

Thesis submitted in partial fulfilment of the requirements for the degree of

DOCTOR OF PHILOSOPHY

by

MUNMI DAS

(Roll No.: 166107113)

DEPARTMENT OF CHEMICAL ENGINEERING

INDIAN INSTITUTE OF TECHNOLOGY GUWAHATI

GUWAHATI, ASSAM - 781039, INDIA

April 2023

Dedicated

To

My Late Grandmother

My Beloved Parents, My Brother, My Husband

and My Mentors

Department of Chemical Enginnering
Indian Institute of Technology Guwahati
Guwahati, Assam 781039

STATEMENT

I hereby declare that the content embodied in this thesis entitled **"Studies on the Synthesis of Bacterial Cellulose and its Utilization in Value-Added Chemical Transformation and Biomedical Applications"** is the result of investigations and experiments carried out by me at the CoE-SusPol Lab, Transit Complex, Department of Chemical Engineering, Indian Institute of Technology Guwahati, India, under the supervision of Prof. Vimal Katiyar and Prof. Bishnupada Mandal. In keeping with the general practice of reporting scientific observations, due acknowledgments have been made wherever the work described is based on the findings of other investigators. The results documented in the thesis are achieved by me and has not been submitted to any other University or Institute for the award of any degree or diploma.

Munmi Das

April, 2023

Munmi Das
Roll no.: 166107113
Department of Chemical Engineering
Indian Institute of Technology Guwahati
Assam, Guwahati – 781039, India.

Department of Chemical Enginnering
Indian Institute of Technology Guwahati
Guwahati, Assam 781039

CERTIFICATE

This is to certify that the thesis called **"Studies on the Synthesis of Bacterial Cellulose and its Utilization in Value-Added Chemical Transformation and Biomedical Applications"**, being submitted by **Munmi Das** (Roll No. 166107113) for the award of Ph.D. degree has been carried out by her at the Department of Chemical Engineering, Indian Institute of Technology Guwahati, under our guidance and supervision. The work documented in the thesis has not been submitted to any other University or Institute for the award of any degree or diploma.

(Prof. Vimal Katiyar)
Professor
Department of Chemical Engineering
Indian Institute of Technology Guwahati
Assam, Guwahati – 781039, India

(Prof. Bishnupada Mandal)
Professor
Department of Chemical Engineering
Indian Institute of Technology Guwahati
Assam, Guwahati – 781039, India

ACKNOWLEDGEMENTS

This thesis becomes a reality with the kind support and help of many individuals. It is a genuine pleasure to express my deep sense of thanks and gratitude to them who helped me in the completion of this thesis.

Foremost, I would like to express my sincere thanks to my thesis supervisors ***Prof. Vimal Katiyar and Prof. Bishnupada Mandal*** *for the continuous support in various stages of my research journey. They have provided me an excellent atmosphere to work with freedom of thinking and execution which grew my interest towards the topic. Also, their positive attitude and encouragement helped me to perform and complete the research objectives. Their support in doing the experiments, analysis of the data and preparing the manuscripts are invaluable. I am fortunate enough to complete my thesis under their supervision. It has really been a notable working experience with them.*

I would like to extend my sincere gratitude to my doctoral committee chairman ***Prof. Amit Kumar****, Department of Chemical Engineering, for his valuable suggestions, evaluation and proper direction during my annual progress seminars and synopsis. I shall always be obliged to other doctoral committee members,* ***Prof. G. Pugazhenthi****, Department of Chemical Engineering, and* ***Dr. A. S. Achalkumar****, Department of Chemistry, for there valuable suggestions, time and efforts.*

I would like to express my sincere gratitude to respected ***Prof. Ing. Petr Sáha*** *and* ***Prof. Nabanita Saha****, Centre of Polymer Systems (CPS), Tomas Bata University in Zlín, Czech Republic, and* ***Dr. Oyunchimeg Zandraa*** *for their constant help in making me learn the techniques of microbiological work in the Cell Biology laboratory, CPS, TBU.*

I would like to acknowledge all the centers for providing me various instrumental facilities required for characterization during the research work carried out at IIT Guwahati specifically, Analytical Lab Facility "Department of Chemical Engineering", "Central Instruments Facility" (CIF), "Centre for Environment".

I am also grateful to all the ***Staff and Faculty Members*** *of the Department of Chemical Engineering for helping and providing me the necessary facilities.*

*I would like to thank my **lab-mates**, all my seniors, juniors and lab-technicians, for their support during my PhD period, **friends** and other **well-wishers** who helped me in my research journey.*

*My final words go to my family and first relatives whom I want to thank for showering their love, care, understanding, sacrifices and encouragements. I would like to thank my beloved grandmother whom I have lost in this journey of life **Late Mrs. Ahalya Das**, my parents **Mrs. Latika Das** and **Mr. Prabhat Kumar Das**, my brother **Mr. Chiranjiv Das**, and my in laws **Mr. Dnyandeo S Kawale** and **Mrs. Neelima D Kawale, Vaibhavi-Parul** and **friends** for their continuous support and inspiration to stay motivated in this journey. I would like to specially thank my husband **Dr. Harshal D Kawale** for being my pillar-of-support and strength in this journey. Lastly, I thank the **Almighty** for blessing me with everything I have today.*

Munmi Das

Contents

Abstract

Replacing the widespread use of petroleum-derived non-biodegradable materials with green and sustainable materials is a pressing challenge that is gaining increasing attention by the scientific community. One such system is bacterial cellulose and its derivative, bacterial cellulose nanocrystals (BCNCs) basically obtained through acid hydrolysis. In this thesis, BC have been fabricated from biomass, *G. xylinus* for their potential application as a commercially viable value-added product with the "waste to wealth" strategy. The fabrication of BC and BCNCs is a promising technology as it opens dimensions with multiple application possibilities. The impregnation of biodegradable polymers, such as PCL into the BC network resulted in the presence of polymer layers on the surface as well as inside the pores of the BC matrix indicating a good fiber-matrix interaction. These fabricated BC and BCP composite membranes were biocompatible and nontoxic to BHK-21 cells even after 72 h, allowing cell proliferation. Electrospun nanofibrous dressings have emerged as an ideal candidate in the biomedical field because they possess multiple criteria as a wound healing material, such as easy absorption of the wound exudates by maintaining a moist environment to promote a faster healing process. The fabricated lidocaine hydrochloride loaded bacterial cellulose/ polycaprolactone (BCP) scaffolds revealed their cytocompatible nature. The utilization of BCNCs can aid in the reduction of carbon dioxide that is responsible for global warming and climate change. BCNCs are excellent candidates for the design and development of functional nanomaterials in many applications due to several attractive features, such as high surface area, hydroxyl groups for functionalization, colloidal stability, low toxicity, chirality and mechanical strength. The strategic functionalization of BCNCs through the sustainable approach avoids the utilization of harmful chemicals. BCNC templated catalysts, are one of the versatile nanomaterials developed in this work, with potential application as biocatalysts in value-added chemical transformation. On the other hand, 5-Hydroxymethyl-2-furfural (HMF) is considered an important platform chemical among other intermediates derived from biomass. In this study, we have used mesoporous BCNC templated zirconium phosphate as a catalyst for the conversion of furfural into HMF. The catalyst was synthesized using a wet-precipitation method and was characterized using powder XRD, FT-IR spectroscopy, FETEM, BET and FESEM. The as-prepared BCNC templated catalyst showed mesoporous structure with high surface area and exhibited excellent catalytic activity as compared to pristine ZrP for the formation of HMF, from

furfural. Also, the HrP-immobilized BCNC hydrogel exhibited good self-healing properties and was reused efficiently for 6 cycles with greater than 50% of its original activity retained even after 60 days, which facilitated their application as promising biomaterials.

Therefore, this doctoral thesis focuses on the utilization of BC and its functionalization for development of polymeric scaffolds, biocatalysts, as well as their advanced applications as biosensors, in biotechnological applications.

List of Figures

List of Tables

List of Schemes

Abbreviations

BC	Bacterial Cellulose
BCNCs	Bacterial Cellulose Nanocrystals
PCL	Polycaprolactone
3-D	Three-Dimensional
WRR	Water Release Rate
WHC	Water Holding Capacity
SM	Streptomycin Sulfate
GEN	Gentamicin Sulfate
LB	Luria-Bertani
HS	Hestrin And Schramm
LID	Lidocaine Hydrochloride
Ag-SD	Silver (I) Sulfadiazine
BHK-21	Baby Hamster Kidney
HRP	Horseradish Peroxide
DAPI	4’,6-diamidino-2-phenylindole
ABTS	2,2′-azino-bis(3-ethylbenzothiazoline-6-sulphonic acid
HCl	Hydrochloric Acid
H_2SO_4	Sulfuric Acid
NaOH	Sodium Hydroxide
DMF	Dimethyl Formamide
$CHCl_3$	Chloroform
DMEM	Dulbecco's Modified Eagle's Medium
DMSO	Dimethyl Sulfoxide
HMF	5-Hydroxymethylfurfural
GA	Gum Arabic
OGA	Oxidized Gum Arabic
PVA	Polyvinyl Alcohol

TGA/DTG	Thermogravimetric and Derivative Thermogravimetric Analysis
DSC	Differential Scanning Calorimetry
FT-IR	Fourier Transform Infrared
XRD	X-Ray Diffraction
FESEM	Field Emission Scanning Electron Microscope
FETEM	Field Emission Transmission Electron Microscope
AFM	Atomic Force Microscopy
BET	Brunauer–Emmett–Teller
UTM	Universal Testing Machine
HPLC	High Performance Liquid Chromatography
WCA	Water Contact Angle
WVTR	Water Vapor Transmission Rate
E. coli	*Escherichia coli*
S. aureus	*Staphylococcus aureus*
BCP	Bacterial Cellulose Based Polycaprolactone
BC-GEN	GEN Loaded BC
BCP-GEN	GEN Loaded BCP
BC-SM	SM Loaded BC
BCP-SM	SM Loaded BCP
ZrP	Zirconium Phosphate
BCNC_ZrP	BCNC Templated Zrp
HG	OGA hydrogel
HG-BCNC(20%)	OGA hydrogel with 20% BCNC Loading
Imm_BCNC	Immobilized BCNC hydrogel
Imm_HG-BCNC(20%)	Immobilized OGA Gel with 20% BCNC Loading
G-glutaraldehyde	Gum Arabic-Glutaraldehyde
BCP-LD	Lidocaine hydrochloride loaded BCP nanofiber
BCP-LSD	Ag-SD coated BCP-LD nanofiber
AgSD-GA	Silver sulfadiazine-gum Arabic solution

Chapter 1

Introduction and Literature Review

1.1. INTRODUCTION

Environmental concerns associated with the hazardous and toxic petroleum resources have created an imperative need to fabricate new biodegradable materials having practically identical properties as that of the present conventional materials at a comparable expense. The selection and utilization of agricultural products, such as biomass is regarded as an intriguing and sustainable method to lessen surplus farm wastes and further transformation to other value–added products making itself the most attractive replacement of fossil resources.

Bacterial cellulose (BC), is an important class of ecological polysaccharide biomaterials of the 21st century, predominantly explored in food, textile, and biomedical applications due to their nontoxic, highly pure, biocompatible, and highly hydrophilic nature. BC is made up of ultrafine and porous fiber network derived from well-arranged three-dimensional (3D) nanofibers, which results in the formation of hydrogel sheets with higher surface area and porosity [1,2]. In comparison to plant-based cellulose although quite similar in chemical structure, BC fibrils are very much smaller in length and diameter (about 100 times) with tailorable properties based on the composition of culture media, carbon source, and on the producing organism used. BC is generally produced from *Acetobacter xylinum*, which is the most efficient cellulose producer as it can absorb several types of sugars leading to higher yields of cellulose at pH ~3-7 and 25-30˚C temperature in liquid medium. BC also has certain promising properties such as high crystallinity (84-90%), high water holding capacity (WHC) of ~106 g water/ g sample, ability to reform into 3D structure during synthesis and higher water release rate (WRR), of which WRR and WHC are the most essential attributes, directly connected to the biomedical applications of BC as a dressing material [1,3–5]. These captivating properties make BC a suitable contender in biomedical applications such as artificial skin, scaffolds, wound dressing materials, dental implants, and in food packaging and paper industry, alone as well as in combination with other polymers and bioactive materials [6]. The easy blending property of BC enables the fabrication of stiff and strong macro fibers with higher tensile strength which could replace synthetic fibers derived from fossil fuel. The presence of abundant hydroxy groups (-OH) on its surface as well the higher surface area to volume ratio

enables the chemical modification of BC with other materials, resulting in better interaction between all the components [7]. The results shown in this thesis are evident of vast characterizations performed for the raw materials and products. Thus, this introductory chapter describes the background research in detail for work presented in this thesis, that includes production of BC, its functionalization, preparation of bacterial cellulose nanocrystals (BCNCs) and various applications associated with BC and BCNCs.

1.1.1. Production of BC

Bacterial cellulose was first reported by Adrian Brown in 1886, and Louis Pasteur defined it as a gel-like, slippery, wet skin formed by the fermentation of coconut water. Examples of bacteria known to produce BC are *Komagataeibacter medellinensis*, *Agrobacterium*, *Aerobacter*, *Komagataeibacter oboediens*, *Achromobacter*, *Sarcina*, *Azotobacter*, *Acetobacter*, *Agrobacterium* etc. [7–9], however *Komagataeibacter xylinus* (previously known as *Gluconacetobacter xylinus* or *Acetobacter xylinum*) is the strongest BC producer. The conventional Hestrin and Schramm (H.S.) medium used to produce BC comprises of glucose, peptone, yeast extract, anhydrous disodium phosphate and citric acid [7].

Production of BC can be carried out in static, agitated or stirred conditions in small-scale or in bioreactors resulting in different forms of cellulose, such as, three-dimensional BC pellicle for static fermentation and spherical particle in agitated conditions [10]. Bacterial cellulose produced by the aerobic bacteria creates a BC film in static culture because of gas-liquid interface generated between the medium and air. Thus, this interface ensures the overall yield of BC in static culture, and it is directly related to the surface area [11]. The methodology for production and purification of pure BC films by static culture is straightforward. As the gas-liquid interface produces the BC films, they are purified by a stream of hot-water and sodium hydroxide. It is necessary to neutralize the pH of the extracted BC films to obtain it in its purest form, and thus the films were washed with large amount of water. Even though this methodology of production and purification of the BC is simple, the low interaction of air in gas-liquid interface of static culture makes it expensive and result in lower yields [12]. Thus, the agitation/stirred culture has been introduced for improvement in the production of BC films. By fact, the agitation culture improves the interaction by increasing the rate of oxygen transport in the medium [13]. Consequently, in comparison with the static culture, agitation culture gives higher yields of BC in small scale. But, when the quality of agitation culture produced BC films were compared with the static culture BC films, it was

found that they have lower crystallinity, lower mechanical properties, and specifically lower degree of polymerization [14]. Overall, the agitation culture method is not significant enough to improve the BC films yield [15,16]. To improve these properties, production of BC was carried out under bioreactor conditions which also takes less time for completion of the reaction than agitation conditions [17]. To be specific, the production of BC films by above listed methods is dependent on the composition of the culture media, as it affects the effectiveness of the process [15]. To date, the static culture is the most commonly adapted method to produce pure BC films on laboratory scale.

For cost effective production of BC, it is advisable to use low-cost carbon and nitrogen sources that are present as industrial wastes or by-products [18]. Some examples of these sources are sugar beet molasses & cheese whey [19], agricultural by-products [20], tobacco waste extracts [21], toxic aromatic hydrocarbons [22], etc. Some studies focused on increased production of BC with improved qualities in terms of crystallinity, particle size, mechanical strength etc. by the addition of certain additives such as agar [23], sodium alginate [24], etc. Still, the production cost and the yield of BC is totally variable and independent of various factors. Therefore, this thesis demonstrates one of such technology to produce BC films by using static culture method to obtain cost effective production along with the improved qualities. Later, it is described that this produced BC can be utilized in various practical applications such as biomedical applications, biosensors, hydrogel and as a green catalyst. The importance of BC has been justified, based on the practical results obtained from the detailed research conducted. The multi-functional properties and application of BC with its chemical and morphological structure is presented in Figure 1.1.

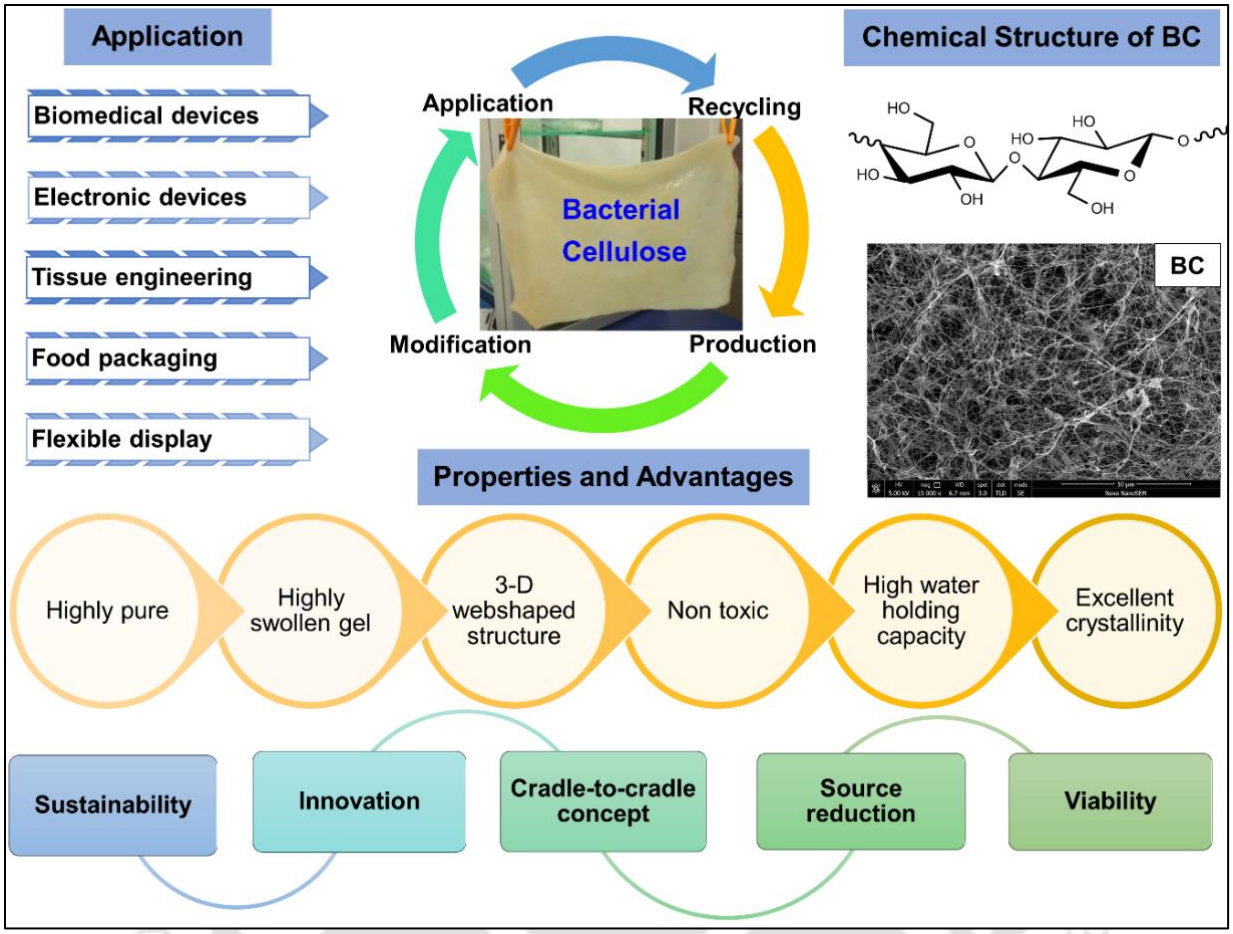

Figure 1.1. The properties and application of bacterial cellulose (BC).

1.1.2. Functionalization of BC

Bacterial cellulose can be modified either during their synthesis or after they are extracted. The in-situ and ex-situ modification typically depends on their future applications. During in-situ fermentation, either the carbon source is changed, or additives/components are introduced into the culture medium, resulting in the formation of functionalized BC based composite materials with improved physical, mechanical and morphological characteristics. Figueiredo et al. [25] demonstrated the in-situ synthesis of BC by incorporating polycaprolactone (PCL powder) into the culture medium, followed by hot-pressing the obtained composites films after the incubation. The compressed films showed a homogenous PCL distribution throughout the BC network, as well as good thermal stability and improved mechanical properties, when compared to pristine PCL. On the other hand, ex-situ modification is carried out either by absorption of active ingredients onto the purified BC pellicle, or by chemical modification. Atta et al. [26] prepared antimicrobial

silver decorated bacterial cellulose food packaging material by dipping BC films in silver nitrate solution. The developed antimicrobial films exhibited better flexibility, biocompatibility towards NIH-3T3 fibroblasts and showed improved thermal properties. Chemical modification is usually carried out to avoid leaching of the active ingredients from the BC surface. Barbi et al. [27] functionalized BC with titanium dioxide (TiO_2) and inorganic clay with various ratios, by a wet mechanical mixing process. The results obtained from the analysis showed that the functionalized BC with clay has porous fragile structure, but TiO_2 functionalized BC showed neat and plastic-like structure. This study discussed an alternative and sustainable pathway to fabricate modified bacterial cellulose based lightweight, textile materials. Taokaew et al. [28] functionalized BCs with organosilanes for medical applications. They modified the BCs chemically to increase hydrophobic or electrostatic interactions of normal human dermal fibroblast (NHDF) by implanting methyl terminated octadecyltrichlorosilane (OTS) or by amine terminated 3-aminopropyltriethoxysilane (APTES). It was seen that the attachment and spreading of NHDF cells improved on modified BCs with APTES conversely to that of OTS modified BCs. Lee et al. [29] worked on esterification of BC nanofibers with organic acids and reported that the time-dependent behaviour of the formed emulsions was showing reliability with unravelling and scattering of freeze-dried modified BC nanofibers into separate nanofiber. Sai et al. [30] worked on surface modification of the BC aerogels with trimethylchlorosilane in liquid phase which improved the surface area, and porosity of the modified BC aerogels and kept the density low. Shao et al. [31] functionalized BC and found that, after functionalization their biocompatibility is improved along with the improvement in their antibacterial property. Enlisted in Table 1 are the in-situ and ex-situ modifications of BC for various applications with modified properties.

Table 1.1. In-situ and ex-situ modifications of BC for various applications.

Application	Bacteria	Additive material	Modified properties	Modification	Reference
Scaffold for tissue engineering	*Acetobacter xylinum*	Collagen	Porosity, thickness, roughness, stiffness, crystallinity, color	In-situ	Luo et al. [32]
	Acetobacter xylinum	Polystyrene and optical fiber	Porosity, crystallinity, swelling behavior, mechanical property	In-situ	Rambo et al. [33]
Wound dressing/ antimicrobial activity	*Gluconaceto-bacter hansenii*	2,3-dialdehyde or cellulase	Porosity, chemical and mechanical properties, degradation rate	Chemical ex-situ	Li et al. [34], Hu and Catchmark [35], Hu and Catchmark [36]
	Acetobacter xylinum	RGDC and gentamicin	Porosity, thickness, chemical property, antimicrobial activity	Chemical ex-situ	Rouabhia et al. [37]
	Gluconaceto-bacter hansenii	*Anogeissus* dhofarica and *Withania somnifera* plant extract	Bactericidal activity, swelling property	Ex-situ	Fatima et al. [38]
Bone regeneration	*Acetobacter xylinum*	Bone morphogenetic protein-2 (BMP-2)	Localized drug delivery system	Physical ex-situ	Shi et al. [39]

1.1.3. Bacterial Cellulose Nanocrystals

The high purity and crystallinity of BC make it a promising starting material for extracting bacterial cellulose nanocrystals (BCNCs). The unique physicochemical properties such as higher specific surface area, nontoxicity, mechanical strength, availability of free hydroxy groups for modification, make the cellulose nanocrystals an object of intense research [40]. Cellulose nanocrystals also aid in the reduction of carbon dioxide responsible for the current climate change, thus their utilization in the development of functional materials with improved properties has become an interesting field in the research fraternity over the past two decades. The introduction of the functional components into the nanocellulose system can lead to the expansion of these materials in specific applications [41]. Some of the potential applications are as an emulsion stabilizer, as templates for functional materials, and as functional organic hybrids [42,43]. So far, various methodologies have been explored to extract cellulose nanocrystals from pure cellulose, such as, chemical modification, enzymatic hydrolysis, or mechanical treatment. Although enzymatic treatment is an eco-friendly process as it retains the thermal stability and structure of cellulose, it is considered an economically challenging process [44]. Kang et al. [42] prepared cellulose nanocrystals (CNCs) from microcrystalline cellulose in deionized water by mechanical treatment of ball milling and obtained 20 % yield of CNCs having 3-10 nm diameter and 120-400 nm length. It was stated by Sofla et al. [45] that, CNCs produced by ball milling has bimodal size distribution and more amorphous structure than that of CNCs obtained by acid hydrolysis which has uniform distribution and increased crystalline structure.

Cellulose nanocrystals are obtained from bacterial cellulose by controlled acid hydrolysis, and the properties of the extracted nanocrystals are dependent on the hydrolysis time, acid strength, temperature, pre and post treatment etc. Generally, the microfibrillar structure of cellulose comprises of alternate amorphous and crystalline regions; and upon acid hydrolysis the crystalline part of the cellulose is isolated since it is acid resistant and the amorphous regions are hydrolysed and removed [46,47]. So, it is very important to understand the process of acid hydrolysis in detail with support of available background data for further processing the BC into BCNCs.

1.1.4. Acid hydrolysis

Various inorganic acids such as sulfuric, hydrochloric, hydrobromic, and phosphoric acids, have been used to isolate cellulose nanocrystals from BC by the penetration of H^+ ions into the

amorphous region of the cellulose molecule [48,49]. The hydrolysis of the amorphous region promotes the hydrolytic cleavage of the glycosidic linkages of BC, thereby releasing the crystalline part. Acid hydrolysis of BC performed with HCl, H_2SO_4 and the mixture of both acids influenced the yields and physical properties of BCNCs. So, it is possible to produce optimized BCNCs by acid hydrolysis according to the specific need of the application. Vasconcelos et al. [50] stated that, high acid concentrations underacid hydrolysis can hydrolyze crystalline as well as amorphous parts of BC. H_2SO_4 intensifies sulfonation of the BC surface whilst HCl implies low-density surface charge on BC. Thus, the researchers focused their study on varying concentrations of H_2SO_4 and HCl together. Roman and Winter [51] researched on sulphuric acid hydrolysis where they engaged their study on hydrolysis conditions, the involvement of sulfate groups, and thermal degradation of cellulose crystals. They noted a substantial decrease in degradation temperature even by involvement of a small amount of sulfate groups whereas a stepwise degradation was noted during involvement of larger amounts of sulphate groups. Hence, the BCNCs obtained by acid hydrolysis are purer and their properties are improved as compared to BCNCs produced by other methods. The prepared BCNCs can be utilized in variety of applications, and they are listed in below section with the overview of comprehensive literature.

1.2. DETAILED LITERATURE ON THE VARIOUS APPLICATIONS OF BC AND BCNCs

1.2.1. Bacterial Cellulose based Polymer Composites

Although BC has unique properties, it has some limitation such as lack of antibacterial properties, optical transparency, and stress bearing capability. To overcome these limitations, BC based composite has been introduced which consist of a matrix and a reinforcement material. BC owns a porous nature arrangement of fibers. The anchored reinforcement materials provide an additional property to BC that impart its natural biological and physiochemical properties [10]. However, BC possess potential as both matrix as well as a reinforcement material. Various BC composites have been synthesized through either in situ or ex situ methods as elaborated in section 1.1.2 and Table 1.1. For the in situ method, reinforcement material is added in the synthesis process while in ex situ, BC is impregnated with reinforcement materials [5].

Various BC composites are synthesized with different function and can be either organic or inorganic material such as polymers [52], metal or metal oxides [53], solid materials and

nanomaterials. However, the preparation of BC composites with other materials affects its structure and physico-mechanical properties, including variations in the pore size, surface area, WHC and WRR. For example, the average pore size of 'BC–Aloe vera' composites was reduced five times while there was significant improvement in properties, such as, mechanical strength, crystallinity, water absorption capacity and water vapor permeability in comparison to those of the unmodified BC film [54].

1.2.2. Bacterial Cellulose based Poly(*ε*-caprolactone) Composites

Altun et al. [55] studied the production of Bacterial cellulose /polycaprolactone scaffolds by using electrohydrodynamic (EHD)-3D-bioprinting technique. The BC/PCL blend was prepared by mixing BC powder in 10% PCL solution (prepared in DCM), followed by stirring at room temperature for 1h. The prepared composite scaffolds exhibited enhanced biocompatibility and facilitated cellular proliferation and were used in a further study for supporting the growth of target tissues with the addition of appreciate drug for skin tissue engineering applications. Figueiredo et al. [56] reported the in-situ synthesis of bacterial cellulose/polycaprolactone blends for hot pressing nanocomposites films production. In this study, PCL powder was incorporated in the BC culture medium, so the obtained films showed a homogenous distribution of PCL throughout the BC network, as well as good thermal stability (up to 200 ℃) and improved mechanical properties, when compared to pristine PCL. Barud et al. [57] investigated the production of optically transparent BC/PCL membrane to be used as fully biocompatible flexible display and biodegradable food packaging, by the impregnation of PCL acetone solution into dried BC membranes, followed by drying. UV-Vis studies revealed an increase in transparency in BC/PCL membrane when compared with pristine BC. The good transparency of the BC/PCL can be related to the presence of BC nanofibers associated with deposition of PCL nano-sized spherulites which are smaller than the wavelength of visible light. Gea et al. [58] melt-compounded particulate BC (PBC) and fibrous freeze-dried BC (FBC) with PCL in a mini twin-screw extruder to prepare biodegradable composites. A significant improvement in mechanical properties, such as Young's modulus of PCL was observed through the addition of both particulate BC and fibrous freeze-dried BC, with the latter giving better mechanical properties compared with particulate BC. PBC was prepared by blending pure BC in water, followed by vacuum drying; on the other haPCL/FBC composites,

based on high-aspect ratio cellulose nanofibers, showed higher tensile strength and strain at break than particulate PCL/PBC while modulus was similar for both types of composites.

The blends and copolymers of PCL have gained attention as they can develop novel polymers suitable for remarkable biomedical applications. However, an increased consumption and global market demand of this polymer, enforce our scientific understanding to replace its synthesis route by a sustainable approach making it more environment-friendly and less expensive.

1.2.3. Biomedical Applications of Bacterial Cellulose and its Nanocrystals

Sharma and Bhardwaj [59] reported the utilization of BCNCs in tissue engineering, drug delivery, wound healing and biosensing. Earlier, Fontana et al. [60] researched on BCNC for direct application of skin tissue repair. Barud et al. [61] reviewed comprehensive applications of BC in medical sector which includes wound dressing, biocompatibility, antimicrobial property, cell adhesion and growth, drug delivery, scaffolds, cardiovascular implants, cartilage/meniscus implants, bone and connective tissue repair, dental/oral implants, neural implants, artificial cornea, urinary conduits, tympanic membranes etc. Xue et al. [62] explained the biomedical applications in detail with various practical examples. They stated that the implementation of BCNC into rats for 12 weeks showed a systematic in-vivo biocompatibility with regards to no foreign body reaction and no histological inflammation. The evident chemical and mechanical properties of BCNC, make it a viable material for wound dressing applications and was introduced in many commercial wound dressing products such as Dermafill®, Xcell®, Biofill®, etc. In another review by Wasim et al. [63], it is reported that the modification of BCNC with metal and metal oxide nanoparticles resulted in strength improvement for bionic design of medical related properties, which includes artificial skin with wound healing, dural prosthesis, arterial stent coating, bone repair graft and biomedicines. Aditya et al. [64] surfaced there study around the properties of BCNC, which shows resemblance with native human tissues and thus BCNCs are one of the best suitable materials to replace the impaired tissues. In this thesis, electrospinning technique has been used to fabricate BC based antimicrobial scaffolds.

1.2.4. Catalytic Applications of BC and BCNCs

Jeremic et al. [65] researched on BCNC as a support material for catalyst preparation from two different transition metals viz., palladium and copper. Prepared catalysts were then utilized for

production of value-added chemicals, biphenyl-4-amine and 4′-fluorobiphenyl-4-amine which can be used in various applications. Khamkeaw et al. [66] researched on BC derived activated carbon (BC-AC) altered with H_3PO_4 to utilize it as a catalyst which performs selective dehydration of ethanol to produce ethylene. The results of this study interpreted that the catalyst P/BC-AC has high thermal stability, and it is very efficient and economical for ethanol conversion into ethylene. Kamal et al. [67] used BC nanofibers as catalyst support due to their high surface area. They used this catalyst support to make carboxymethyl cellulose cobalt (CMC-Co) catalyst. The results were compared between CMC-Co catalyst with BC support and without support, and the results showed the repeatability for multiple use by the CMC-Co catalyst with BC nanofibers support. Song et al. [68] worked on BC aerogels for dispersing Cu and Ni nanoparticles to prepare the catalyst. Their study showed that the synthesized catalyst has improved reusability and stability with excellent performance in 4-nitrophenol reduction reaction. Pagliaro et al. [69] stated that BC composites are used in polluted water treatment by organic contaminants catalytic activity. Their review also showed hydrogenation reaction for conversion of phenol into cyclohexanone, by transition metal palladium nanoparticles (NPs) catalyst doped with the nanocellulose, the conversion was not reported for just palladium NPs. Thus, BCNCs can be utilized as catalyst for variety of applications including conversion of raw materials into platform chemicals and value-added products.

1.2.5. Cellulose based Hydrogels

Wichterle and Lim [70] introduced hydrogels in the 1960s for the first time. The use of plastics, such as glycolmonomethacrylate in the formation of transparent, soft gels was studied in the 1960s. From then onwards, researchers and industries had started to work on them extensively [71]. In present day world, hydrogels are used in a variety of applications such as food, biomedical, and other relevant fields [72,73]. Hydrogels are nothing but a heterogenous mixture of two or more phases basically having three dimensional solid network as solid phase and water as liquid or dispersed phase [74]. Usually, these hydrogels are procured from the chemical reactions of the heterogeneous mixture but the obtained hydrogels possess some drawbacks like low tensile strength, low toughness, and low stiffness [75]. To overcome these drawbacks, hydrophilic CNC based hydrogels can be prepared and lot of studies has already been done and reported elsewhere for this research [76–78]. In this thesis, our study is focused on the preparation on hydrogels from CNCs extracted from the BC. The research on BCNC based hydrogels is performed for the first

time as a composite polymer with the addition of modified gum arabic (GA), and the fabricated hydrogels have shown superior qualities in terms of improved self-healing properties, high mechanical strength, and high porosity. Self-healing hydrogels are beneficial in biomedical applications as they can facilitate proper healing of wounds by automatically repairing themselves via hydrogen bond mechanism.

1.3. STRUCTURE AND OBJECTIVES OF THE THESIS

Bacterial cellulose (BC) due its highly pure, biocompatible, nontoxic and highly hydrophilic nature have been considered the novel material of this thesis. Crystalline bacterial cellulose nanocrystals (BCNCs) are extracted from BC as the source material, through acid hydrolysis. Various studies have been carried out using BC and BCNCs as the major component in each objective, and after obtaining captivating results from these studies multi-domain application of the developed materials have been discussed. The results obtained by this thesis work, fulfilled the aim and objective decided prior to the selection of biomass and materials.

To be specific, the objectives of this thesis are structured are as follows:

1. Synthesis of Bacterial Cellulose and its derivative, Bacterial Cellulose Nanocrystals: A Lab Scale approach
2. Studies on Fabrication of Bacterial Cellulose based Polycaprolactone Composite Scaffolds for Wound Dressing Applications
3. Studies on Surface Functionalization of Bacterial Cellulose Nanocrystals and their Catalytic Applications in Value-Added Chemical Processes
4. Studies on Fabrication of Bacterial Cellulose based Polycaprolactone Electrospun Bandages for Wound Dressing Applications
5. Studies on Fabrication of Immobilized Bacterial Cellulose Nanocrystals/modified Gum Arabic Hydrogel

1.4. OUTLINE OF THE THESIS

Based on the above discussion, this thesis work is divided into eight chapters as summarized below.

Chapter 1: This chapter belongs to the background information and different studies associated with bacterial cellulose and cellulose nanocrystals, their surface functionalization for utilization in various applications as "Introduction and Literature Review". The research objectives formulated to accomplish the research goal has also been listed in this chapter.

Chapter 2: The second chapter presents complete information about the "Materials and Method" utilized in this thesis work along with the qualitative and quantitative analyses, using various characterization techniques to investigate the desired properties of the fabricated materials.

Chapter 3: This chapter discusses the synthesis of Bacterial cellulose (BC) in standard HS (Hestrin-Scharmm) medium using *G. xylinum* CCM 3611. Focus had been given on production of bacterial cellulose on the basis of its yield, size and shape. Further, acid hydrolysis was used to extract needle-like BCNCs from the obtained bacterial cellulose. Various characterization techniques were used to determine the properties of the synthesized BC and BCNCs. These two materials were then used in the subsequent chapters to develop new materials with enhanced characteristics.

Chapter 4: This chapter deliberated the mechanism of poly(ε-caprolactone) impregnation into the bacterial cellulose membrane and discussed the performance of the fabricated composite. The use of bacterial cellulose as the reinforcing agent enhanced the crystallinity and flexibility of the prepared composites. Additionally, this chapter also investigated the biocompatibility of the prepared composites to further use them as wound dressing materials.

Chapter 5: This chapter relates to the utilization of bacterial cellulose nanocrystals for producing a novel and efficient BCNC templated heterogeneous catalyst which could be further utilized in a hydroxymethylation reaction. The developed mesoporous catalyst with comparatively higher surface area, helped in the conversion of furfural to HMF.

Chapter 6: This chapter discussed the use of electrospinning technique for the fabrication of bacterial cellulose/ polycaprolactone (BCP) scaffolds. A comprehensive study has been performed to determine the physico-chemical, antimicrobial and biocompatible properties of the scaffolds. The results obtained interpreted that the prepared drug-functionalized cellulosic scaffolds have a great potential as a wound dressing material in biomedical applications.

Chapter 7: In this study, the preparation of immobilized BCNC based hydrogels and their possible applications is summarized based on the results obtained from the analyses. The formulated hydrogels exhibited good self-healing and improved mechanical properties, good porosity, which facilitated their application as promising biomaterials. The cross-linking was confirmed through characterization by FTIR spectroscopy, SEM morphology, thermal studies and water absorption capacity.

Chapter 8: This chapter summarizes and concludes the thesis work based on previous chapters and presents the "Future scope" of work in this area along with associated further processes.

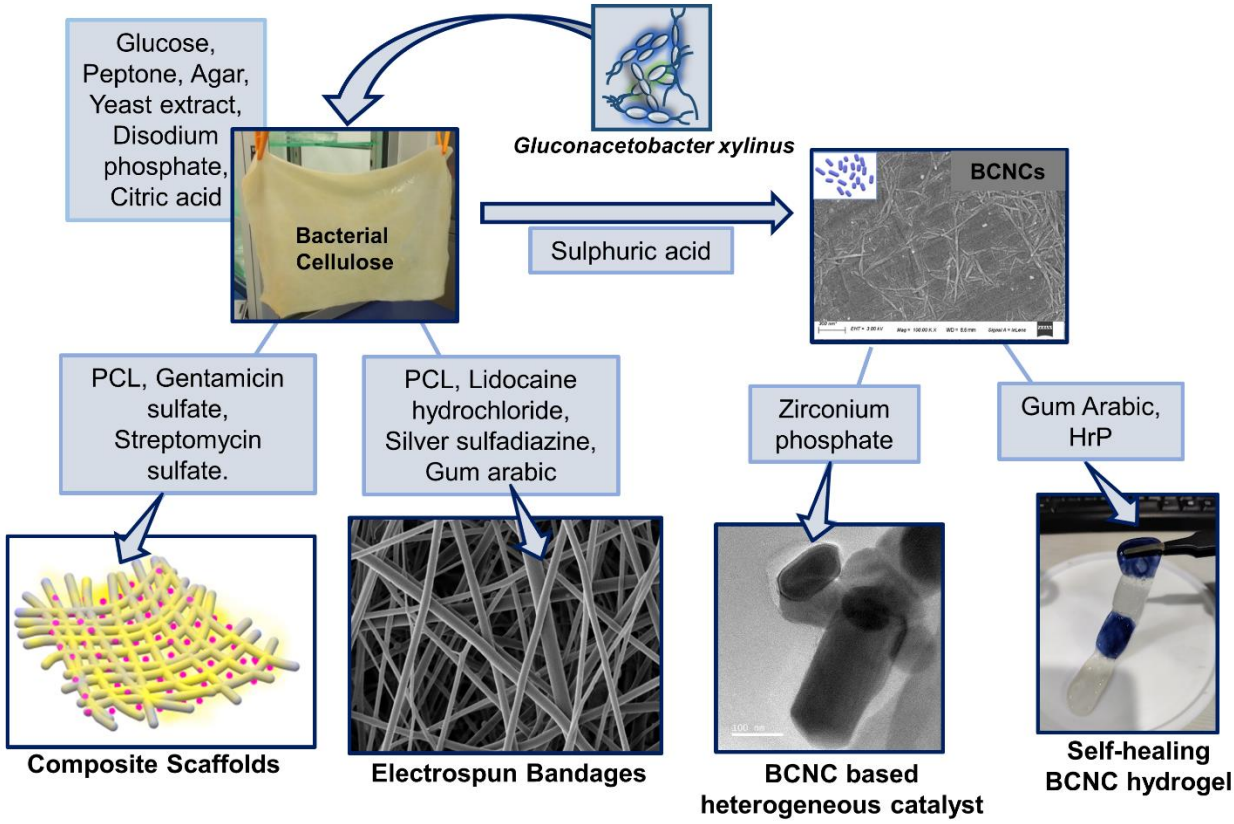

Figure 1.2. Structural representation of the thesis with the mentioned objectives along with the materials used, as discussed in Chapter 2.

Chapter 2

Materials and Method

This chapter provides details of the materials and methodologies followed for performing the experiments involved in this Thesis work. Fabrication of bacterial cellulose (BC) on different lab-scale approaches from *Glucanoacetobacter xylinus* strain have been discussed. The fabrication of needle-like bacterial cellulose nanocrystals (BCNCs) using acid hydrolysis have also been discussed. Surface modification of BC with polymer, PCL and different drug particles to fabricate BCP-GEN, BCP-SM as wound dressing materials has been described. Preparation of BCNC templated ZrP nanosheets, and the utilization of their catalytic activity in value-added chemical synthesis has been also reported. Fabrication of electrospun BC-based polymeric bandages functionalized with different drug has been reported. Preparation of immobilized BCNC based gum arabic hydrogel has been detailed. The experimental methodologies followed along with the analytical instrumentation used for characterization of the aforementioned materials have also been discussed in this chapter.

2.1. MATERIALS

Bacterial strain *Gluconacetobacter xylinus* CCM 3611 used for the synthesis of Bacterial Cellulose, was purchased, and conserved in the Microbiology Laboratory of the Centre of Polymer Systems, Zlin, Czech Republic. Glucose, peptone, agar, yeast extract, anhydrous disodium phosphate and citric acid were purchased from Sigma-Aldrich and Himedia (Czech Republic and India). To obtain bacterial cellulose powder, the extracted wet BC was first homogenized into a uniform suspension in distilled water, followed by freeze-drying. Poly(ε-caprolactone) of M_n~78 KDa was laboratory synthesized by a solvent-free polymerization technique under inert atmosphere in the Centre of Excellence for Sustainable Polymers, Dept. of Chemical Engineering, IIT Guwahati, India. In the polymerization process, initially ethylene glycol (>99% purity, initiator) and tin octoate (>99% purity, catalyst) was allowed to stir for some time followed by the addition of monomer, Ɛ-caprolactone (98% purity) and the reaction time and temperature were optimized to achieve the desired molecular weight. The initiator to monomer ratio was maintained

at 1:1000. The as-synthesized PCL exhibited a density higher than its monomer (~1.130 g/cm^3) and a maximum intrinsic viscosity 74.0 cm^3/g [79]. Commercial poly(ε-caprolactone) Capa™ 6800 (M_w=80 kDa) used in Chapter 6 was purchased from Ingevity, United Kingdom. Gentamicin sulfate (GEN) salt, Furfural (99%), Gum arabic from acacia tree, Lidocaine hydrochloride, Silver (I) sulfadiazine (98%), Poly(vinyl alcohol), was purchased from Sigma-Aldrich, India. Streptomycin sulfate (SM), Zirconium chloride oxide octahydrate ($ZrOCl_2.8H_2O$), sodium dihydrogen phosphate ($NaH_2PO_4.2H_2O$), Nitric acid, Sulphuric acid (97%), Sodium (meta)periodate, di-Sodium Tetraborate (Borax), Hydrogen peroxide 30% were purchased from Himedia, India. Formalin (37% aqueous formaldehyde stabilized with 10% methanol), Chloroform, dimethyl formamide (DMF), glutaraldehyde solution (25%), aniline blue diammonium salt were purchased from Merck, India. Dulbecco's modified Eagle's Medium (DMEM) supplemented with 10% fetal bovine serum (FBS) was purchased from Gibco™ and Luria-Bertani (LB) broth, Agar, DAPI (4',6-diamidino-2-phenylindole), used as a staining agent for cell adhesion studies was also purchased from Himedia Laboratories, India. Peroxidase from horseradish and ABTS {2,2′-azino-bis(3-ethylbenzothiazoline-6-sulphonic acid)} used for immobilization study was purchased from Sigma-Aldrich and SRL, India, respectively. Deuterium oxide (Sigma-Aldrich, India) was used as the reagent for NMR analysis. All the chemicals were used as received.

2.2. METHODS

2.2.1. Synthesis of Bacterial Cellulose and Fabrication of Bacterial Cellulose Nanocrystals: A Lab Scale approach

(i) Synthesis and Purification of Bacterial Cellulose

The standard Hestrin and Schramm (H.S.) medium comprising of glucose, peptone, yeast extract, anhydrous disodium phosphate and citric acid was used as the medium for the BC production [80]. Bacterial strain, *G. xylinum* was cultured in agar plates for 3 days at 28°C. Briefly, 5 loopful of the grown bacteria were collected and inoculated in a tube containing 5 mL H.S. medium to prepare initial inoculum for BC production and was incubated for 2 days at 28°C under static condition. This prepared inoculum was then transferred to sets of sterile 250 mL glass bottles filled with 100 mL H.S. medium each and the culture bottles were then covered with perforated parafilm for aeration incubation at 28°C for 15 days under static state. Large scale synthesis of BC was also

carried out in glass trays (295*230*210 mm) containing 4-6 L of medium to obtain BC membranes of larger size (295*230 mm and 15 μm height) and wet weight ~125g. The H.S. medium used was autoclaved at 121°C for 20 min. before use. The BC pellicles formed on the surface of the culture vessels were then collected and soaked in distilled water overnight, and then treated twice with 0.5 N NaOH for 30 min. at 80°C followed by washing with distilled water until neutral pH was achieved.

(ii) Fabrication of Bacterial Cellulose Nanocrystals (BCNCs)

Oven-dried bacterial cellulose membranes were first cut into small pieces and then treated with 50 % (v/v) sulphuric acid solution in a cellulose/acid ratio of approximately 20 g/L, at 50 °C for 2 h. The hydrolysis reaction was then stopped by diluting the reaction suspension around 8-fold with cold deionized water. Later, the suspension was centrifuged and washed with deionized water at 5500 rpm for 15 min at 20°C to precipitate the BCNC and this step was repeated for 3 times. Finally, the BCNC suspension was dialyzed in deionized water to obtain a neutral pH and final concentration of ~1 % w/v, which was further freeze-dried at -80°C for 48h to obtain BCNC powder [81].

2.2.2 Fabrication of Bacterial cellulose-based poly(ε-caprolactone) composite scaffolds

(i) Preparation of BC/PCL composite films

The previously treated and purified BC pellicles were placed in a beaker, to which 1:1 (weight) ratio of distilled water was added. A fine suspension of BC in water was achieved in 20 min. with the use of a hand blender (Powermaxx, BOSCH, 750W). This suspension was then cast on a silicon tray and allowed to air dry overnight to get a uniform BC membrane. To develop uniform bacterial cellulose based polycaprolactone (BCP) composites, dried BC membranes were first cut (3×4 cm2) and incubated in acetone for 24 h. Thereafter, all the acetone soaked samples were immersed in glass vials containing PCL solution in acetone (2wt% and 3wt% PCL) [57]. The impregnation of PCL into the BC membrane was facilitated with the use of a 2D-Benchrocker. After each incubation (48h, 72h and 120h), the BC membranes immersed in the PCL solution were taken out, washed with acetone to remove the excess polymer, placed in petriplates and allowed to dry at room temperature. The average thickness of the BC and BCP films were calculated as 15μm and 23μm, respectively.

(ii) Functionalization of BC based composite films

Two different drug concentration (0.2 mg/mL and 0.5 mg/mL) of gentamicin and streptomycin salts, each were prepared in 50 mL deionized water. The BC and BCP membranes were then immersed in the prepared drug solutions for 24 h at 37°C in a shaking incubator. After 24 h, the membranes were taken out and washed with deionized water and dried at room temperature overnight. BC-GEN, BCP- GEN, BC-SM and BCP-SM are the abbreviations used for GEN loaded BC, GEN loaded BCP, SM loaded BC, SM loaded BCP membranes, respectively.

2.2.3 Surface Modification of Bacterial Cellulose Nanocrystals with Metallic Nanoparticles

(i) Fabrication of Bacterial cellulose nanocrystals (BCNC) templated zirconium phosphate catalyst

Zirconium phosphate (ZrP) catalyst with a molar ratio of 2:1(P/Zr) has been prepared according to literature and used as a reference catalyst [82]. For the preparation of ZrP, dropwise addition of 0.2 M sodium dihydrogen phosphate (100 mL) aqueous solution to 0.1 M $ZrOCl_2.8H_2O$ (100 mL) was done with continuous stirring at 70°C for 1h. The pH of the reaction mixture was maintained at 1-2. After 1h of stirring, a gelatinous precipitate was obtained, which was then filtered and washed with water, followed by drying under vacuum at room temperature. Then, the acidification of the obtained material was done with the treatment of 1 M HNO_3 for 30 min, atleast for five times with occasional stirring. The sample was then washed and centrifuged with distilled water to separate the acidic part, for several times followed by drying at room temperature. To synthesize the BCNC_ZrP catalyst, BCNC with two different loading of 2-3 wt% was first added to the 0.1M aqueous $ZrOCl_2.8H_2O$ solution and allowed to stir at 70°C. To this solution mixture, 0.2 M sodium dihydrogen phosphate was added dropwise and stirred for 1h. Then, the above-mentioned same procedure is followed to obtain the bacterial cellulose nanocrystal templated ZrP catalyst.

(ii) Conversion of raw material furfural to 5-hydroxymethylfurfural using BCNC templated ZrP

The reaction was performed in a two-necked round bottom flask attached to a condenser. At first, formalin (5mL) and solid catalyst were allowed to mix well under continuous stirring (500rpm) at ~90°C for 30 min. To this reaction mixture, furfural (82µL) without purification treatment was

injected to initiate the target reaction. Then, after 12-24 h of reaction, the reaction mixture was centrifuged and the obtained filtrate was analysed. The reusability of the developed catalyst was also tested. After each reaction, the catalyst was filtered and separated by centrifugation, washed with ethanol, dried under vacuum overnight at 60°C, and again was used for the next reaction.

2.2.4 Fabrication of Bacterial Cellulose/Polycaprolactone electrospun bandages

(i) Preparation of bacterial cellulose powder

To obtain bacterial cellulose powder, the extracted wet BC was first homogenized into a uniform suspension in distilled water, followed by freeze-drying.

(ii) Fabrication of BC-PCL nanofiber scaffolds loaded with lidocaine hydrochloride by electrospinning

An electrospinning unit (Nanotech, India) was used to produce the nanofibers. The prepared polymeric solution was loaded into a 5 mL plastic syringe connected to a pump which controls the flow-rate of the solution. A high voltage supply was applied (15 kV) between the spinneret and the electrode and the thin jet fibers were collected on an aluminium grid placed on the collector plate. The working distance between the aluminium grid and the needle was kept as 15 cm, with a flow rate of 1 mL/h to produce the desired nanofibers. The electrospinning experiment was carried out at room temperature (25-30 ℃), at a relative humidity of 35%.

To prepare the polymer solution, PCL, 9% (w/v) was allowed to dissolve in a binary mixture of $CHCl_3$/DMF (9:1) with overnight stirring. Then, BC powder (1-2 wt%, with respect to polymer volume taken for electrospinning) was added to the PCL solution and allowed to stir overnight. Both the solutions were then separately subjected to the electrospinning unit to fabricate pure PCL and bacterial cellulose based polycaprolactone (BCP) mats. To prepare LID loaded BCP mats, 1wt% LID was added into the BC-PCL solution and allowed to further stir for 12h. The obtained nanofibrous mats (PCL, BCP and BCP-LD) were then allowed to vacuum dry overnight to remove the trapped residual solvent.

(iii) Surface treatment of BCP-LID scaffolds using glutaraldehyde

A gum arabic (2% w/v) solution was prepared in glutaraldehyde (2% v/v) solution, to which 0.5 wt% silver-sulfadiazine (Ag-SD) was added and the mixture was allowed to stir for 4h. The fabricated nanofiber scaffolds (BCP-LD) were then dipped in the GA-glutaraldehyde solution loaded with the drug for 30 min. to crosslink, taken out and rinsed with water to remove excess glutaraldehyde, followed by drying in dark at room temperature. The samples (BCP-LSD) were then stored in a vacuum desiccator for characterization.

2.2.5. Fabrication of Immobilized Bacterial Cellulose Nanocrystal based Gum Arabic Hydrogel

(i) Preparation of modified Gum Arabic

The oxidation of gum arabic was carried out using sodium metaperiodate to synthesize a natural aldehyde crosslinker, oxidized gum Arabic (OGA) as reported in literature [83,84]. At first, gum arabic (5% w/v) solution was prepared in 20mL of distilled water, to which 10 mL aqueous sodium metaperiodate (5% w/v) solution was added dropwise, and the reaction mixture was continuously stirred for 24h at 20 °C in dark. After 24 h, the unreacted periodate present in the solution was neutralized using 5 mL of ethylene glycol followed by the addition of ethanol (~200 mL) to precipitate the reaction mixture. The obtained precipitate was then washed, centrifuged several times with water-ethanol mixture, and then freeze-dried to obtain powdered OGA.

(ii) Preparation of BCNC loaded modified Gum Arabic hydrogel

OGA powder (300 mg) and BCNC (5,10,20 wt%) w.r.t OGA were taken in a beaker and to this 3mL of PVA (5% w/v) solution was added and allowed to stir. The addition of BCNC to the mixture resulted in a slightly viscous solution. To this viscous solution, about 1.5mL of borax solution (5% w/v) was poured and allowed to mix for about 20min, which resulted in the formation of a hydrogel. The prepared gels were then stored at 4°C for further use. OGA hydrogels without BCNC loading was also prepared for comparison. The hydrogels prepared with 5, 10, 20 wt% BCNCs were named as HG-BCNC(5%), HG-BCNC(10%), and HG-BCNC(20%), while the hydrogel without BCNC was named as HG.

(iii) Immobilization of BCNC-modified GA hydrogel

For immobilization studies, 0.1 mg/mL HRP solution was prepared in Phosphate buffered saline, PBS 7.0 and HG-BCNC(20%) was investigated. 20 mg of prepared hydrogel was first allowed to crosslink in 10 mL of aqueous glutaraldehyde (4% v/v). After 2h, the gel was taken out washed with water to remove the excess aldehydes and then added to 5mL of HRP solution for immobilization. After the immobilization, the hydrogels are first separated from the HRP solution by centrifugation, and the first supernatant is collected and stored at 4℃. The hydrogels are then washed with PBS many times and all the supernatants are stored at 4℃ for enzyme activity assay.

2.3. ANALYTICAL INSTRUMENTATION AND CHARACTERIZATION

Fourier transfer infrared (FT-IR) spectroscopy. The chemical characteristic of the fabricated samples was done using Fourier transfer infrared (FTIR) spectroscopy in attenuated total reflectance (ATR) mode at room temperature (PerkinElmer, U.S.A). The spectra were recorded in the frequency range of 4000 to 400 cm^{-1} wavelength, with 64 scans and 4 cm^{-1} resolution.

Thermogravimetric Analysis (TGA/DTG). The thermal behavior of all the prepared samples was studied in an inert atmosphere of nitrogen at 10 °C/min heating rate using thermogravimetric and derivative thermogravimetric analysis (TGA-4000, PerkinElmer, U.S.A.) with flow rate maintained at ∼20 mL/min. The temperature profile of the analysis was set as 30−700 °C.

XRD analysis. The X-ray diffraction analysis was conducted to analyze the crystalline structure of the samples. The experiment was performed using a Micromax-007HF (Rigaku, Japan). The scans were performed in the range of $2\theta = 4°–80°$ at a speed of 5°/min utilizing a foil filtered CoKβ radiation (λ of 0.179 nm) at 40000 V voltage and a current of 15 mA. The divergence slit was maintained at 0.1° all throughout the experiment.

Differential Scanning Calorimetry (DSC). The change in physical properties of the fabricated BC, BCP samples was studied using DSC (Phoenix DSC 204 F1 NETZSCH, GmbH) in 30-400°C range.

BET Surface Area Analysis. The surface area and pore size distribution based on N_2 adsorption of the synthesized catalysts was studied using BET Analyzer (Tristar II; Make: M/s Micromeritics, U.S.A.) at liquid nitrogen temperature.

Field Emission Transmission Electron microscopy (FETEM). FETEM of the prepared BCNC and catalysts were carried out using JEOL, Model :2100F. BCNC was dispersed in deionized water under ultrasonic radiation for 1h and drop casted on copper grid before analysis. Similarly, the catalyst samples were prepared by dispersing the catalyst powder in ethanol under ultrasonic radiation for 30 min, and then the resulted solution was drop-casted on a copper grid followed by slow evaporation of solvent under vacuum at room temperature. Elemental mapping of the catalysts was also done using FETEM.

Field Emission Scanning Electron microscopy (FESEM). For morphological analysis of the BCNC and the catalyst samples, the sample suspensions were dropcasted on aluminium paper and investigated at an accelerating voltage of 3 kV (ZEISS Sigma 300, FESEM, USA).
The surface morphology of the samples was analyzed at different magnification (10 000× magnification 14 000×, 100 000×, 250 000 × etc.). Energy dispersive X-ray analysis (EDX) (Zeiss, Gemini) was performed with an aim to identify the chemical compositions of prepared samples in terms of weight percentages (wt.%) of elements Carbon (C), oxygen (O), nitrogen (N), and sulfur (S). The surface and cross-sectional morphology of the prepared BC and BCP scaffolds studied in Chapter 4 was characterized using a field emission scanning electron microscope (Nova NanoSEM™ by FEI™, CZ s.r.o, Brno).

Atomic Force Microscopy (AFM). The surface topography of the membranes was assessed using AFM (Oxford, Model: Cypher) equipped with a silicon cantilever with spring constant of 42 N/m and resonance frequency 320 kHz.

Wettability. The contact angle of the dried samples was evaluated using Kruss GMBH DSA25 (Germany), where a sessile drop of water (~2 µl) was placed on the sample and the change in behavior of the water droplet in contact with the sample was observed as a function of time (10s to 60s) at 25ºC.

Swelling studies. Fabricated scaffold immersed in phosphate buffered saline (PBS), pH 7.4 was used for swelling study for 24h. The initial and final weight was recorded before and after immersion to determine the swelling percentage.

Water vapor permeability studies. The water vapor transmission rate (WVTR) through the fabricated scaffolds was investigated using a PERMATRAN-W Model 1/50 (Mocon, U.S.A.). The wet and dry chamber's relative humidity (RH) was set as 100% and 10% respectively, and a mat of 1cm^2 was characterized at 37.8°C in the atmospheric pressure.

Mechanical studies. The tensile and compression properties of the prepared materials were studied using a universal testing machine (UTM) with a 5kN load cell (Zwick Roell : Z005TN).

In vitro cytotoxicity assay and cell staining

Baby Hamster Kidney fibroblast cells (BHK-21) were cultured in Dulbecco's modified Eagle's Medium (DMEM) (Gibco™) supplemented with 10% fetal bovine serum (FBS) (Gibco™). The cytotoxicity assay was determined by a colorimetric assay (MTT Assay), where MTT stock solution of 5mg/mL was prepared in Phosphate-buffered saline (PBS), stored at 4°C. BHK-21 cells, at a density of 2×10^3 cells/well, were seeded and allowed to grow overnight in a 96-well microplate, at 37°C in a humidified atmosphere with 5% CO_2. After discarding the media, the samples (6 cm^2 of area) were UV sterilized for 1h and the extract of the test materials was prepared as per International Standard ISO 10993- 12, and the material surface to extract fluid ratio was kept as 6 cm^2/mL. Then the sterilized samples were placed in BHK-21 cell's growth medium for 24 h. After that the cultures were treated for 24 h, 48 h and 72 h with the prepared extracted media and the standard culture medium containing only the cells was used as control. After the specific incubation period, all the samples were removed and MTT solution was diluted to 0.5 mg/mL in plain DMEM (without FBS) and the incubation was maintained for further 3 h. Dimethyl sulfoxide (DMSO) was added to each cell well to dissolve the formazan pigment and the absorbance was recorded at 570 nm wavelength using a microplate reader (ELISA). Wells containing only DMSO was considered as blank, and the comparison of relative cell viability was calculated in four replicates. The mean values and their standard deviations were calculated, and the graphs were plotted using the closest absorbance values of three replicates out of the four samples.

To study the biocompatibility of the fabricated scaffolds, the same procedure as above was followed to seed BHK-21cells in a 96-well plate and circular sample films were cut and placed on it. After specific time (24h, 48h and 72h), the incubated samples were treated with 4% formaldehyde for 10 min to fix the cells followed by rinsing thrice with PBS. Then DAPI (4',6-diamidino-2-phenylindole) (100µL) was added to the wells containing the sample and allowed to incubate in dark for 15 min. The cells were then again rinsed with PBS thrice and the images were taken using blue/cyan filter under the fluorescence microscope (Nikon H600L).

Antimicrobial assay

Antimicrobial activity of the drug-loaded samples was determined against *Staphylococcus aureus* and *Escherichia coli.* Luria-Bertani (LB) broth, Agar (HiMedia Laboratories) was used for this study. At first, the cultures were inoculated in LB broth and allowed to grow at 37°C, overnight. Further, the cultures were diluted to get a concentration of 2×10^9 CFU/mL for *E. coli* and 2×10^{10} CFU/mL for *S. aureus* and used as an inoculum for the antimicrobial assay. Circular discs of each sample were cut in triplicates and UV-sterilized for 1h before use. The discs were then placed on agar plates containing both the model bacteria separately and allowed to incubate for 24 h at 37°C and the zone of inhibition was measured in millimeter from the growth inhibited by the discs. Gentamicin (10 mcg) control (Himedia Laboratories) was also placed separately on agar plates containing *E. coli* and *S. aureus* to check the bacterial inhibition.

In vitro drug release study

In-vitro release profile of the drug-loaded scaffolds were carried out by placing each sample in plastic vials containing 10 mL phosphate-buffer saline solution (PBS, pH 7.4). These vials were then incubated at 37°C and at specific time interval, 3mL of sample medium was removed and replaced with fresh buffer solution. The cumulative drug release into the PBS solution was measured using an UV/Vis Spectrometer (Lambda 25, PerkinElmer USA) at wavelengths 232 nm, 240 nm, 241 nm and 263 nm for GEN, SM, LID and Ag-SD, respectively.

High Performance Liquid Chromatography (HPLC)

The obtained HMF filtrate was analysed using a Hypersil GOLD^{TM} column (250 x 4.6 mm, 5µm, Thermo Fisher Scientific). The injection volume for each sample was 20 µL, the solvent system

was water with 20% methanol(v/v). The flow rate was maintained at 0.8 mL/min and the detection wavelength for HMF was 277 nm.

Enzyme Assay

For the enzyme activity of horseradish peroxidase, ABTS (2,2′-azino-bis(3-ethylbenzthiazoline-6-sulfonic acid) was used. The sample was prepared by placing 2.9 mL of 9.1 mM ABTS solution in a cuvette, followed by the addition of 0.1 mL of 0.3% (w/w) hydrogen peroxide. To this solution mixture, 2 mg of immobilized hydrogel was added and the cuvette is subjected to UV-Visible spectroscopy for 20 min at absorbance, λ_{max} = 405 nm. Blank solution for this assay was prepared by using 0.05mL of PBS (pH 5.0) and 0.25% (w/v) bovine serum albumin (BSA) along with 2.9 mL ABTS solution [85]. The leakage test of the immobilized hydrogel was also done by mixing the gel with PBS and incubation at 4 ℃. Then the immobilized gel was collected and the supernatant was tested for HRP activity using ABTS assay and this test was conducted for six times. The specific enzyme activity was determined using the following equation;

$$UL^{-1} = \frac{\Delta A.V_t.D_f.10^6}{t.\varepsilon.d.V_s} \quad \text{Equation (1)}$$

where,

V_t is the final volume of reaction in mL (3.05 mL),

ΔA is the difference in absorbance recorded after an interval of 20 min,

D_f is the dilution factor of the enzyme, which is 1 in this case,

t is the time of analysis (20 min),

ε is the millimolar extinction coefficient of oxidised ABTS, at λ_{max} = 405 nm (36.8), and

V_s is the volume of enzyme used for the assay (0.05 mL).

Chapter 3

Synthesis of Bacterial Cellulose and its derivative, Bacterial Cellulose Nanocrystals: A Lab Scale approach

Motivation

The need to protect the environment and alertness to use renewable and biodegradable substitutes for the synthesis of biocompatible and eco-friendly materials have open possibilities in the scientific research community. Bacterial cellulose (BC) is a novel biomaterial derived from microorganisms with excellent purity and crystallinity, high mechanical stability and low toxicity, compared to plant-based cellulose. Due to their inherent higher water absorption and porosity, BC can be easily functionalized or combined with other materials for application in food, biomedical, tissue engineering, and textile industries. The extraction of bacterial cellulose nanocrystals (BCNCs) from BC is more efficient than plant-based cellulose since separating hemicellulose and lignin involves energy consumption and is environmentally challenging. Also, CNCs produced by conventional methodologies require around 7-10 days, whereas BCNCs can be easily obtained in 4-12h. Hence, we have developed methods to synthesize bacterial cellulose and BCNCs in a cost-effective and environment-friendly approach, and this process can be upscaled to produce larger quantities of BC and BCNCs for use in multiple applications in future.

Abstract

This chapter focuses on the synthesis and characterization of bacterial cellulose; and the subsequent extraction of BCNCs from BC through acid-hydrolysis. The biosynthesis of BC is conducted using Bacterial strain, *G. xylinum* under static aeration incubation at 28°C for 15 days. Pure BC membrane showed well-defined, closely intertwined and oriented fibrils with long and smooth fibers of diameter in the range of 35-200 nm in a typical 3-dimensional web-like highly porous network structure which also confirmed its high crystallinity. It is found that the BC examined in the present study was highly pure and can be readily processed into nanocrystals. BCNCs have been produced with a homogeneous morphology of well-defined, needle-like fibers with an average width of 13±9 nm and lengths in the range of 159-356 nm.

Graphical Abstract

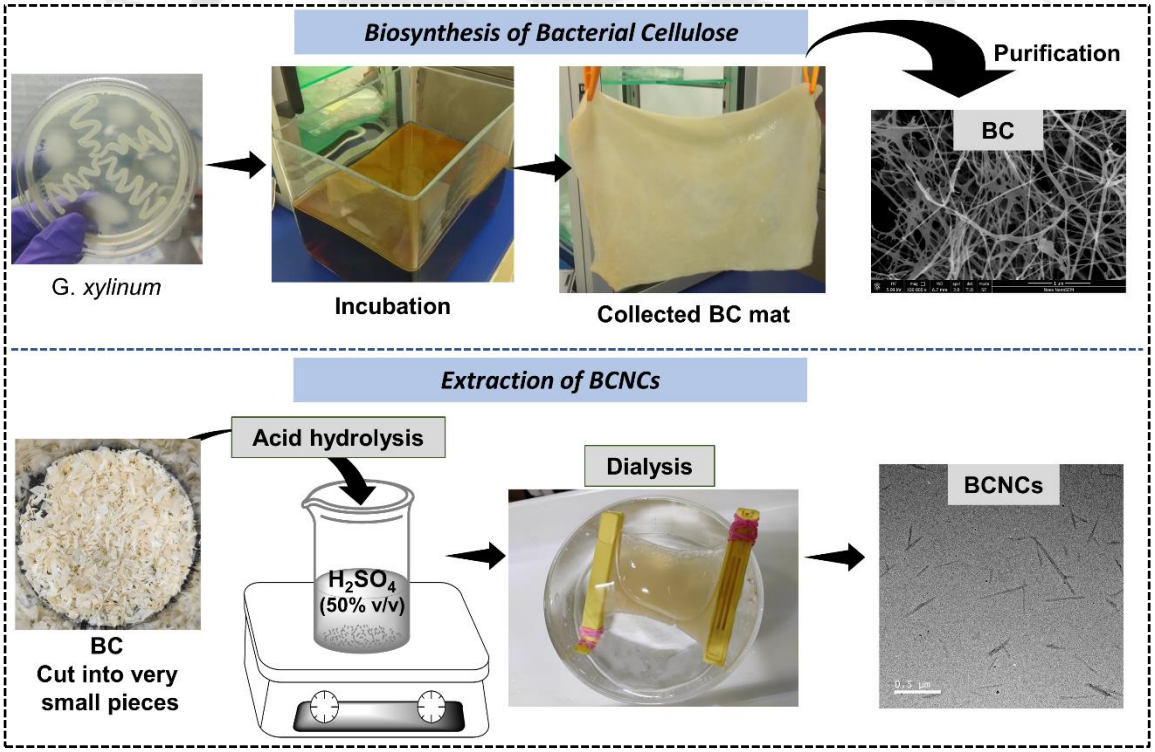

3.1. INTRODUCTION

Bacterial cellulose (BC) is a fascinating biomaterial possessing a range of noteworthy characteristics, such as, high water holding capacity and crystallinity, tensile strength, an ultrafine fiber network and the ability to be molded into three-dimensional (3D) structures during synthesis [3]. The fibrillar structure of BC consists of repeated dimers of β-1→4 glucan chain connected by inter- and intra-molecular hydrogen bonding with molecular formula $(C_6H_{10}O_5)_n$. The ultrafine network and high degree of polymerization of BC elaborates its application in textile industries, for making electronic paper, etc. [86,87].

Generally, bacterial strain *Acetobacter xylinum* is used in BC synthesis as it produces both ribbon-like and thermodynamically stable polymer (cellulose I and cellulose II) which are pure-forms of cellulose. The production of bacterial cellulose is carried out either through static or agitating oxidative fermentation, depending on the type of cellulose required, for example, static fermentation of BC leads to the formation of an interconnected three-dimensional structure [10]. In the synthesis process, the glucose chains secrete intermediate fibrils through the bacterial cell wall and these fibrils combine together to form nanofibrillar ribbons of pure cellulose at the air-medium interface which controls the oxygen supply to the medium [88].

Nanocrystals are structures with at least one of their dimensions in nanometer scale (1-100 nm), and they contribute as bio-crosslinking or reinforcing material for a wide range of applications. Usually, micro-cellulose fibers are resized to nano-form using top-down approaches, such as homogenization, acid hydrolysis, or combined chemical and mechanical approaches [40]. The highly pure and crystalline nature of BC make it a convenient source for the efficient extraction of bacterial cellulose nanocrystals (BCNCs). BCNCs extracted from bacterial cellulose leads to the minimization of energy consumed as well as it is an eco-friendly and sustainable process. The large specific surface area, higher strength and crystallinity, and abundance of hydroxy groups on their surface enables the easy dispersion of BCNCs in aqueous solutions [89]. The most commonly used technique to produce cellulose nanocrystals is acid hydrolysis, which involves the penetration of H^+ ions into amorphous cellulose part which release the crystallites of BC as a result of splitting of the glycosidic linkages [41].

Therefore, the possibility of tuning the inherent characteristics of BC and BCNCs to fabricate new and improved materials have been studied and discussed in the subsequent chapters of this thesis.

3.2. RESULTS AND DISCUSSIONS

3.2.1. Morphological analysis of the fabricated bacterial cellulose (BC) and bacterial cellulose nanocrystals (BCNCs).

The cellulose examined in the present study was derived from bacteria as this type of cellulose is highly pure and can be readily processed into nanocrystals. Figure 3.1(a) shows the FESEM image of pure BC with a typical 3-dimensional web-like highly porous network structure of well-defined, closely intertwined and oriented fibrils confirming their higher crystallinity [25,37]. The FESEM micrograph of the synthesized BCNCs shown in Figure 3.1(b) indicates a homogeneous morphology of well-defined, needle-like fibers with an average width ranging between 13.77 and 22.03 nm and lengths ranging between 159.8 and 356 nm. Small agglomerates or bundling of BCNC fibers were occasionally observed, most possibly due to the nanoparticle overlapping during drying. The distribution of the width and length of the nanocrystals could be assumed due to the breaking up of coarse aggregates of microfibrils by sulfuric acid hydrolysis and sonication.

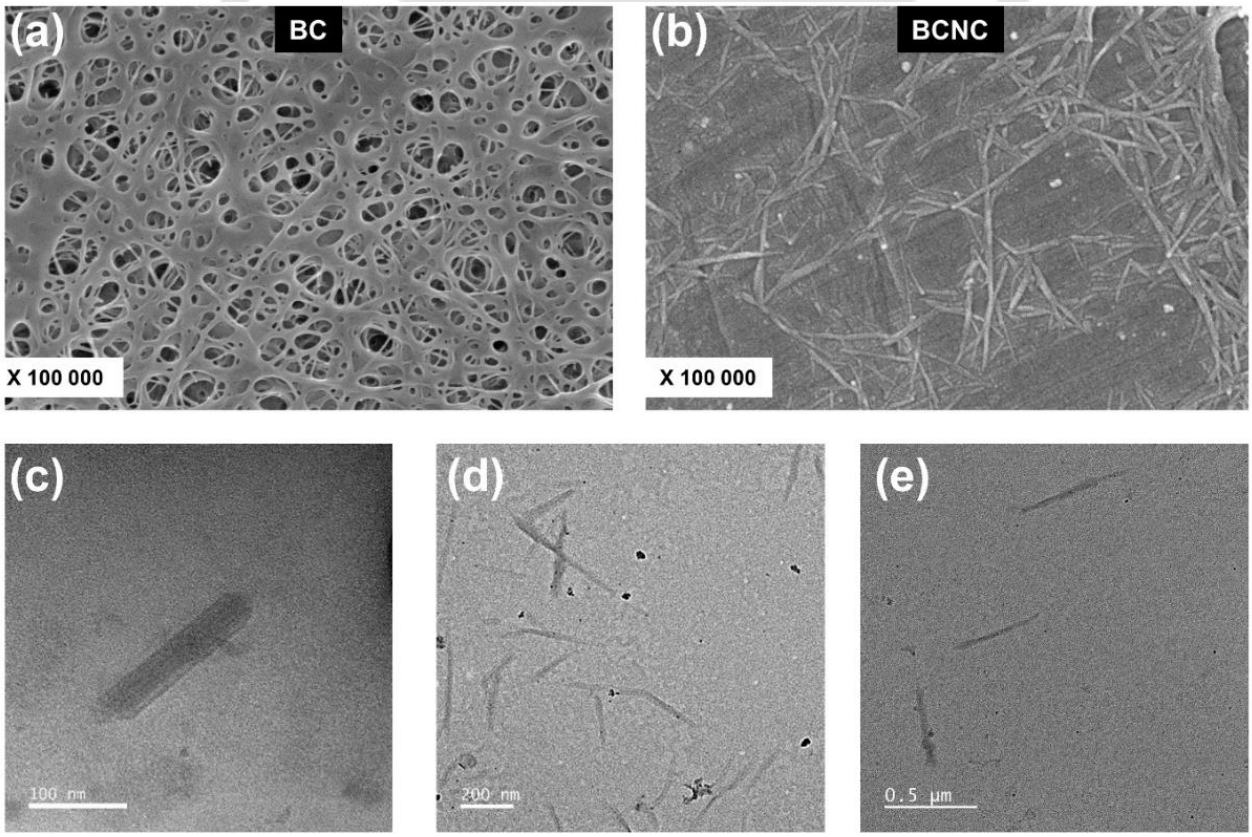

Figure 3.1. (a)FESEM image of BC, (b)FESEM image of BCNCs, and (c,d,e)FETEM micrographs of BCNC, confirming needle-like morphology.

Figure 3.1(c,d,e) shows the FETEM photograph of BCNCs with well-dispersed needle-shaped structures, which is an expected pattern for acid hydrolysis nanocrystals. The BC nanocrystals had a length ranging from 156 to 560 nm and width ranging from 9.85 to 20 nm.

3.2.2. Physico-chemical properties of the synthesized BC and BCNCs.

The FTIR spectra of native BC and BCNCs (Figure 3.2a) showed typical cellulose vibration bands, such as 3341 cm^{-1} (stretching of O-H bonds), 1427 cm^{-1} (asymmetric angular deformation of C-H bonds), 1363 cm^{-1} (symmetric angular deformation of C-H bonds), 1159 cm^{-1} (asymmetrical stretching of C-O-C glycoside bonds), 1103 cm^{-1} and 1046 cm^{-1} (stretching of C-OH and C-C-OH bonds in secondary and primary alcohols, respectively), and 892 cm^{-1} (angular deformation of C-H bonds)[41]. A sharp band corresponding to half-sulfate ester groups due to the reaction of BC with sulfuric acid is observed around 1256 cm^{-1}.

Crystallinity is a major factor that specifically influences the mechanical properties of materials. Therefore, the XRD patterns were used to determine the Crystallinity index (CrI) of BC and the BC nanocrystals. The results showed that BCNCs had a greater CrI than native BC [90]. The percentage crystallinity of BCNCs was calculated and found to be ~91% as compared to that of pure BC (~89% crystallinity) shown in Table 4.1. The increase in crystallinity after acid hydrolysis reaction was due to a reduction of the amorphous content, as this region is more accessible to acid attack. The XRD patterns of pure BC and BCNCs showed three 2θ diffraction peaks at 16.3°, 18.8°, 25.74° 14.7°, 16.7°, and 22.78°, respectively which are usually attributed to the crystallographic planes of 101 (amorphous region), 10(amorphous region), and 200 (crystalline region), respectively (Figure 3.2b). The presence of these 3 diffraction peaks characterizes cellulose type Iα (triclinic), which is prevalent in BC.

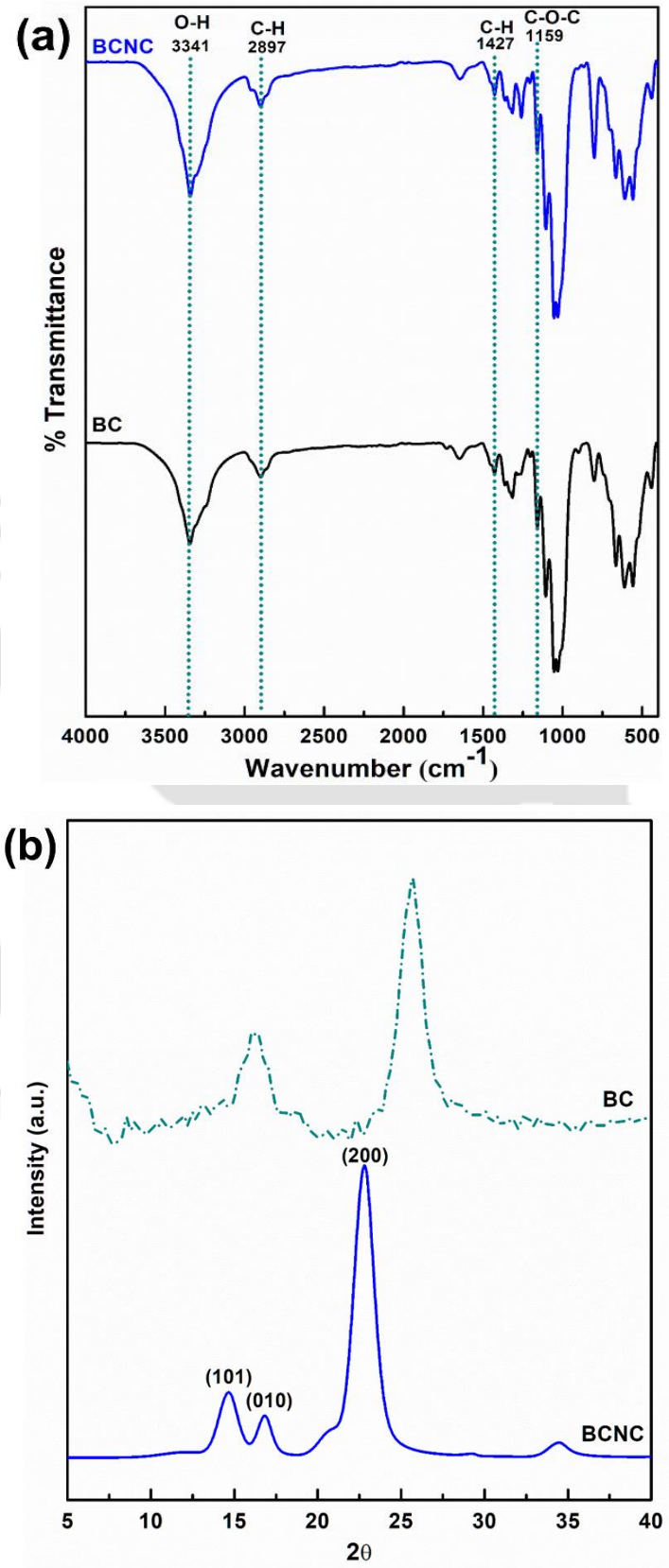

Figure 3.2. (a)FTIR spectra and (b)XRD patterns, of pure BC and the synthesized BCNCs.

The thermo-gravimetric analyses shown by TGA and the respective DTG curves of BC and BC nanocrystals obtained by acid hydrolysis (Figure 3.3a,b) revealed that the mass-loss profiles were similar. Three mass-loss events can be observed during thermal analysis of the sample. The first event, occurring at approximately 50–150 °C, is attributable to the evaporation of residual water present in the material. The second event, occurring in the temperature range of 250–500 °C, is characterized by a series of reactions in the degradation of cellulose, including dehydration, decomposition, and depolymerization of the glycoside units. This second mass-loss event is associated with a high loss of mass of cellulosic material, which is characterized by the onset temperature (T_{onset}), 316°C and 349°C for BCNCs and BC, respectively. The third thermal event, which extends from 550 to 650 °C, is related to oxidation and breakdown of carbonaceous residues, yielding gaseous products of low molecular weight. The degradation temperature of pure BC was slightly higher than that of BCNCs. The high surface area of BCNCs may play an important role in reducing the thermostability. Moreover, hydrolysis reactions with H_2SO_4 promote the formation of nanostructures with low thermal stability due to the presence of sulfate groups ($–OSO^{3–}$) on the BCNC surface.

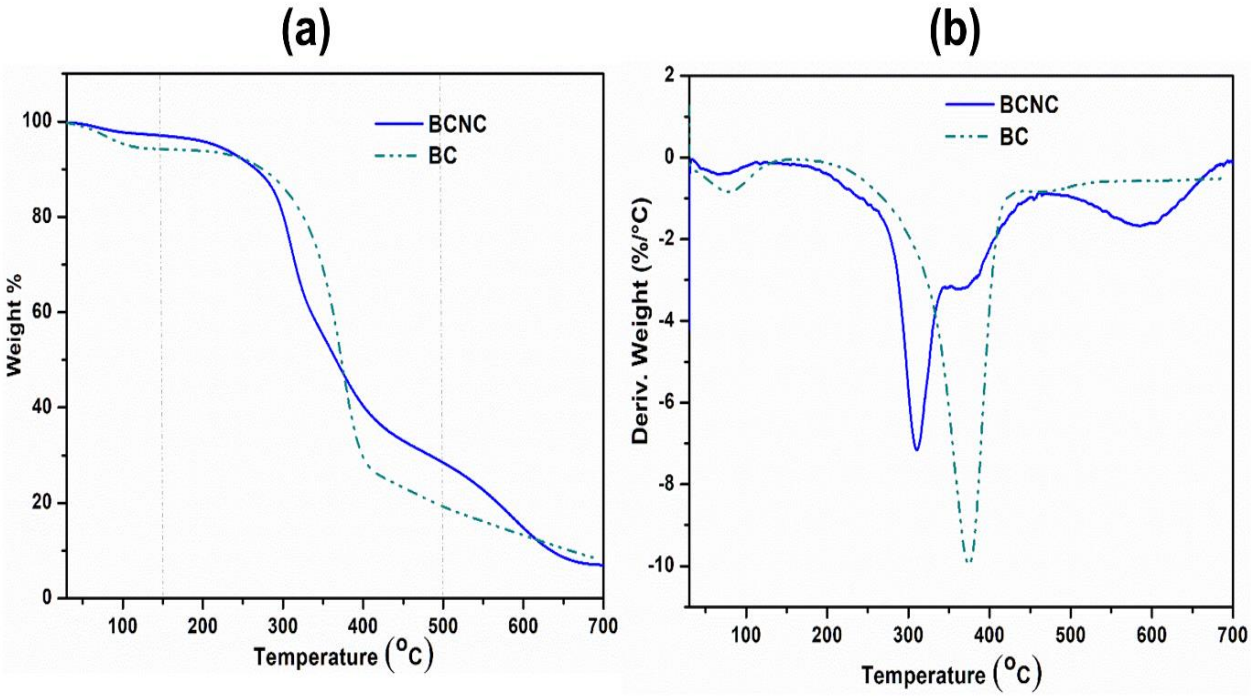

Figure 3.3. (a)TGA, and (b)DTG curve of pure BC, and BCNCs obtained after acid hydrolysis.

3.3. CONCLUSIONS

The synthesis of highly crystalline and ultrafine, pure bacterial cellulose was successful, as established by FESEM, XRD and FT-IR spectroscopy results. This highly pure BC can be effectively converted to BCNCs through acid hydrolysis. BCNCs fabricated from BC exhibited a higher crystallinity with a needle-like morphology. The fabricated BC and BCNCs are hydrophilic in nature and they can be easily blended with other bioactive molecules or polymer matrices through hydrogen bonding, due to their interfacial interaction. Based on these captivating properties, BC and BCNCs are considered as the base materials of this thesis and discussed elaborately in the subsequent chapters with their targeted applications.

Chapter 4

Studies on Fabrication of Bacterial Cellulose based Polycaprolactone Composite Scaffolds for Wound Dressing Applications

Motivation

Bacterial cellulose is an excellent biomaterial with exceptional properties to be used in biomedical applications however they lack in antimicrobial properties. On the other hand, polycaprolactone is a biodegradable polymer also used in biomedical applications, due to its flexibility, biocompatibility and chemical stability. However, BC is highly hydrophilic in nature while PCL is hydrophobic, thus the blending of these two materials is a challenging task. To overcome this problem, we have developed a sustainable approach to modify the BC surface by a simple PCL impregnation method which resulted in flexible BCP membranes. The surface-functionalization of the developed membranes through dip-coating improved the structural, antimicrobial, biocompatibility and cell adhesion properties of BCP, making it suitable for wound dressing applications.

The work in this chapter is published as:

- ***M. Das**, O. Zandraa, C. Mudenur, N. Saha, P. Sáha, B. Mandal, V. Katiyar, (2022). "Composite Scaffolds Based on Bacterial Cellulose for Wound Dressing Application", ACS Applied Bio Materials, 5, 8, 3722–3733, https://doi.org/10.1021/acsabm.2c00226.*

Abstract

This chapter deals with the fabrication of a wound dressing material using a biocompatible polymer, bacterial cellulose (BC), which is quite relevant for medical applications with exceptional properties in terms of biocompatibility, high purity, crystallinity (~88%), and high water holding capacity. However, the lack of antibacterial activity slightly restricts its application as a wound dressing material. So, in this study polycaprolactone (PCL) was first impregnated into the BC matrix to fabricate flexible bacterial cellulose-based PCL membranes (BCP), which was further functionalized with antibiotics gentamicin (GEN) and streptomycin (SM) separately, to form wound dressing composite scaffolds to aid infectious wound healing. In-vitro studies of the BC and BCP scaffolds against baby hamster kidney (BHK-21) cells revealed their cytocompatible nature, also the wettability studies indicated the hydrophilicity of the developed scaffolds, qualifying the main criterion in wound dressing applications. The prepared scaffolds also exhibited excellent antimicrobial activity against *Escherichia coli* and *Staphylococcus aureus* and the release profiles initially indicated a burst release (6 h) followed by controlled release of GEN (**~42%)** and SM (**~58%)** from the prepared scaffolds within 48 h. Hence, these results interpret that the prepared drug-functionalized cellulosic scaffolds have a great potential as a wound dressing material in biomedical applications.

Graphical Abstract

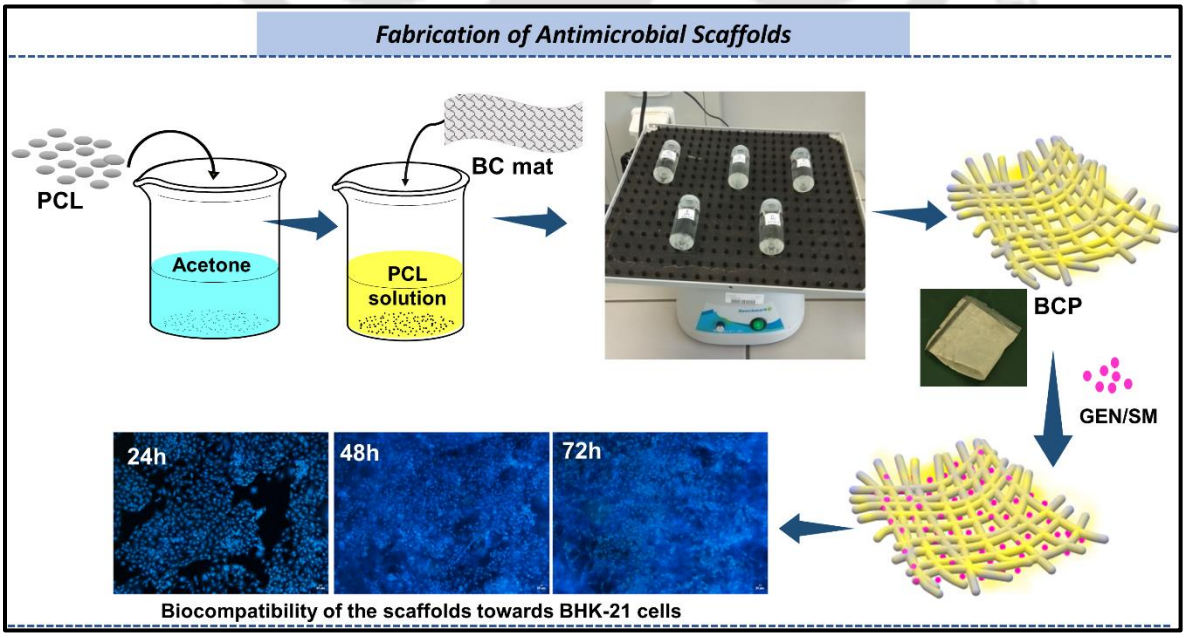

4.1 INTRODUCTION

Skin, the human body's largest organ plays a substantial role in protecting the body from pathological organisms by acting as a natural barrier, maintaining the body temperature, homeostatis and dehydration [91]. However, these characteristics are disturbed whenever there is an injury or wound, leading to the invasion of bacteria through the site of injury. Thus, to repair these tissues, dressing materials are prepared. A proper wound dressing material should impart a moist environment, allow easy transport of gases, inhibit bacterial infections, should be nontoxic, nonallergenic, and promote heat insulation [92]. In the recent studies, bacterial cellulose (BC) has grabbed attention in the biomedical field due to its highly pure, biocompatible, nontoxic and highly hydrophilic nature. These captivating properties make it a suitable contender in biomedical applications such as artificial skin, scaffolds, wound dressing materials, dental implants, and also in food packaging and paper industry [6]. BC is generally produced from *Acetobacter xylinum*, which is the most efficient BC producer as it can absorb several types of sugars leading to higher yields of cellulose at pH ~3-7 and 25-30˚C temperature in liquid medium. BC is made up of ultrafine fiber network derived from well-arranged three dimensional (3D) nanofibers, which results in the formation of hydrogel sheets with higher surface area and porosity [1,2]. As compared to plant-based cellulose, BC fibrils are very much smaller in diameter as well as length (about 100 times) with tailorable properties based on the composition of culture media, carbon source, and also on the producing organism used. BC also has certain promising properties such as high crystallinity (84-90%), high water holding capacity (WHC) of ~106 g water/ g sample, ability to reform into 3D structure during synthesis and high water release rate (WRR), of which WRR and WHC are the most essential attributes, directly connected to the biomedical applications of BC as a dressing material [1,3–5]. Although, BC has quite a few unique properties, it also has some limitation such as lack in antibacterial activity, and optical transparency, which limits its use as an effective wound dressing material for highly infectious wounds [93]. To meet such application standards, BC is functionalized with various organic or inorganic material such as polymers, metal or metal oxides, solid materials, and nanomaterials possessing antimicrobial property via impregnation, either by in situ or ex situ and several other techniques. Recently, nanofibrous polymer composites (NFPC) has acquired attention in biomedical applications due to their superior properties, such as larger surface-to-volume ratio and flexibility. Examples of

materials used along with BC in NFPC preparation for wound dressing applications are silver nanoparticles, graphene oxide, chitosan, and aloe vera [5,92–96].

Due to its biocompatibility, controlled degradability and miscibility with other polymers, polycaprolactone (PCL) has a wide range of application in controlled drug-delivery and tissue engineering as a scaffold material and as a solid plasticizer in soft compostable packaging [97,98]. The production route of PCL is comparatively economical as compared to counterpart aliphatic polyesters, hence its utilization in the biomedical devices development is highly demanding. PCL is a linear, semi-crystalline polymer possessing rubbery character at room temperature and comprises of hexanoate repeating units, obtained by ring-opening polymerization (ROP) of ε-caprolactone. It is permeable to low molecular compounds at body temperature, and hence it's an excellent entrant for controlled drug release and widely practiced as a wound dressing material [25,99,100].

Gentamicin (GEN) is a highly hydrophilic aminoglycoside antibiotic and is often used against a wide range of bacterial infections, such as *P. aeruginosa*, *E. coli*, and *E. aerogenes*, and is also used in the treatment of bone infections caused by *S. aureus* and many others [101–103]. Several studies have reported the use of GEN in controlled drug delivery, as for example Rouabhia et al. [37] prepared gentamicin activated bacterial cellulose dressings containing 3-aminopropyltriethoxysilane (APTES) as a coupling agent for drug delivery and wound healing applications. Another widely researched aminoglycoside antibiotic is Streptomycin (SM), which is also antibacterial and is mainly used in the treatment of serious infections caused by tuberculosis (*Mycobacterium tuberculosis*), plague (*Yersinia pestis*), and avium (*Mycobacterium avium*), and is considered as one of the most effective and safe medicines for human health system as documented by World Health Organization (WHO) [104–106].

Till date, BC have been utilized as an antimicrobial material, however, the utilization of GEN and SM functionalized BC is to be further explored. It is well known that BC has abundant hydroxy groups on its surface, which enables its easy functionalization and interaction with other materials ultimately resulting in beneficial applications. Thus, considering the unique properties of BC and PCL together, in terms of biocompatibility and biodegradability, herein we propose the fabrication of BC based composite scaffolds by the impregnation of PCL into the BC network structure. The

developed scaffolds showed good biocompatibility towards baby hamster kidney fibroblast cells (BHK-21). The composite scaffolds were then functionalized by the incorporation of antibiotics, GEN and SM separately to form antimicrobial wound dressing material and the resultant scaffolds showed a wide spectrum of antibacterial inhibition against *E. coli* and *S. aureus*.

4.2 RESULTS AND DISCUSSIONS

4.2.1. Fabrication of BCP membranes and their characterization.

This study discusses the property enhancement of bacterial cellulose membranes with the impregnation of PCL into its matrix, by incubating the cellulose films in PCL solution. The presence of ester bond in the structure of PCL is expected to react with the abundant hydroxy groups present on the BC surface resulting in the formation of flexible BCP membranes. These membranes were then functionalized with GEN and SM to produce antimicrobial scaffolds. As both the antibiotics used are aminoglycosides, the amino groups present in their structure react with the hydroxy groups present in the BCP structure (Scheme 4.1).

The surface morphology of BC and BCP membranes are shown in Figure 4.1 (a,b). The FESEM and AFM images suggested well-defined fibrillar orientation of BC with long and smooth fibers of diameter in the range of 35-200 nm. The high surface area of the BC matrix allowed the successful impregnation of PCL into its interpenetrating porous structure in the BCP membranes, as observed in the figures. A smooth and dense morphology is observed for both BCP (2%)_48h and BCP (2%)_72h membranes, where the polymer layers are present on the surface as well as inside the pores of the BC matrix indicating a good fiber-matrix interaction. The average thickness of each BC bundle was calculated to be ~121 nm in Figure 4.1(b), whereas in case of BCP, the BC bundles were almost covered and filled with PCL, so a few small bundles of average thickness ~54nm appeared on the surface. The root mean square surface roughness value of BC and BCP membranes was estimated to be 3.46 nm and 5.61 nm, and the height profiles of BC and BCP suggested a maximum height of ±37 nm and ±70 nm, respectively shown in Figure 4.2. Also, it is noteworthy that even after 72h incubation of the BC mat in PCL solution, some pores are still visible on the surface of BCP membrane which could further facilitate the cell colonization in the membranes when used as a drug carrier. The surface morphology of the drug loaded BC membranes, BC-GEN, and BC-SM shown in Figure 4.3, further indicated the intact microstructure

of BC with the presence of agglomerated drug particles spread over the surface and inside the pores [107].

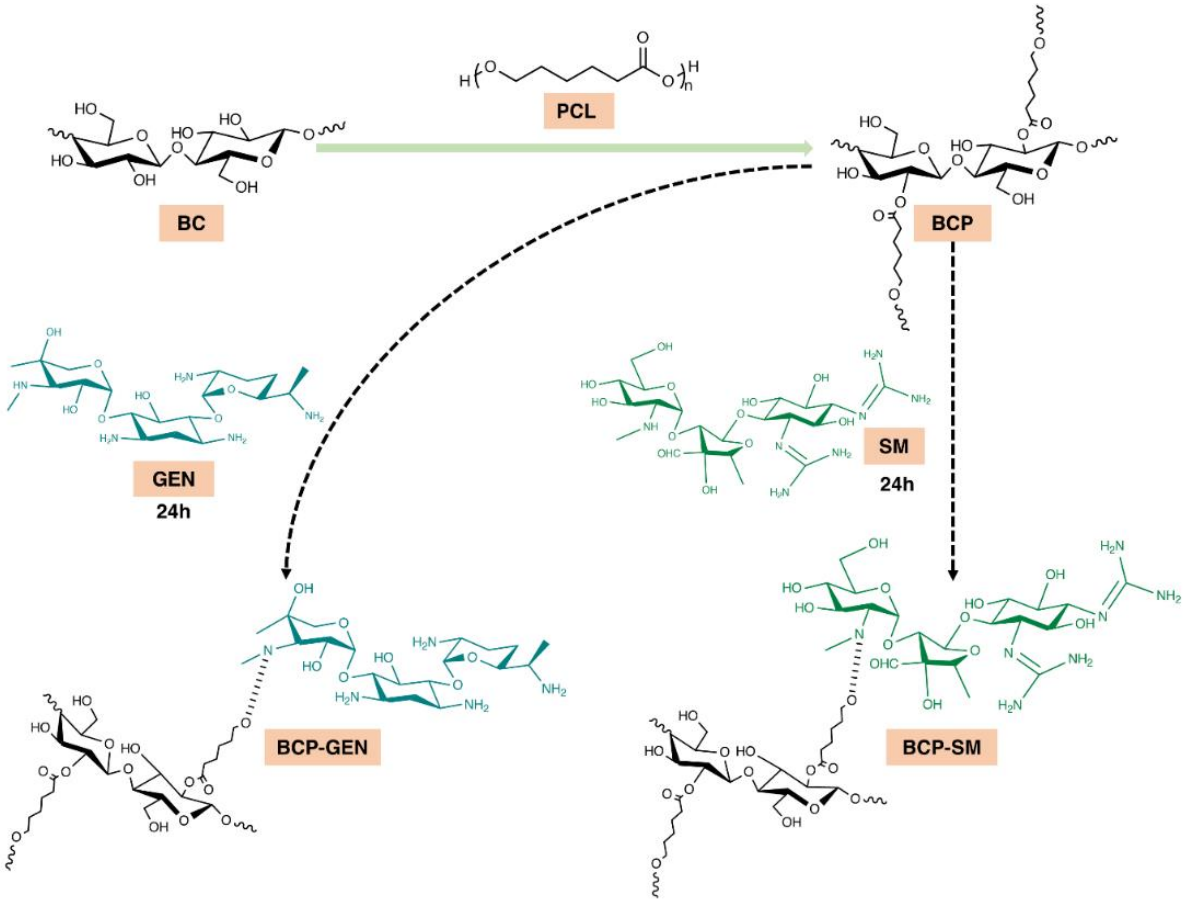

Scheme 4.1. Reaction mechanism showing impregnation of PCL into the BC membrane, followed by surface functionalization with gentamicin (GEN) and streptomycin (SM).

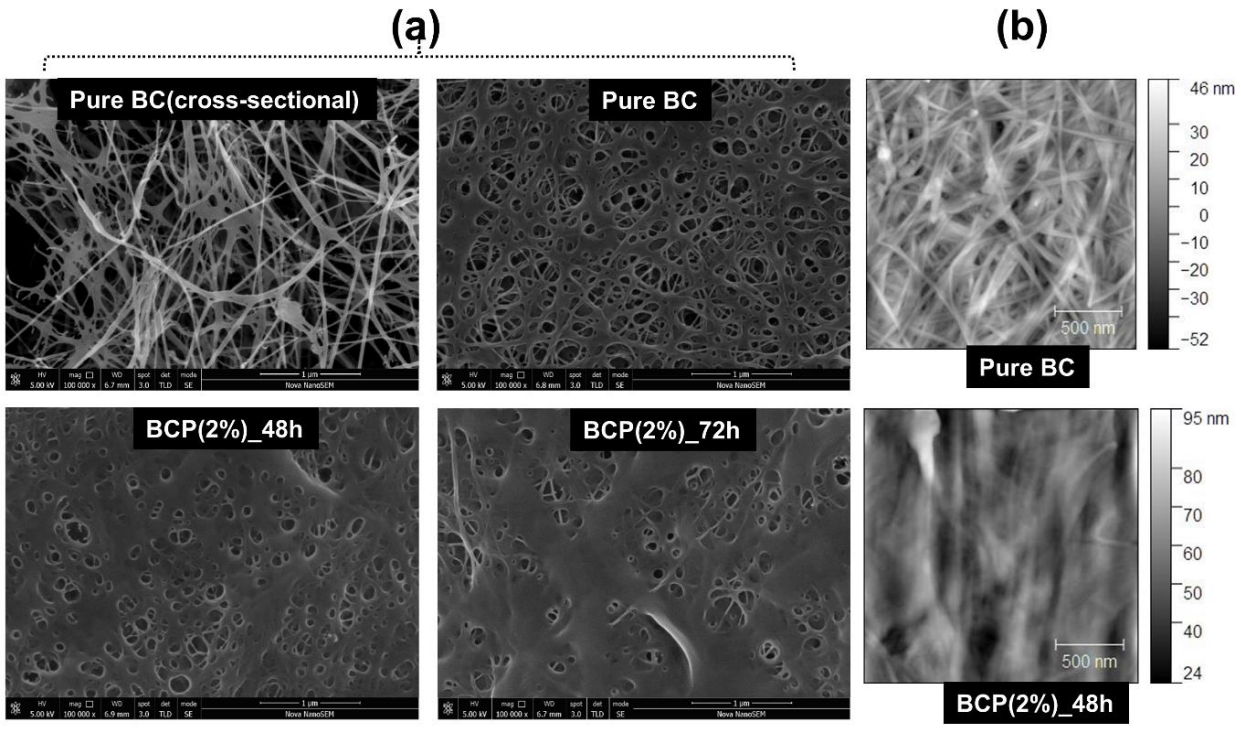

Figure 4.1. (a) FESEM micrographs of pure BC (cross-sectional and surface view), BCP (2%)_48h and BCP (2%)_72h. (b) AFM image of pure BC and BCP (2%)_48h.

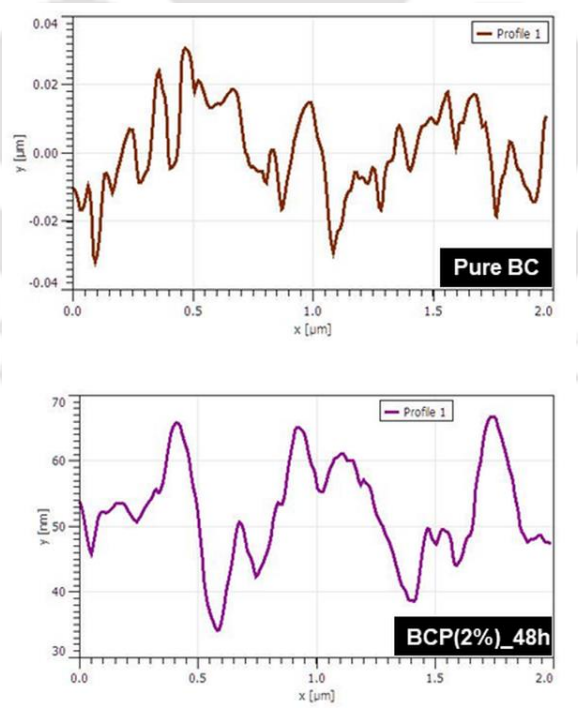

Figure 4.2. AFM-height profile of BC and BCP membranes.

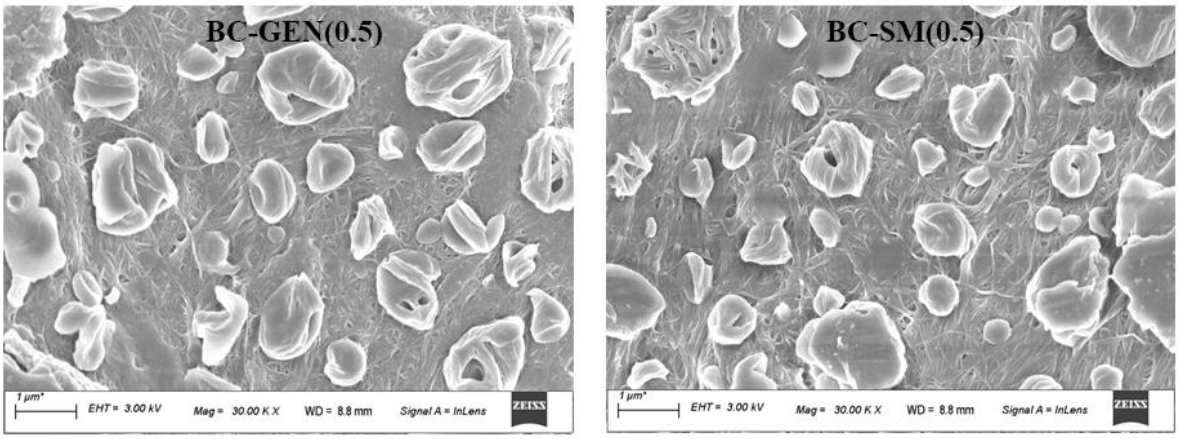

Figure 4.3. FESEM micrographs of BC-GEN(0.5) and BC-SM(0.5).

The chemical and physical attributes of the synthesized BC and its composites (BCP) were studied using FT-IR as shown in Figure 4.4 (a). Pure BC exhibited a strong O-H stretching around 3349 cm^{-1} conforming the intramolecular H-bond, C-H vibration stretching at 2895 cm^{-1} and the C-O-C stretching vibration is observed around an intense peak at 1054 cm^{-1}[31,108]. The ~75% crystallinity of PCL could be justified by the presence of C=C and C=O stretching vibration bands at 1291 cm^{-1}. Similarly, a strong C=O stretching band is located at 1720 cm^{-1}, which also refers to the high crystallinity% of PCL. The characteristic symmetric and asymmetric CH_2 stretching was found around 2858 cm^{-1}, and 2945 cm^{-1}, respectively [109]. The BCP membranes showed the presence of the characteristic cellulose and PCL peaks around 3400 cm^{-1} and 2895 cm^{-1} related to BC and 2945, 2858, 1720 cm^{-1} from PCL [31]. Thus, the interaction between BC and PCL is confirmed, which is also consistent with the change in surface morphology of the prepared composite membranes as shown by SEM images (Figure 4.1.a). The crystallinity of the prepared membranes was studied using XRD analysis as shown in Figure 4.4(b). Pure BC exhibited a highly crystalline structure, with strong polymeric chain network and slightly lower flexibility [110]. Broad diffraction peaks were observed at 16-17° and 27°, which indicates the formation of cellulose type I for the pure BC membrane. PCL also exhibited its crystallinity with two diffraction peaks, at around 25 and 27.6 degrees [79,111].

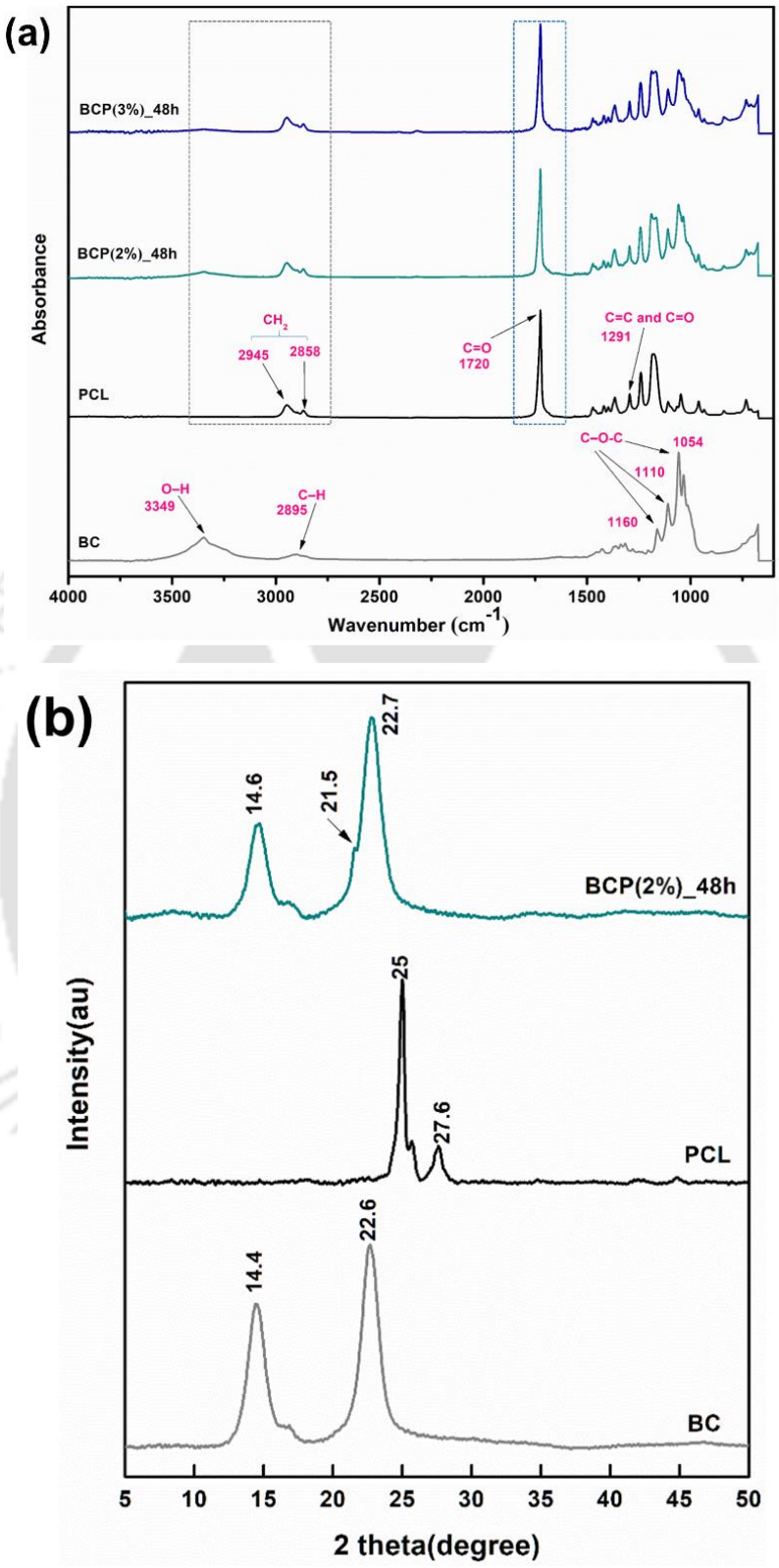

Figure 4.4. (a)FTIR spectra and (b) XRD plot of BC, PCL and BCP membranes.

The presence of cellulose type I peaks in the composite membrane suggests the BC structure was not disturbed in the composite preparation. The sharp intensity of the peaks indicates highly crystalline nature, however there is a slight difference in the relative intensity of the peaks, which could be contributed as the change in orientation of the cellulose fibers in interaction with the polymer. Pure BC and PCL revealed a highly crystalline nature (~88% and ~75% crystallinity, respectively). The addition of PCL into the BC network resulted in composites with nearly 84-86% crystallinity exhibiting the same crystalline phase as BC and PCL. The calculation of percentage crystallinity for each membrane is shown in Table 4.1.

Table 4.1. Calculation of percentage crystallinity of the BC and BCP membranes.

Sample Code	Area of individual peaks	Area of crystalline peaks	Area of all peaks	% Crystallinity
BCP(2%)_48h	3958.51	14485.13	16699.74	86.74
	579.99			
	9946.64			
PCL	548.97	830.59	1104.74	75.18
	106.36			
	175.26			
BC	8533.76	24281.24	27313.89	88.90
	560.32			
	15187.17			

From the thermal studies (TGA-DTG) as shown in Figures 4.5 (a,b), it was observed that the thermal stability of the composites increased significantly with the incorporation of PCL into the BC matrix. Clearly, it was evident that the inherent higher thermal stability of PCL enhanced the thermal property of the final composite membranes.

An initial smaller weight loss was observed for BC (~3%) below 150 °C caused by the evaporation of water from its polysaccharide structure which is not that prominent in the PCL and BCP membranes [112]. The most significant degradation leading to weight and structural change occurred in the 250-450 $^{\circ}$C range for all the samples, which is attributable to the degradation of crystalline part and depolymerization of the glyosidic units. The final stage above 500 $^{\circ}$C could be associated with the carbonaceous residue breakdown leading to char oxidation [113]. As observed from Figure 5, PCL exhibited a maximum weight loss temperature (T_{max}) at ~441°C while native BC has a T_{max} ~378 $^{\circ}$C. An increase in onset degradation temperature (~ 43 to 54 $^{\circ}$C) for the composite samples as compared to BC could be projected as the presence of PCL in its structure.

The lower thermal stability of pure BC compared to pure PCL is due to the chemical composition of BC which comprises of hydroxy end groups, resulting in the restriction of the chain mobility. All the samples showed one-step degradation and the initial and maximum degradation temperature along with weight residue of all the samples are compiled in Table 4.2. The ash content of BC and BCP samples were ~4% whereas PCL almost completely degraded at 600 °C.

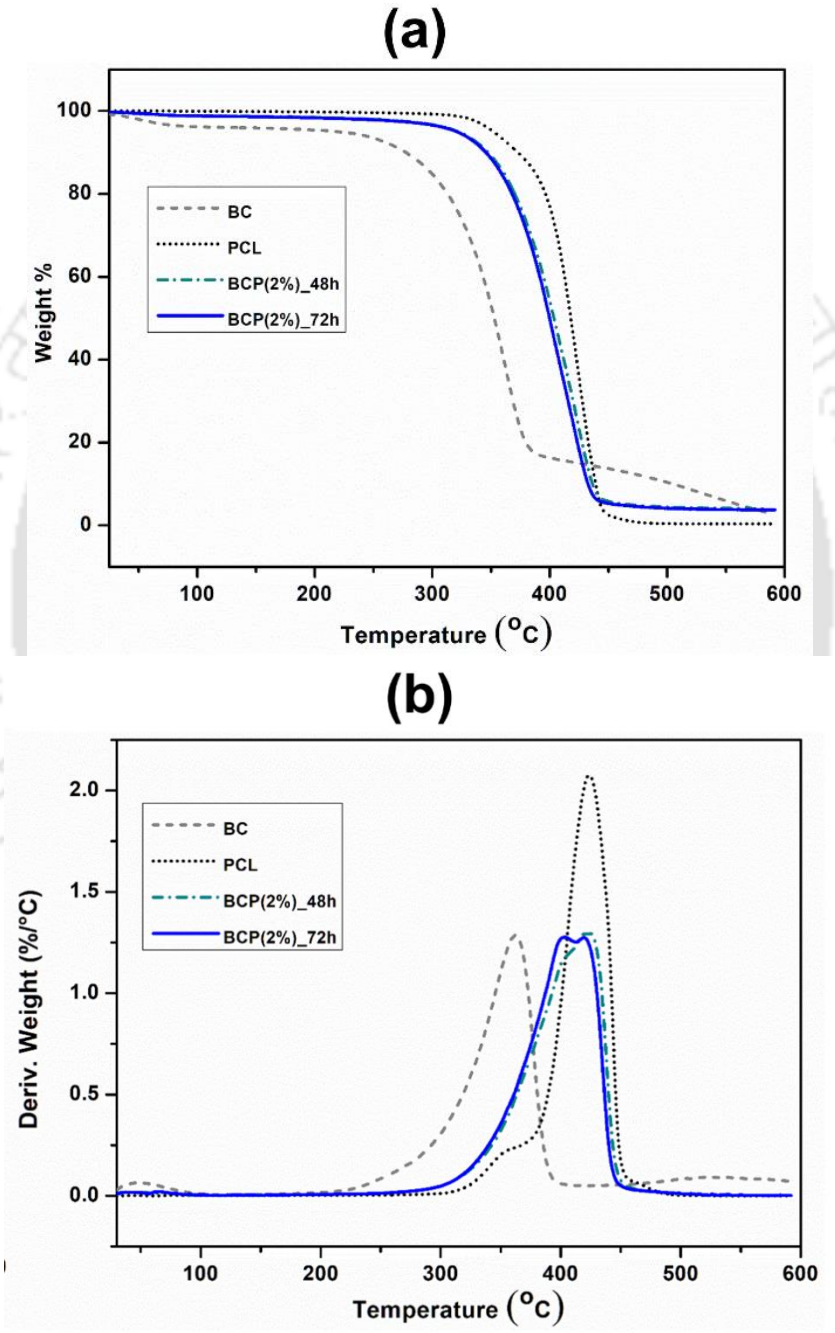

Figure 4.5. (a)TGA and (b)DTG thermographs of the fabricated BC, PCL and BCP membranes.

Table 4.2. Thermal analysis of the BC, PCL and BCP samples.

Sample	T_o (°C)	T_{max} (°C)	Weight residue at 600°C (%)
BC	318.28	378.36	3.38
PCL	394.76	441.82	0.38
BCP(3%)_48h	368.98	438.84	4.29
BCP(3%)_72h	361.14	435.04	4.00

The thermal transition of BC and the prepared composites was studied using DSC as shown in Figure 4.6, where from 27 to 124 °C, an endothermic event was observed indicating the dehydration of surface water mostly around 70 °C for both BC and BCP membrane. The endothermic events around 348 to 372 °C for both BC and BCP could be attributed to the melting of crystalline regions of respective polymers. This decomposition is also confirmed by the single-step degradation in TGA analysis (Figure 4.5), which overall concludes that the melting phenomenon is followed by degradation for all the samples. The higher thermal stability could also be connected with the highly crystalline and oriented structure of the cellulose matrix and its composites [114,115].

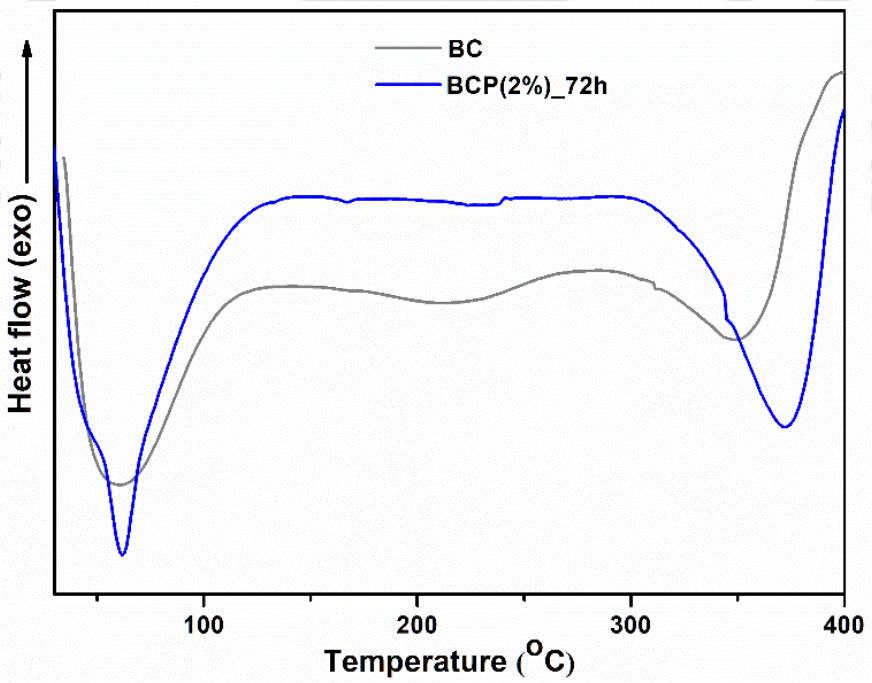

Figure 4.6. DSC scans of BC and BCP(2%)_72h.

Contact angle measurement was carried out to understand the water absorption and hydrophilicity of the developed BC and BCP membranes shown in Figures 4.7 (a,b). The high surface energy and the presence of abundant –OH group within and in between the adjacent cellulose structure create an extensive hydrogen bonding (-OH….O-), thereby making BC a highly hydrophilic material. So, whenever a water droplet falls on its surface, BC absorb it immediately leading to a lower contact angle (~36° in 60s) as shown in Figure 4.7(b). However, as most of the –OH groups present in the surface becomes already occupied, the water contact angle tends to remain constant after a certain time (60s). The absorption of water droplet onto the surface is also dependent on the porosity of the sample [116]. It was observed that the contact angle of BCP samples increased from 74° to 99° (in 60s) with increase in incubation period of the BC membrane in PCL solution, i.e., from 48 h to 72 h. As a result, the BCP membranes became resistant to water because of the impregnation of hydrophobic PCL in its surface and network. However, the motive behind the incorporation of PCL into the BC membrane is to produce a stretchable wound dressing material, so BCP membranes incubated for 48h were used for the antimicrobial and cytotoxicity tests as they have contact angle of ~74° which is satisfactory for wound dressing applications [117]. The images of the water droplets on the BC and BCP membranes recorded at 60s time period are shown in Figure 4.7(b).

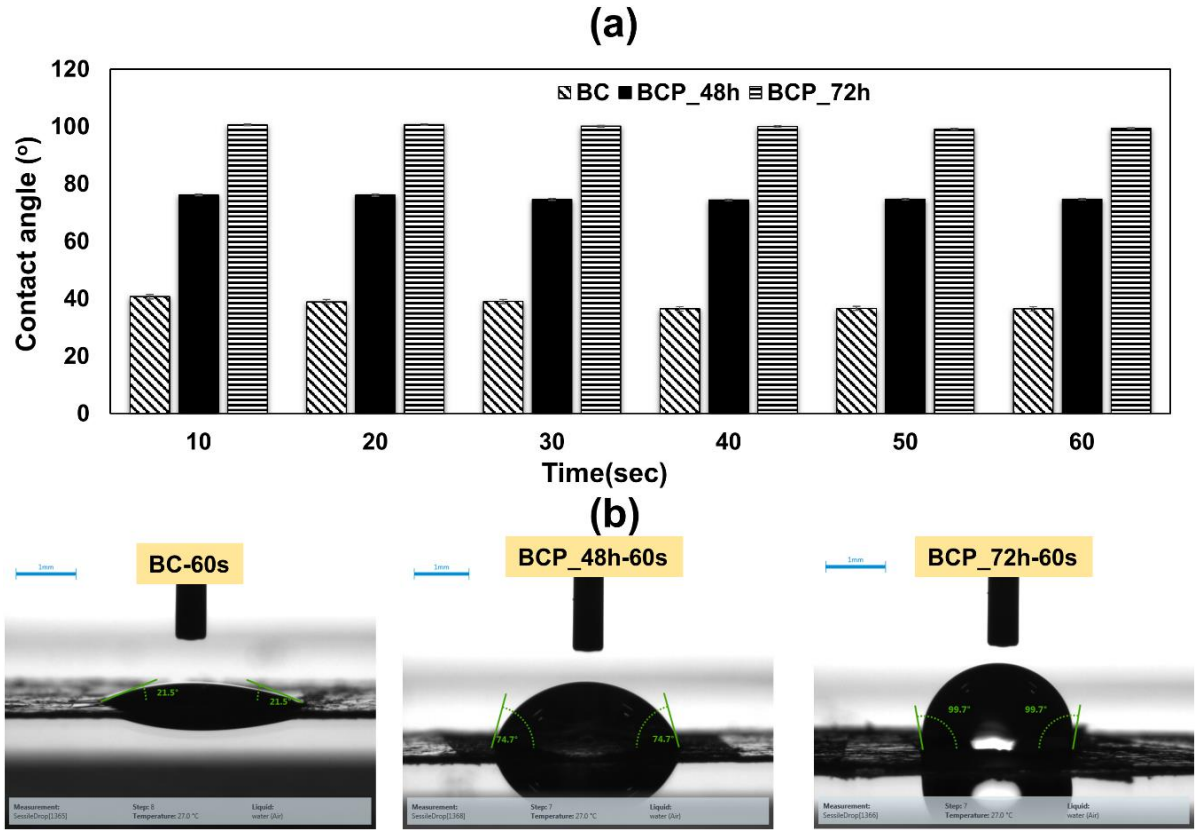

Figure 4.7. (a)Contact angle measurement of BC, BCP_48h and BCP_72h membranes over a time period of 10 to 60sec. (b)Images of water contact angles of BC, BCP_48h and BCP_72h recorded at 60 sec.

4.2.2. Antibacterial activity of drug-loaded films and their elemental composition

The bacterial growth of the pure and drug-loaded films was evaluated with the inoculation of the sample discs in gram-negative and gram-positive bacteria, *E. coli* and *S. aureus*. The hydrophilicity associated with BC is an added advantage to be used as a drug carrier system for wound healing applications, as it provides a moist environment and promotes the healing process by enhancing angiogenesis and collagen synthesis, and inhibits bacterial infections [118]. However, pure BC lacks antibacterial characteristics which is an important aspect in wound dressing applications, with this motive antibiotic-loaded BC and BCP films are being developed in this work. After 24 h of incubation, wider bacterial growth inhibition was evident for the gentamicin and streptomycin loaded discs (BC-GEN, BCP- GEN, BC-SM and BCP-SM) against *S. aureus* (Figure 4.9a),

however in *E. coli* only gentamicin loaded discs exhibited inhibition zone as the bacteria provides resistance to streptomycin due to its genetic encoding [119]. Pure BC and BCP clearly does not influence the bacterial growth, with no inhibition zone observed in Figure 4.9(a). The quantitative evaluation of zone of inhibition exhibited by each sample is shown in Figure 4.9(b). Both the tested drugs (GEN and SM) showed a concentration-dependent killing activity, which is specific to the drug carrier systems. BC showed a better performance as a drug carrier at a lower dose of ~0.2 mg/mL, whereas the BCP samples showed better inhibition at slightly higher doses of ~0.5 mg/mL, which is due to the easy penetration of drug into the voids of porous BC matrix as observed from FESEM images (Figure 4.1a). The morphology of the drug loaded BC membranes shown in Figure 4.3 indicates the presence of agglomerated drug particles on the BC surface. Gentamicin control also exhibited an inhibition of ~28 mm and ~33 mm against *S. aureus* and *E. coli*, respectively as shown in Figure 4.8. The impregnation of PCL into the BC matrix is expected to impart flexibility in the prepared drug-loaded films, which when used as a wound dressing material will possess the ability to adapt to any shape of the wound [92,94]. Also, the biocompatible nature of PCL will help in controlling the drug release for treating the local infections caused due to severe injuries. Generally, infection at the site of injuries is due to the presence of microorganisms and the effectiveness of the gentamicin and streptomycin loaded membranes showed promising results by inhibiting the cell multiplication with the release of the loaded drugs.

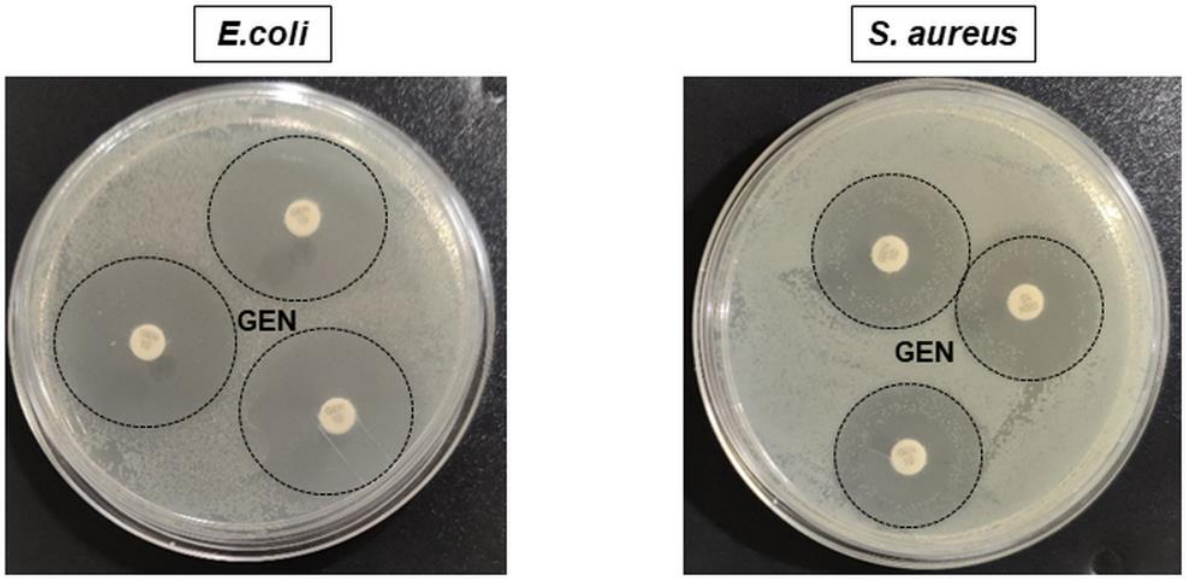

Figure 4.8. Photographs of gentamicin control showing antibacterial activity against *E. coli* and *S. aureus*.

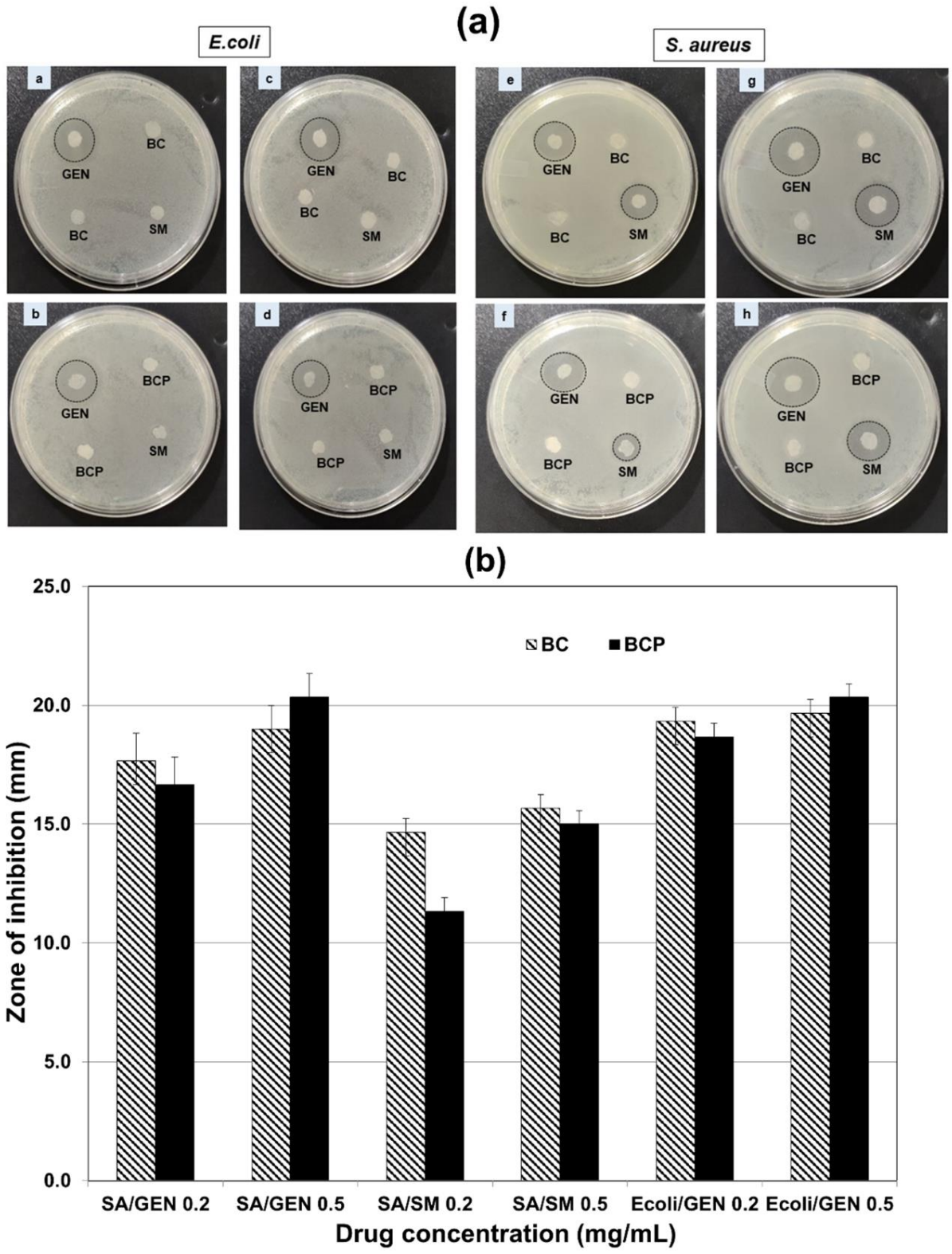

Figure 4.9. (a) Photographs of gentamicin and streptomycin loaded BC and BCP discs showing antibacterial activity against bacteria, *E. coli* and *S. aureus*. (b) Zone of inhibition in millimetres of the drug loaded films against both the bacteria.

The elemental composition of BC and drug-loaded BC membranes, BC-GEN and BC-SM was studied using EDX and represented in Figure 4.10(a). Pure BC membrane comprises of carbon (C) and oxygen (O) level of around 51% and 48%, respectively in terms of weight percentage. However, the surface modification of BC with gentamicin sulphate and streptomycin sulphate resulted in an increase in nitrogen (N) level thereby increasing the overall C+N along with the presence of sulfur (S), confirming the functionalization of BC membrane with GEN and SM (Figure 4.10a) [37]. The presence of N could be justified due to the presence of amine groups in both the aminoglycosidic antibiotics [120]. As the drug solutions prepared were of very low concentration (0.2 mg/mL and 0.5 mg/mL), the elemental composition did not reveal a higher percentage of sulfur. However, even that amount of drug loading was sufficient to inhibit the bacterial growth as shown in the antimicrobial assay (Figure 4.9a). The structural and chemical composition of the fabricated drug-loaded scaffolds was studied by FT-IR spectroscopy and shown in Figures 4.10(b,c). The characteristic O-H and C-O-C stretching vibration bands present in BC are observed in the gentamicin and streptomycin loaded BC membranes (BG and BS, respectively) as shown in Figure 4.10(b). Similarly, in Figure 4.10(c), characteristic carbonyl and symmetric-asymmetric CH_2 stretching related to BCP are predominantly observed in both gentamicin and streptomycin loaded BCP membranes (BCG and BCS, respectively). The typical absorption bands corresponding to amide I, II and III linkages are respectively observed at 1638, 1531 and 1261 cm^{-1} in the BG sample and 1646, 1544 and 1235 cm^{-1} in the BS sample, in Figure 4.10(b) [121,122]. A slight shift and overlapping of the peaks have appeared due to inter and intra-molecular hydrogen bonding, confirming the efficient encapsulation of the BCP membranes with gentamicin and streptomycin.

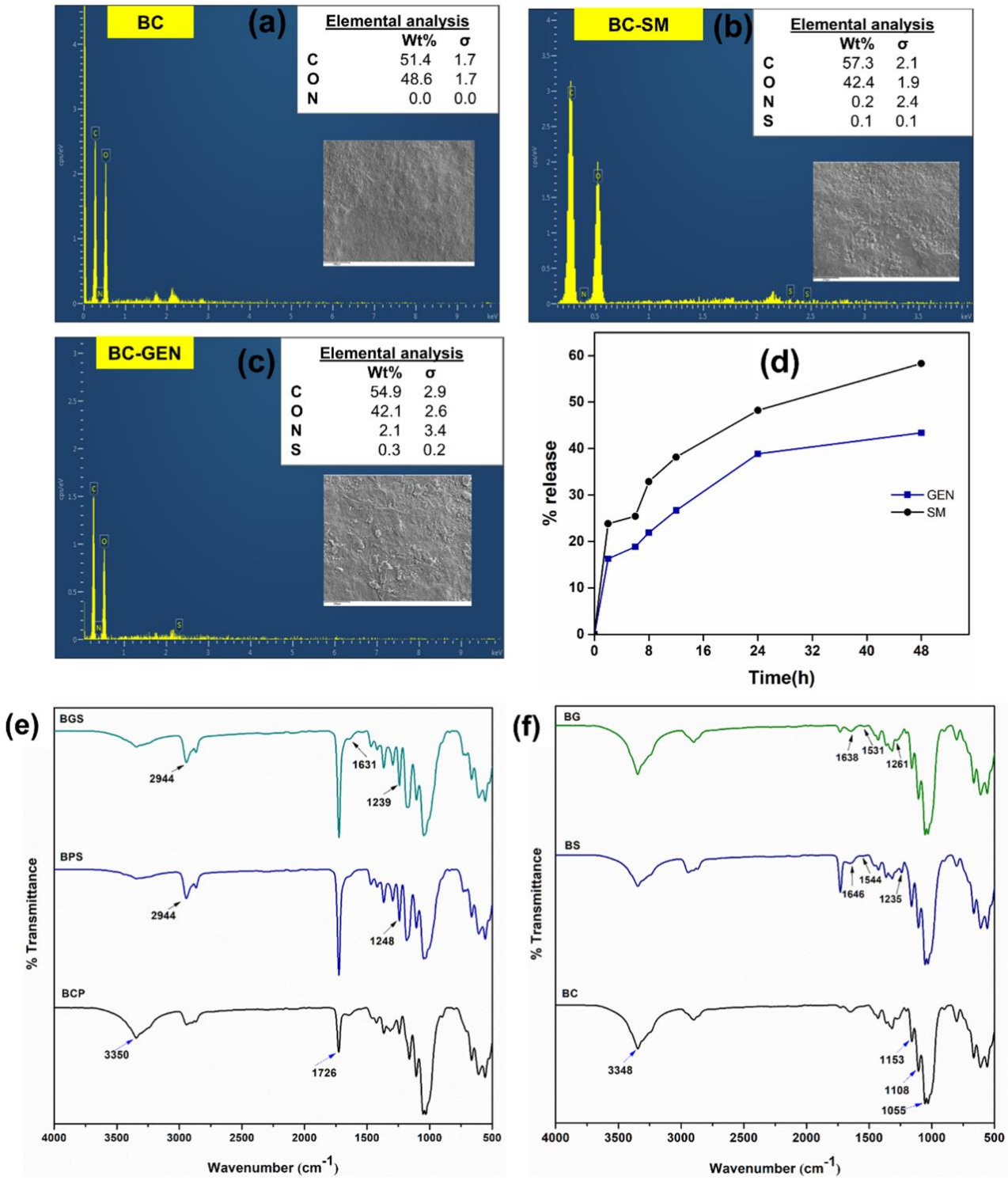

Figure 4.10. EDX patterns and elemental composition of (a) BC, and drug loaded BC membranes, (b) BC-GEN and (c) BC-SM. (d)Release behaviour from the GEN and SM-loaded BCP films at pH 7.4, (e) FTIR spectra of BC, BS and BG, and (f) FTIR spectra of BCP, BPS and BPG.

4.2.3. In vitro cytotoxicity of the fabricated scaffolds.

The prepared BC and BCP membranes were subjected to cytotoxicity test against baby hamster kidney cells to understand their biocompatible behavior. Figure 4.11(a) illustrates the cell attachment ability of the pure BC and developed BCP membranes. Pure BC has no cytotoxicity against BHK-21 cells and exhibited an excellent cell viability (~103%). This could be due to the presence of abundant hydroxy groups in the BC structure, which benefitted the cell growth and adhesion [123]. Generally, BC is non-cytotoxic in nature, however the impregnation of usually biocompatible PCL into the BC matrix was carried out in this work to understand the overall biocompatibility of the prepared composite membrane (BCP) for biomedical application. As shown in Figure 4.11(a), BCP membrane extract also showed no toxicity against the BHK-21 cells and exhibited 94% viability after 72 h. To use these membranes for long-term application, the cells were treated with the BC and BCP extracts for 24 h, 48 h and 72 h and it was observed that the extracts were non-toxic to the cells even after the long incubation period. Also, from Figure 4.11(b), it was clearly observed that the DAPI stained nuclei of the cells showed cell adhesion and proliferation on the BC and BCP surfaces, indicating their intact nature. Therefore, these results indicate that the fabricated BCP membranes exhibited biocompatibility towards baby hamster kidney cells and thus could be utilized as wound dressing material for infectious wounds.

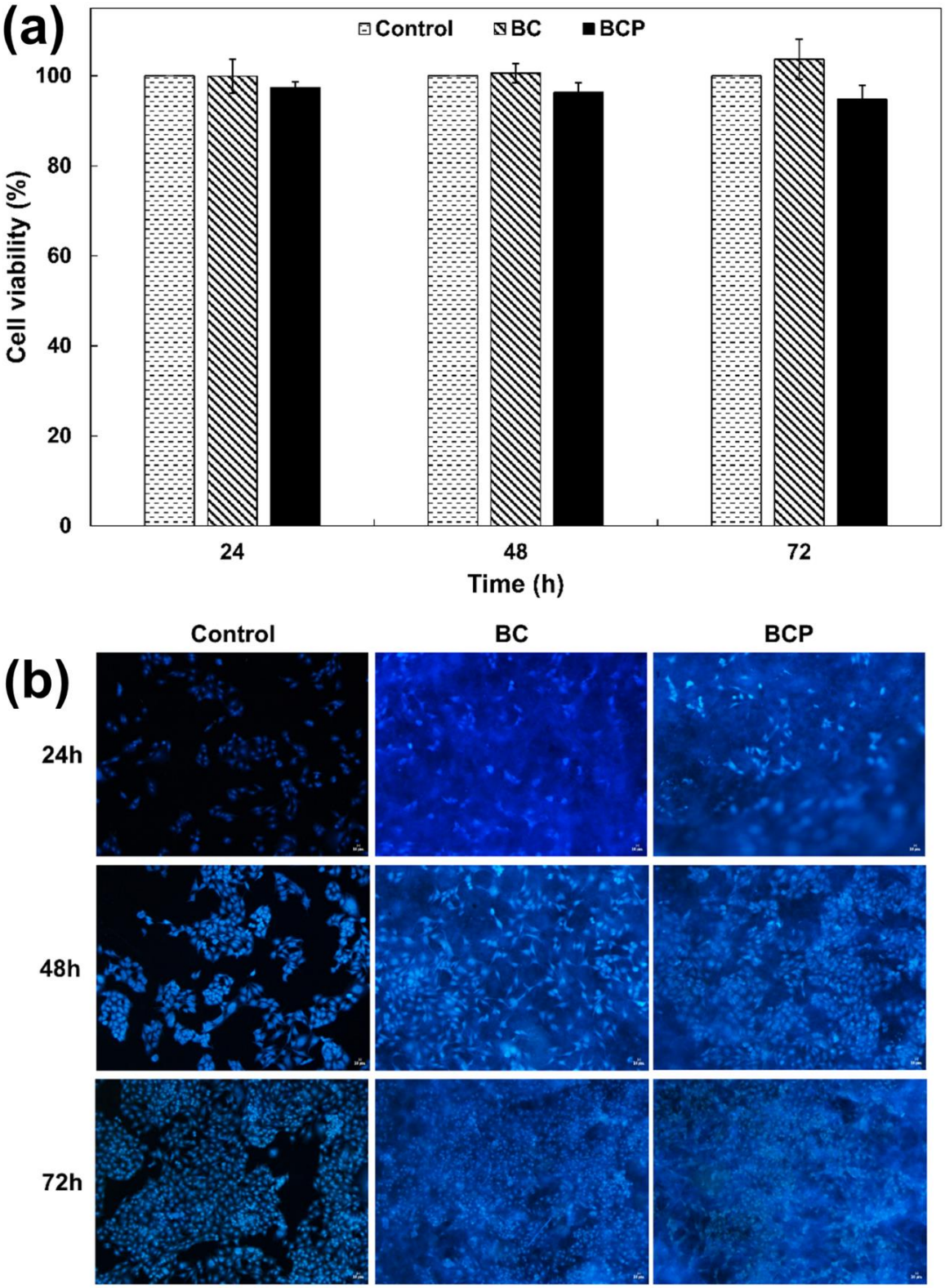

Figure 4.11. (a) Cell viability(%) of baby hamster kidney cells in contact with BC and BCP membranes incubated for 24 h, 48 h and 72 h. (b) BHK-21 cell proliferation on the BC and BCP surfaces, after 24 h, 48 h and 72 h of incubation, stained with DAPI.

4.2.4. In vitro drug release.

As observed from Figure 4.10(d) , both streptomycin and gentamicin exhibited burst release effect at around 6 h with the release of 23% of SM and 16% of GEN respectively into the phopshate buffered saline system. Rest of the streptomycin and gentamicin were slowly diffused to the system and ~58% and ~42% of the drugs were released into the system after 48h. The drug release profiles indicate a uniformly distributed BCP scaffold which could be utilized as a wound dressing material.

4.3 CONCLUSIONS

The current research elucidates the BC and BCP based antimicrobial scaffolds produced by their functionalization with GEN and SM antibiotics. PCL has been used as a biomaterial in wound healing and other biomedical applications, due to its flexibility, biocompatibility and chemical stability. So, the BC membranes were first impregnated with PCL and the FTIR, SEM, and TGA analyses confirmed the interaction between BC and PCL resulting in the formation of flexible cellulose membranes. These membranes were then functionalized with the antibiotics, GEN and SM and the resultant membranes exhibited excellent antimicrobial properties against model bacteria, *E. coli* and *S. aureus*. The fabricated BC and BCP composite membranes were biocompatible and nontoxic to BHK-21 cells even after 72 h, allowing cell proliferation. Thus, these results suggest that the GEN and SM functionalized BC and BCP membranes are ready to be utilized as an effective dressing material in future.

Chapter 5

Studies on Surface Functionalization of Bacterial Cellulose Nanocrystals and their Catalytic Applications in Value-Added Chemical Processes

Motivation

Cellulose based catalytic systems are advantageous to use because of their low toxic and biocompatible nature, and thus have expanded application in food and pharmaceutical industry. These cellulose nanocrystal-supported catalysts can be utilized for the upgradation of C5 to C6 furaldehydes in biorefineries, as BCNCs are inexpensive material with excellent surface area, porosity and mechanical strength. Also, the easy modification of BCNCs make it a potential candidate to develop new environment friendly and sustainable energy materials.

Abstract

The present study relates to the utilization of bacterial cellulose nanocrystals for producing a novel, efficient and mesoporous heterogeneous catalyst BCNC templated ZrP. It has been confirmed by surface morphology that BCNCs are useful in the formation of porous support of intertwined nanosheets within its structure. Direct hydroxymethylation of furfural to HMF proceeded smoothly with the highest values of yield of ~28% in the presence of BCNC_ZrP in a two-necked round bottom flask equipped with condenser system. Thus, cellulose nanocrystal-catalyzed hydroxymethylation reactions could be beneficial in the upgradation of C5 to C6 furaldehydes in biorefinery.

Graphical Abstract

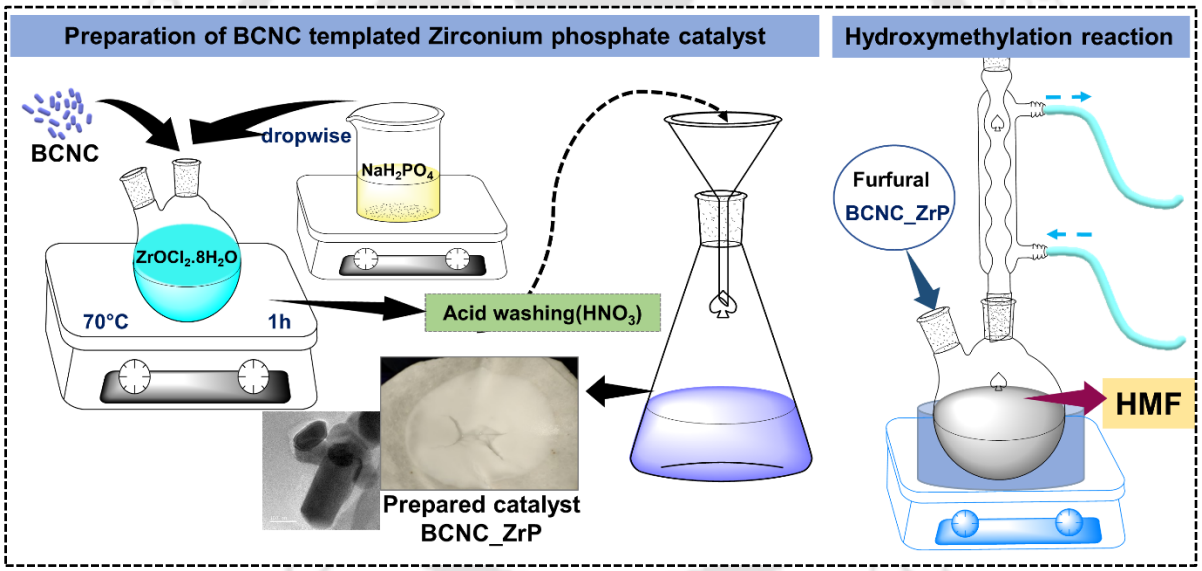

5.1 INTRODUCTION

The transformation of biorefinery waste into value-added products is regarded as an intriguing and sustainable approach. The replacement of petroleum-derived non-biodegradable materials with sustainable green materials, and the selection and utilization of bioresources is a pressing challenge that has gained attention in the scientific community. Therefore, it is an urgent need to develop our know-how in generating green platform chemicals to self-sustain our environment.

The unique physicochemical properties such as higher specific surface area, mechanical strength, availability of free hydroxy groups for modification, nontoxicity, make the bacterial cellulose nanocrystals (BCNCs) an object of intense research. BCNCs also aid in the reduction of carbon dioxide responsible for the current climate change, thus their utilization in the development of functional materials with improved properties has become an interesting field in the research fraternity over the past two decades. The introduction of the functional components into the nanocellulose system can lead to the expansion of these materials in specific applications [124]. Some of the potential application of BCNCs are as an emulsion stabilizer, as templates for functional materials, as functional organic hybrids, etc.

Zirconium phosphate (ZrP) based materials possess high thermal stability and biocompatibility alongwith the presence of abundant active sites and ion-exchange capability; also, the easy intercalation of ZrP with other materials make them suitable for fabrication of novel materials and useful in fundamental applications. ZrPs can be classified into two categories, based on their crystallinity and structural components, as crystalline ZrP and amorphous ZrP [125,126].

Furfural is derived generally from C5 sugars, mainly from xylose and arabinose, present in the hemicellulose of lignocellulosic materials. Amongst the wide-ranging chemicals derived from lignocellulose, furfural is a key chemical with possible applications in oil refining, plastics, pharmaceutical and agrochemical industries. The possibility of furfural conversion into low cost monomer to biodegradable plastics, make it the most attractive replacement of conventional plastics production [127,128]. On the other hand, 5- hydroxymethylfurfural (HMF) is a fine chemical obtained from hexose after the acid-catalyzed dehydration reaction, and it has various applications which deliberates it's property of platform chemical during the synthesis of biofuels and valuable intermediate chemicals, and also as a precursor to biobased-monomer [129,130].

The hydroxymethylation of furfural to HMF is dependent on the catalyst and its purity, so proper selection and quantification of catalyst is required. In this study, we have used mesoporous BCNC templated zirconium phosphate as a catalyst for the conversion of furfural into HMF.

5.2 RESULTS AND DISCUSSIONS

5.2.1. Characterization of the synthesized catalysts.

The catalysts ZrP, BCNC-ZrP (2% and 3% BCNC loading) used in this chapter were synthesized using a wet-precipitation method. The addition of BCNCs into the aqueous solution of zirconyl chloride octahydrate, to enable binding of ZrP onto the nanocellulose structure resulted in increase in surface area of the prepared support catalyst. The concentration of cellulose nanocrystals was slightly varied with specific amounts to the pristine ZrP, which resulted in change of morphology and surface area.

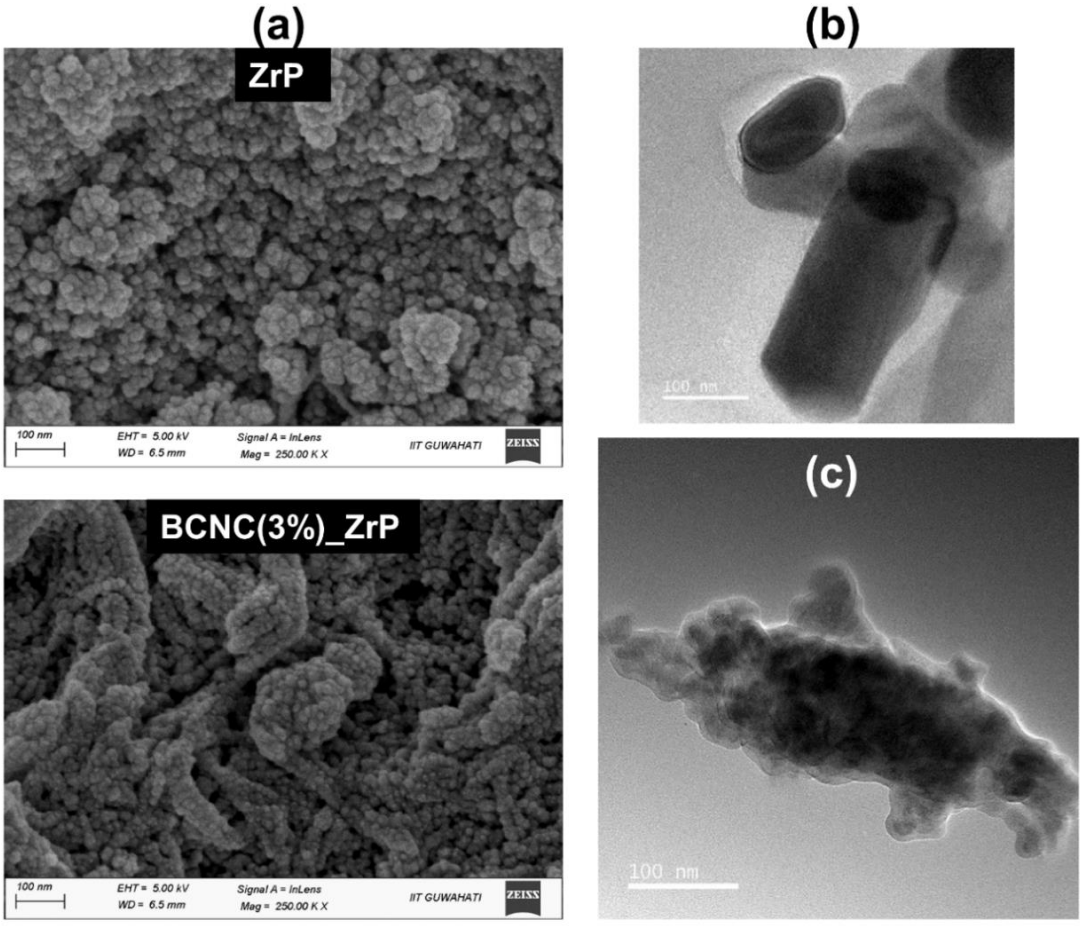

Figure 5.1. (a)FESEM image of the synthesized catalysts, ZrP and BCNC(3%)_ZrP, (b,c) FETEM micrographs of BCNC(3%)-ZrP.

The surface morphology of heterogeneous ZrP and BCNC(3%)_ZrP catalyst is illustrated in Figure 5.1 (a). ZrP exhibited the formation of spherical as well as agglomeration of the particles containing rough surfaces, while the BCNC templated catalyst showed the attachment of ZrP onto the BCNCs indicating a agglomeration loaded fibrillar morphology. The FETEM micrograph of an edge of BCNC_ZrP, as observed in Figure 5.1(b,c) showed ordered arrangement of multi-layered ZrP sheets rolled with the BCNC needles encapsulated in its core and surface. This type of alignment confirms the presence of long-pore channels in the catalyst resulting in a mesoporous structure [131]. The distinct hexagonal nanoplatelets of ZrP attached to the BCNC surface is shown in Figure 5.1(b).

An elemental mapping via FETEM of BCNC(3%)_ZrP containing the relevant elements (C,O,Zr and P) is shown in Figure 5.2. A homogeneous and uniform distribution of Zirconium(Zr) and Phosphorus(P) throughout the catalyst is observed. The presence of Carbon(C) and oxygen(O) all over could be due to the use of carbon grid in the sample preparation as well as presence of atmospheric air.

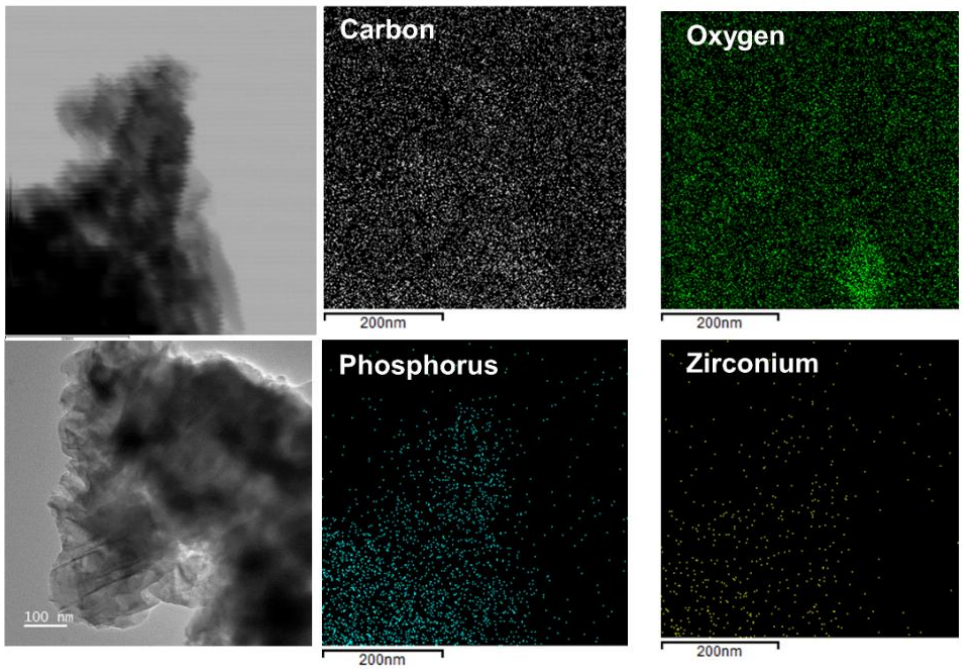

Figure 5.2. FETEM image of a selected region and the corresponding elemental mapping, confirming the arrangement of different elements.

The thermo-gravimetric profiles of the synthesized catalysts are shown in Figure 5.3(a), which indicates two weight-loss regions when heated from 30-700°C. The first weight-loss region (≈18% up to 180°C) in case of ZrP, and ≈15-17% up to 210°C in case of BCNC_ZrP is attributed to loss

of moisture or the loss of hydrated water. The second weight loss in the range 250–550°C for all the phosphates is attributed to the condensation of structural hydroxy groups. All the three samples ZrP, BCNC(3%)_ZrP and BCNC(2%)_ZrP exhibited a maximum weight loss of 36%, 31% and 28%, respectively; and no weight loss was observed beyond 500°C which indicates complete removal of the structural units without any transition of the catalyst structure. However, it was found in literature that the material may get converted to pyrophosphate at temperatures greater than 700°C and oxide at very high temperatures [132].

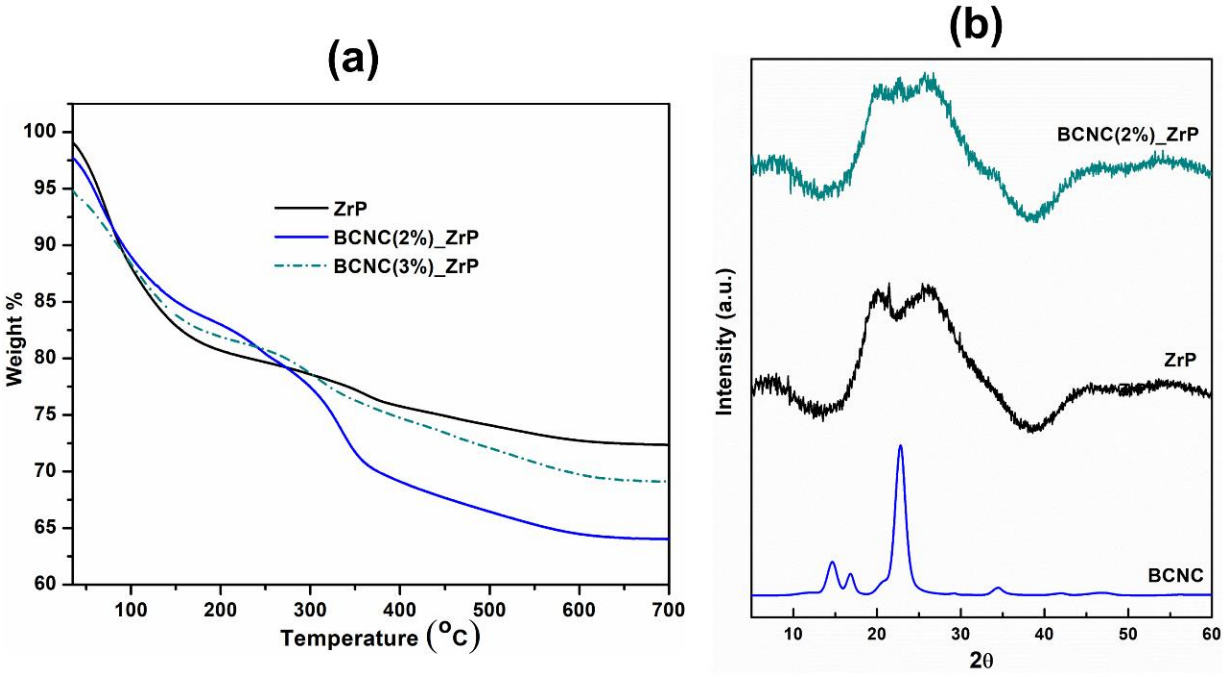

Figure 5.3. (a)TGA spectra of the synthesized ZrP and BCNC_ZrP catalysts, (b) XRD patterns of BCNC, ZrP and BCNC(2%)_ZrP.

The absence of any sharp peaks in the X-ray diffractograms for ZrP and BCNC_ZrP catalysts, and the presence of two broad peaks in 2θ ranges of 10–40° and 40–70° (Figure 5.3b), indicates the amorphous nature of the synthesized materials which is unlike the crystalline characteristics of BCNC [133]. The introduction of phosphorus into the mesoporous catalytic system resulted in their amorphous nature.

5.2.2. Chemical composition and structure of the synthesized catalysts.

The pore-size distribution of the synthesized catalysts depicting their Brunauer-Emmett-Teller (BET) data is shown in Figure 5.4(a). The specific surface area of the synthesized zirconium phosphate, BCNC(2%)_ZrP and BCNC(3%)_ZrP was found to be 153, 192 and 227 m^2/g, respectively. The gradual increase in surface area with increase in the BCNC loading during the catalyst preparation could be due to the intercalation of ZrP nanosheets into the BCNC fibers. Figure 5.4(a) shows the N_2 adsorption and desorption isotherms of all the catalysts. The adsorption−desorption pattern shows a type IV isotherm with a narrow hysteresis loop measured at a relative pressure (p/p^0) of 0.0−1.0 exhibiting mesoporous structures of the cellulose nano-crystal templated ZrP. The higher specific surface area of BCNC(3%)_ZrP is expected to provide abundant sites to the reactants, hence serving as a promising catalyst for the hydroxymethylation reaction.

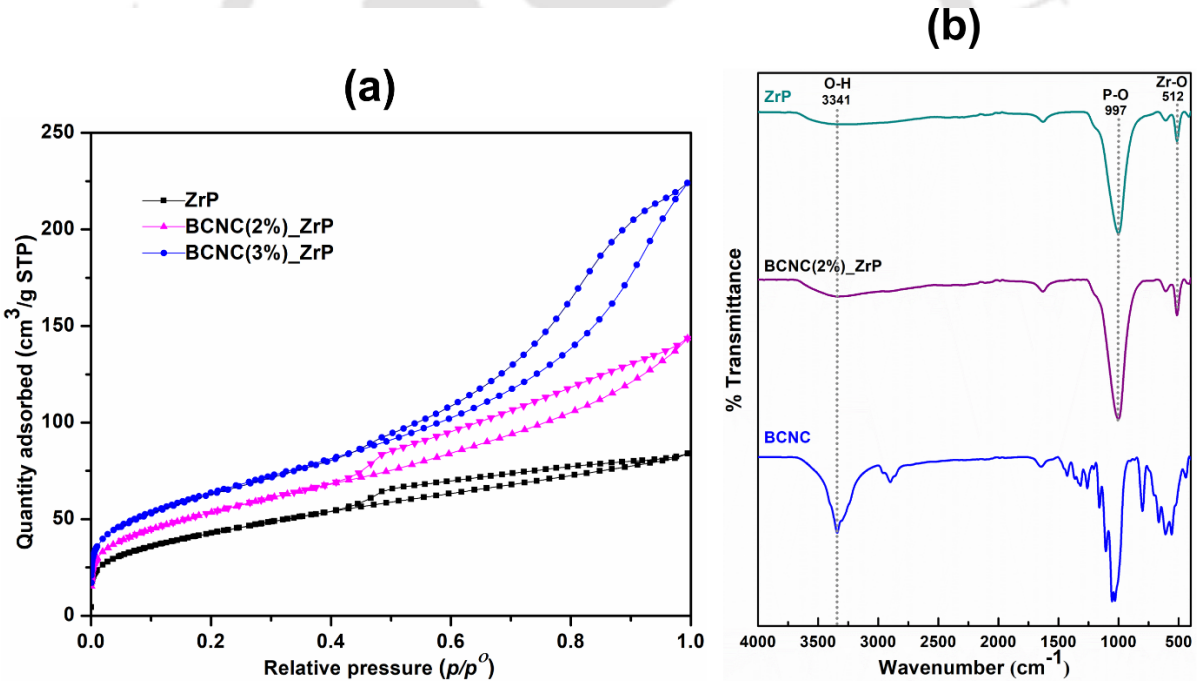

Figure 5.4. (a)N_2 adsorption-desorption isotherm of the synthesized ZrP and BCNC_ZrP catalysts, and (b)FTIR spectra of BCNC, BCNC(2%)_ZrP.

The chemical structure of the synthesized ZrP, BCNC_ZrP was characterized with an FTIR spectrometer over the spectral region of 400–4000 cm^{-1}. As shown in Figure 5.4(b), the –OH extending vibrations in water are clearly visible at 3341 cm^{-1}; the peak at 997 cm^{-1} can be assigned

to pyrophosphate groups; and finally, the peak at 512 cm^{-1} can be associated to Zr–O extending vibrations [134]. Similar bands are observed in the BCNC_ZrP spectra with a slightly broader –OH and phosphate bands. These bands indicate the presence of structural hydroxy groups or protonic sites in the synthesized catalyst.

5.2.3. Catalytic performance of BCNC to produce 5-hydroxymethylfurfural.

Previous literatures have been reported about the use of ZrP as an efficient catalyst in the conversion of xylose to HMF [133]; however, to date, no reports are available on the catalytic utilization of ZrP in the transformation of furfural to HMF. In this chapter, catalytic performance of the synthesized mesoporous BCNC(3%)_ZrP was investigated in the conversion of furfural to HMF.

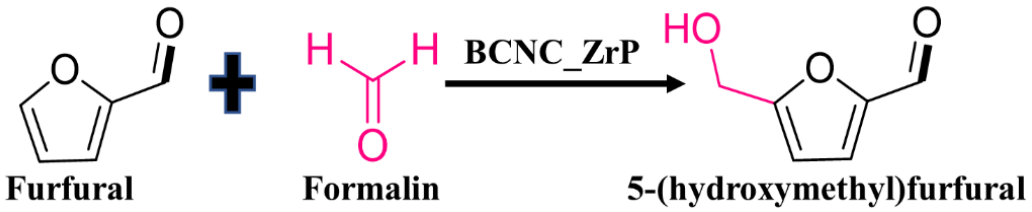

Scheme 5.1. Reaction mechanism showing hydroxymethylation of furfural to obtain HMF.

The hydroxymethylation reaction (Scheme 5.1) was initiated by adding the catalyst in a two-necked round bottom flask equipped with a condenser system and continued till 12h at 90°C. The reaction carried out using BCNC gave a yield of 0.7% with furfural conversion of 18.5%. It was observed that the pristine ZrP had no effect in the conversion of C5-C6 furaldehydes, however BCNC(3%)_ZrP was able to convert 67% of the reactant, with a highest HMF yield of 28%. Table 5.1 shows the effect of reaction time and type of catalyst on the HMF yield, and it was observed that HMF yield increased with increasing concentration of BCNC, while the yield decreased when the reaction time exceeded from 12h to 24h.

Table 5.1. HMF yield with respect to reaction time and catalyst used

Sl.no.	**Catalyst**	**Reaction time (h)**	**HMF yield (mol%)**
1	BCNC	12	0.7
2	ZrP	12	nil
3	BCNC(2%)_ZrP	12	~22
4	BCNC(2%)_ZrP	24	~16
5	BCNC(3%)_ZrP	12	~28
6	BCNC(3%)_ZrP	24	~17

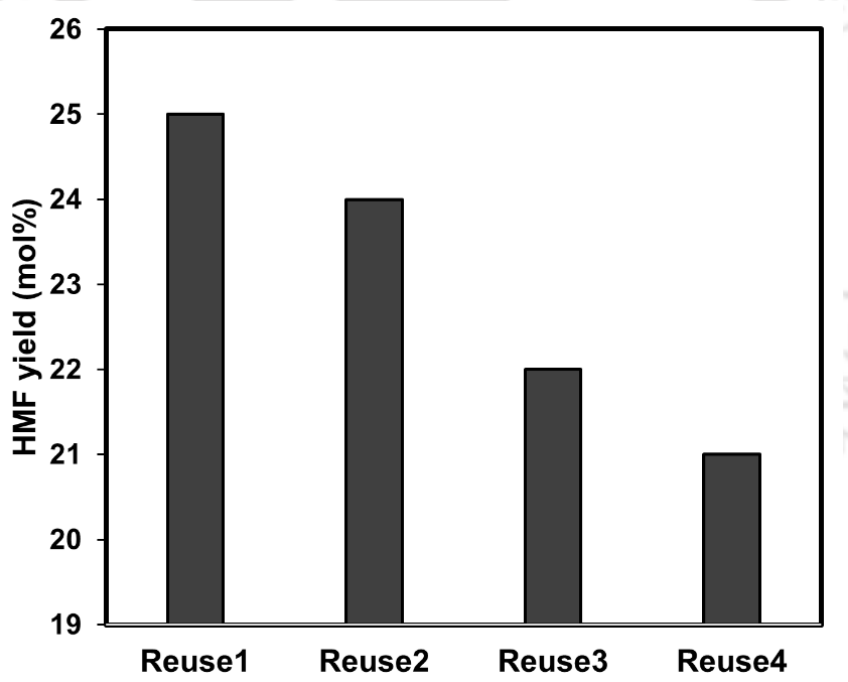

Figure 5.5. Re-usability of BCNC(3%)_ZrP for the conversion of furfural to HMF.

The efficiency and reusability of the synthesized catalyst was also studied for the furfural conversion into HMF under the same reaction conditions. The catalyst after each reaction was separated by centrifugation and washed with water-ethanol mixture several times, dried and reused in the fresh reaction. The synthesized BCNC_ZrP catalyst was successfully reused for four times,

and a slight decrease in HMF yield was observed as shown in Figure 5.5. The deposition of organic by-products during the reaction gave a brownish tint to the spent catalyst as shown in Figure 5.6. These results conclude that the synthesized cellulose nanocrystal templated catalyst is highly efficient in transforming furfural to HMF with good reusability.

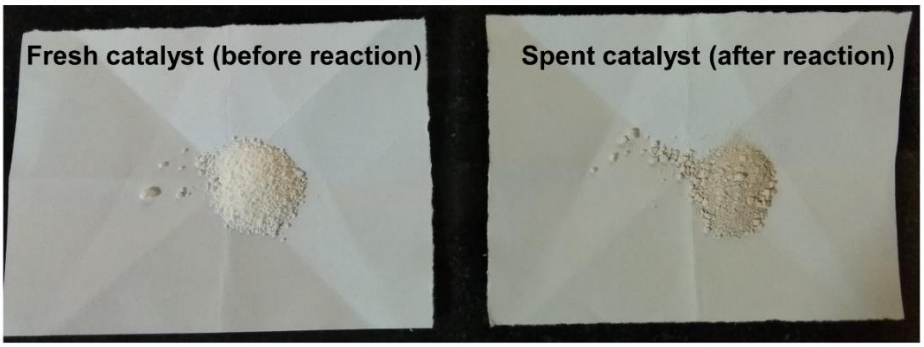

Figure 5.6. Photographic images of fresh and spent, BCNC(3%)_ZrP catalyst.

Figure 5.7(a) shows a typical HPLC chromatograph with the corresponding peaks of HMF and furfural, when a mixture of methanol/water of 20:80 (v/v) was employed as the mobile phase, and Figures 5.7(b,c) displays the standard calibration of furfural and HMF, respectively.

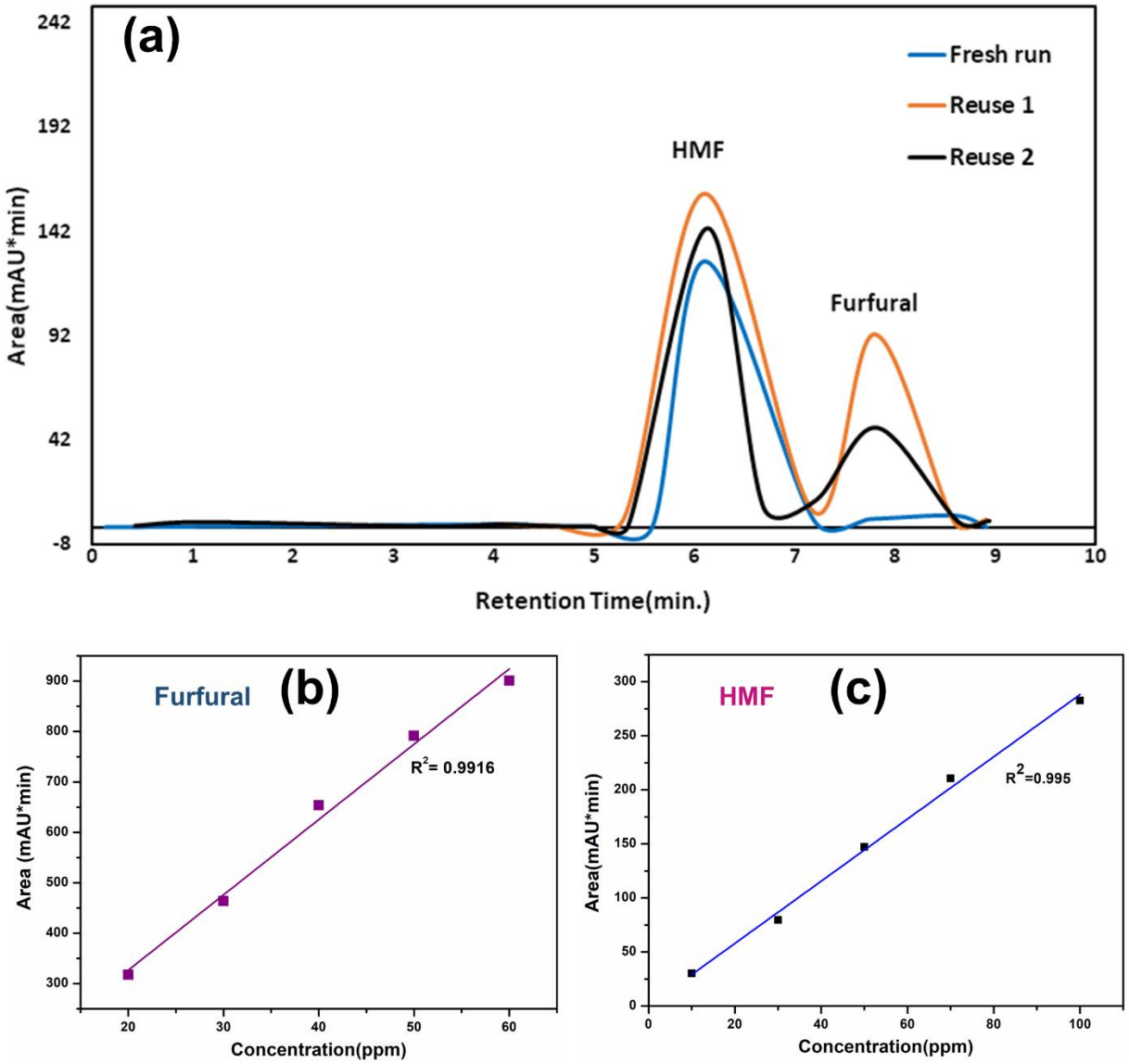

Figure 5.7. (a) HPLC chromatogram showing HMF and furfural as per their retention times, (b,c) Calibration curve of furfural and HMF standards obtained using HPLC.

5.3 CONCLUSIONS

In this study, BC nanocrystals were used as a template to synthesize ZrP catalysts. The prepared BCNC templated catalyst exhibited porous structure and showed a high surface area which facilitated its excellent catalytic activity as compared to pristine ZrP in the conversion of furfural, into HMF. The effect of reaction time on HMF yield was also investigated and it was found that heating for longer time had negative impact on HMF yield due to the formation of side products. Also, regeneration of the synthesized catalyst was done upto four times with minimal change in HMF yield. Thus, cellulose nanocrystal-catalyzed hydroxymethylations, could be beneficial in the upgradation of C5 to C6 furaldehydes in biorefinery.

Chapter 6

Studies on Fabrication of Bacterial Cellulose based Polycaprolactone Electrospun Bandages for Wound Dressing Applications

Motivation

Bacterial cellulose is a fascinating biomaterial obtained from microorganisms, with high purity, excellent biocompatibility and biodegradability. One of the most important characteristics of BC is its moisture retention capacity making it a suitable material for biomedical applications. The advancement of nanotechnology using the electrospinning technique to fabricate bacterial cellulose nanofibers blended with biodegradable polymer, PCL along with the inclusion of drug nanoparticles is highly beneficial. Thus, to utilize the overall benefits of nanotechnology, in this chapter we have fabricated drug-loaded nanofibrous dressings based on bacterial cellulose for wound-dressing applications.

Abstract

In this study, nanofibrous lidocaine hydrochloride loaded bacterial cellulose/ polycaprolactone (BCP-LD) scaffolds were fabricated using electrospinning technique. The developed scaffolds were then surface modified using silver-sulfadiazine loaded gum arabic solution to prepare a wound dressing material (BCP-LSD). The biocompatibility and improved cell proliferation of the fabricated scaffolds was successfully established with baby hamster kidney (BHK-21) cells using MTT assay and cell staining method. Water vapor permeability and wettability studies confirmed the improvement in hydrophilicity of the scaffolds, convincing their use as wound dressing materials. The BCP-LSD scaffold also showed excellent inhibition against model bacteria, *Escherichia coli* and *Staphylococcus aureus*. In-vitro release behaviour was studied in PBS (7.4), with an initial 28% burst release of SD in 30 min followed by controlled release of remaining drug in 84h and LID was fully released into the PBS system in 108h with an initial burst release of 29% in 30 min. Based on these results, BCP-LSD nanofiber scaffold is considered a good contender as a wound dressing material, providing both antimicrobial as well as pain-relieving effect on the wound.

Graphical Abstract

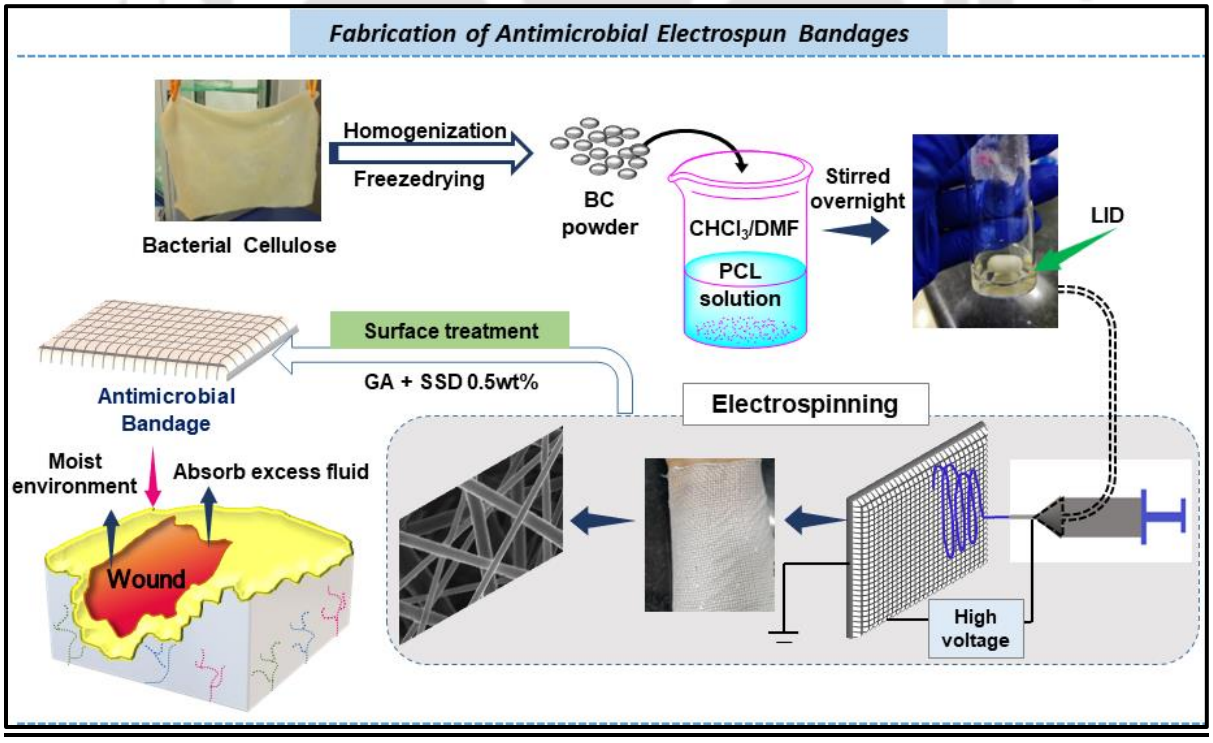

6.1. INTRODUCTION

Our skin plays an essential role by protecting the human body from pathological microorganisms with its natural defense mechanism; and also maintain a balanced homeostatis in the body [135,136]. Generally, wound dressing materials are prepared with an aim to protect the infected site by providing an excellent moist environment, allowing better absorption of the exudate, inhibit bacterial infections; also, they should be biocompatible and can be easily removed from the wound site [137,138].

Electrospinning technique have enabled the fabrication of nanofibrous dressing materials which are highly efficient as compared to the conventional dressings. The fibers obtained from electrospinning resembles with the natural extracellular matrices (ECM), thus acts as good support allowing cell adhesion and proliferation [139,140]. The highly porous structure as well as the higher surface area to volume ratio enables the passage and absorption of exudates from the wound maintaining a moist environment and protect the wound from dehydration [140,141]. These nanofibrous dressings also reduces bacterial infections and are suitable for direct contact with the skin [142]. Another advantage of using electrospinning is the ease of incorporating drugs and bioactive substances into the fibers, and the porous structure enables good release behavior of the drugs into the system [143,144].

Bacterial Cellulose (BC) is an essential class of ecological polysaccharide biomaterials of the 21st century, predominantly explored in food, textile, and biomedical applications due to their biocompatibility, nontoxicity, high purity, and hydrophilicity [5,92,145]. BC is generally extracted in the form of wet hydrogel sheets, with a porous, three-dimensional (3D) nanofibrous network of high surface area [1,2]. One of the most important characteristics of BC is its moisture retention capacity making it a suitable material for biomedical applications [5,108]. The employment of BC in biomedical applications largely attributed to its antigenicity, biocompatibility, and liquid absorbing potential [146]. However, batch-to-batch variability and difficulty in controlling morphology, diameter, porosity, and structure of pristine BC harvested from bacteria limits its applicability [115,147]. Therefore, synthetic production of an ideal BC scaffold with tailored properties to satisfy varying needs of wound-healing sites is highly imperative using electrospinning [96,148]. Moreover, the poor solubility of BC in most organic solvents does not allow the formation of monodispersed and continuous nanofibers. So, blending of BC with other

biomaterials or biopolymers results in enhanced processability and physico-mechanical properties, also the presence of polar OH group on BC act as binding site for interaction resulting in a stable composite material [31,56,146].

On the other hand, polycaprolactone (PCL) is a biodegradable and biocompatible polymer extensively investigated in tissue engineering applications owing to its miscibility in various solvents, tunable viscoelasticity, bioresorbability, miscibility, and mechanical characteristics [149–152]. Many approaches have been investigated to fabricate porous composite material to attain biocompatible scaffold. For example, in a study bacterial cellulose nanocrystal (BCNC), PCL, and gelatin were used for preparation of 3D scaffold composite. The fabricated electrospun nanofiber composite showed well-mimicked extracellular matrix of glioblastoma tumor. Biocompatibility was tested using U251 MG glioblastoma cells which suggested PCL/GEL/BCNC are excellent candidate for biomimetic scaffold application [153]. Aydogdu et al. prepared BC-PCL composite nanofibers using electrospinning. Cell viability test performed on Saos-2 cells indicated good biocompatibility of scaffold for wound healing applications [147]. Furthermore, other investigations such as keratin/ cellulose nanofiber mats produced by concurrent utilization of electrospinning and electrospraying [154], oxygenated bacterial cellulose with controlled oxygen release and antimicrobial properties for effective wound healing application [155], bacterial cellulose and silver nanowire based wound dressing as stretchable, robust, antimicrobial, and sustained controlled release of silver ions [156], supports the use of bacterial cellulose blended with biomaterials as an efficient wound healing scaffold with great promise for cell proliferation, attachment, and biocompatibility.

Silver sulfadiazine (Ag-SD) is an antimicrobial agent often used topically to treat wound caused by burns. Ag-SD is released into the wound with a burst release in the initial 2-8 h inhibiting the microbial growth on the wound [157]. On the other hand, lidocaine hydrochloride (LID) is mostly used as an anesthetic agent to treat painful wounds [136].

Herein, we have investigated the advancement of nanotechnology using the electrospinning technique to fabricate bacterial cellulose nanofibers blended with biodegradable polymer, PCL along with the inclusion of drug nanoparticles (Fig. 1). Thus, the hypothesis of this study is based on the successful fabrication of antimicrobial and biocompatible scaffolds with good wettability, and swelling properties, directing their utilization in wound dressing applications. This study aims

in the optimization of electrospinning conditions in producing uniform nanofibers to improve their cellular interaction and compatibility. Also, the use of LID and Ag-SD are expected to improve the antimicrobial and biocompatible nature of the fabricated scaffolds. The cell adhesion on the scaffolds was assessed using a cell staining method and MTT assay. The chemical properties, and surface morphology of the scaffolds were characterized by Fourier-transformed infrared spectroscopy (FTIR) and Field emission scanning electron microscopy (FESEM). Thus, this research article is expected to provide an essential understanding of the use of electrospun nanofibrous dressings in wound dressing applications.

6.2. RESULTS AND DISCUSSIONS

6.2.1. Chemical and structural characteristics of the drug-loaded BCP nanofiber scaffolds

Ag-SD coated BCP-LD scaffolds were successfully fabricated, and the resultant material appeared as a uniform nanofibrous mat replicating a bandage. The FT-IR spectra of the fabricated scaffolds are shown in Figure 6.1(a and b). The pure BC and PCL spectra are included for comparison and the formation of the composites was evaluated based on their structural characteristics. A broad peak is observed at 3306 cm^{-1} due to -O-H stretching in the cellulose structure, C-H stretching appeared at 2846 cm^{-1} and an intense band attributing the C-O-C stretching appeared at 1028 cm^{-1} as shown in Figure 6.1(a). The carbonyl stretching band was observed around 1718 cm^{-1}; and the asymmetric and symmetric -C-H vibrations at 2938 and 2865 cm^{-1}, respectively in the PCL spectrum. From the BCP (1% and 2%) plots, the characteristic peaks of cellulose and PCL are observed around 3400 cm^{-1}, 2875 cm^{-1} and 2940, 1724 cm^{-1}, respectively which confirms uniform blending of BC in the PCL nanofibers [158]; and is also evident from the uniform fibrous FESEM micrographs shown in Figure 6.5. In Figure 6.1(b), the characteristic -O-H, N-H and C=O acid stretching bands of LID was observed at 3383 and 1656 cm^{-1} [136,159]; while for Ag-SD, $-NH_2$ stretching bands were observed around 3388 and 3340 cm^{-1}, aromatic C=C bending around 1501 and 1549 cm^{-1}, and SO_2 symmetric stretching was observed at 1123 cm^{-1} [157]. The presence of these characteristic bands in the BCP-LSD scaffolds at 1165, 1602 and 1032 cm^{-1} indicated the physical interaction of the drugs with BCP during the electrospinning process.

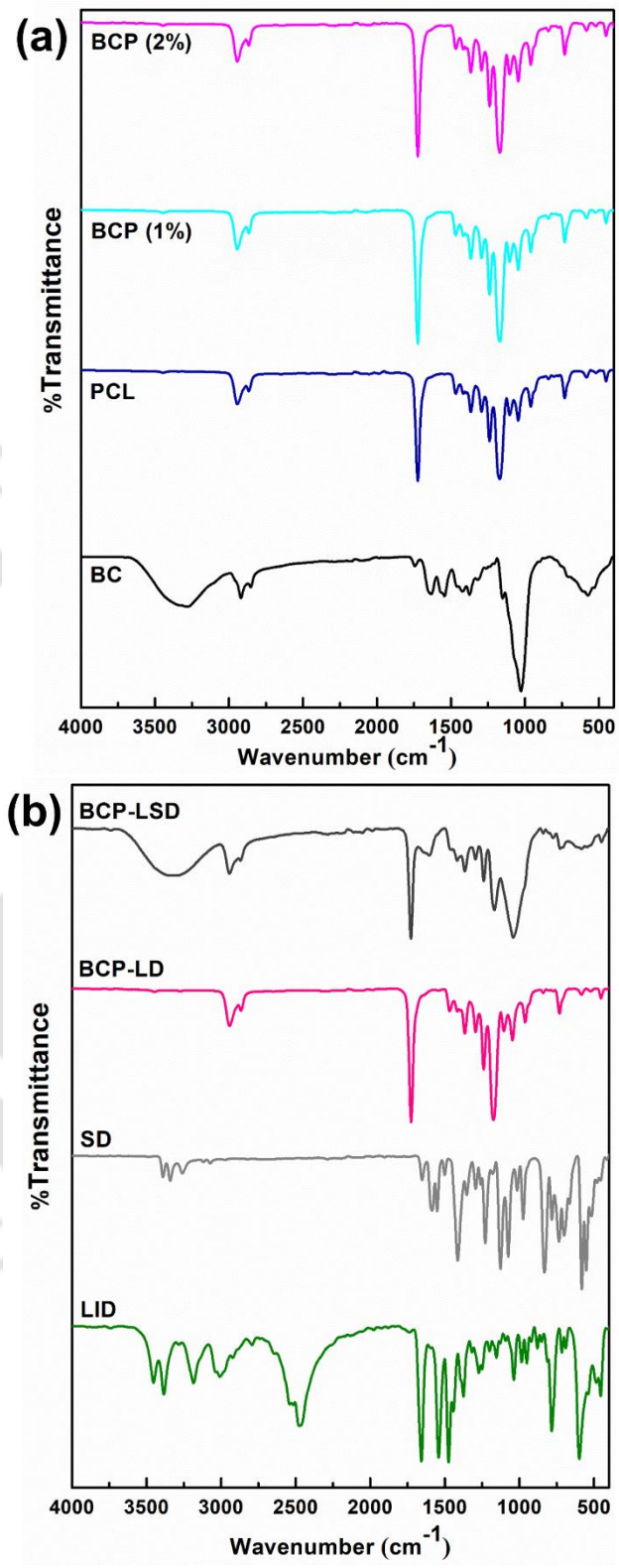

Figure 6.1. FT-IR spectra of (a) BC, PCL, BCP, and (b)LID, SD, and the fabricated scaffolds BCP-LD, BCP-LSD.

The uniform blending of BC and PCL investigated using XRD, resulted in highly crystalline nanofibers as shown in Figure 6.2. The diffraction peaks corresponding to cellulose-I of BC, and semi-crystalline peaks of PCL at 21° and 23° is observed in all the spectra, with a slight change in peak intensities as a result of the re-orientation of the nanofibers in the BC-PCL interaction. Thus, these results conclude that the addition of drug into the BCP nanofibers did not alter the diffraction pattern.

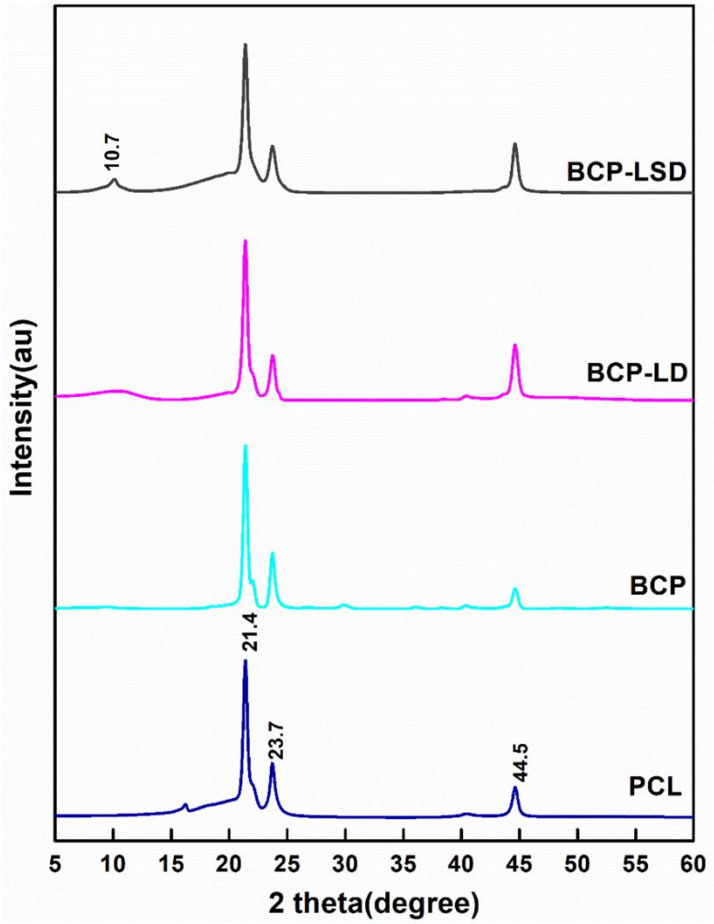

Figure 6.2. XRD plot of PCL, BCP, BCP-LD and BCP-LSD.

6.2.2. Mechanical and thermal properties of the fabricated scaffolds

For wound dressing applications, a material should possess good mechanical properties to support cell proliferation. Pure BC generally exhibits a lower elongation at break as compared to flexible PCL [108], and with increase in BC concentration the overall stiffness of the composite scaffold is expected to increase. Hence, we have optimized BC concentration of 2 wt% with respect to PCL

used for the fabrication of nanofibers. The fabricated scaffolds (PCL, BCP and BCP-LD) showed an average thickness of ±8 μm. The use of PCL in the fabrication of the nanofibrous scaffolds resulted in their improved flexibility with percentage elongation of ~ 40% as shown in Figure 6.3. This improvement in % elongation is a very important parameter in wound dressing materials as they enhance the cell growth mechanism providing an adequate toughness. All the nanofiber scaffolds showed a rupture upon ultimate stress due to the plastic behaviour of PCL, with a maximum tensile strength of 0.4 MPa in the BCP-LD scaffolds.

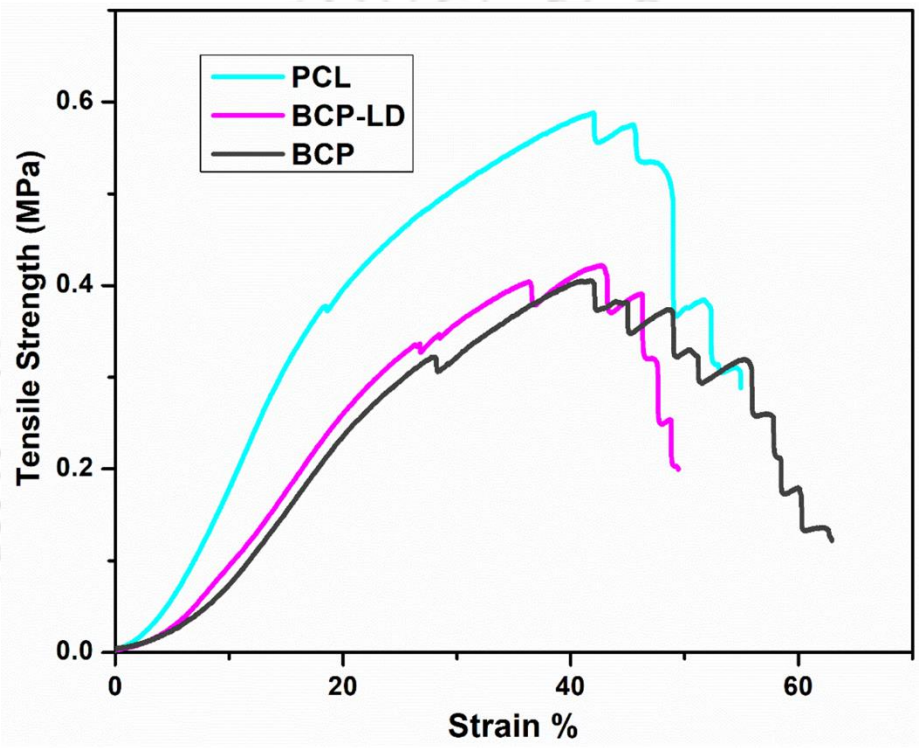

Figure 6.3. Stress-strain plot of the PCL, BCP and BCP-LD nanofibers.

An overall increase in thermostability of the BCP nanofibers with the incorporation of BC into the PCL nanofibers has been observed, and depicted in Figure 6.4(a and b). Pure BC showed an initial water evaporation of ~4% from its polysaccharide structure, while negligible moisture was present in the PCL, BCP and BCP-LD scaffolds. Further, a total of 18% weight loss from 55-365 ˚C was observed in the BCP-LSD nanofibers due to the moisture present on the GA surface. All of the fabricated scaffolds showed a single-step degradation profile with the maximum degradation happening in the 272-475 ˚C temperature range, due to the crystalline part degradation as well as the glycosidic unit depolymerization [109]. Also, it was observed that all the samples completely degraded around 700 ˚C leaving behind negligible ash content.

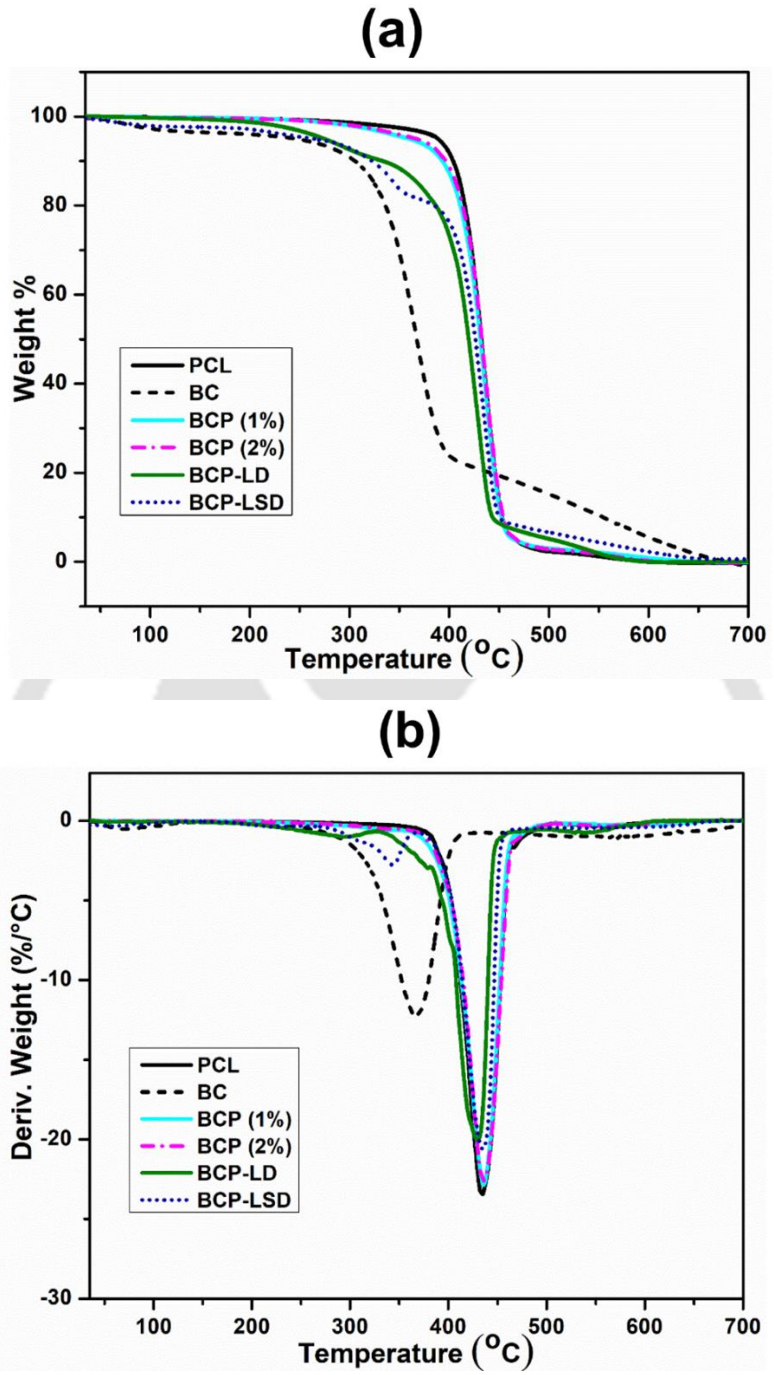

Figure 6.4. (a) TGA, and (b) DTG thermographs of BC, PCL, BCP (1% and 2%), BCP-LD and BCP-LSD.

6.2.3. Morphology of the electrospun nanofiber scaffolds

The BCP-LD and BCP-LSD nanofiber scaffolds offered multifunctional properties as a wound dressing material along with a controlled drug release. An electrospinning process was used to

fabricate the nanofibrous dressings. Figure 6.5 shows the surface morphology of the electrospun neat PCL, BCP, BCP-LD and BCP-LSD nanofiber scaffolds. All the structures showed uniform, homogenous distribution of nanofibers. It was observed that the incorporation of BC into the PCL electrospinning solution resulted in uniform beadless nanofibrous mat. The lidocaine blended BCP resulted in beadless and uniform fibers with a rough surface, and the BCP-LSD coated fibers were also found to be rough and uniform with the appearance of AgSD-GA layer above the fibers. The average fiber diameter of the BCP fibers (111.18 nm) was significantly lower than that of the neat PCL fibers (223.35 nm) and the average diameter of the BCP-LD and BCP-SD fibers was calculated as198.46 nm. A slight swelling of the BCP-SD fibrous mats was observed due to the attachment of AgSD-GA on its surface which also resulted in the increase in wettability of the fabricated mats as shown in Figure 6.6.

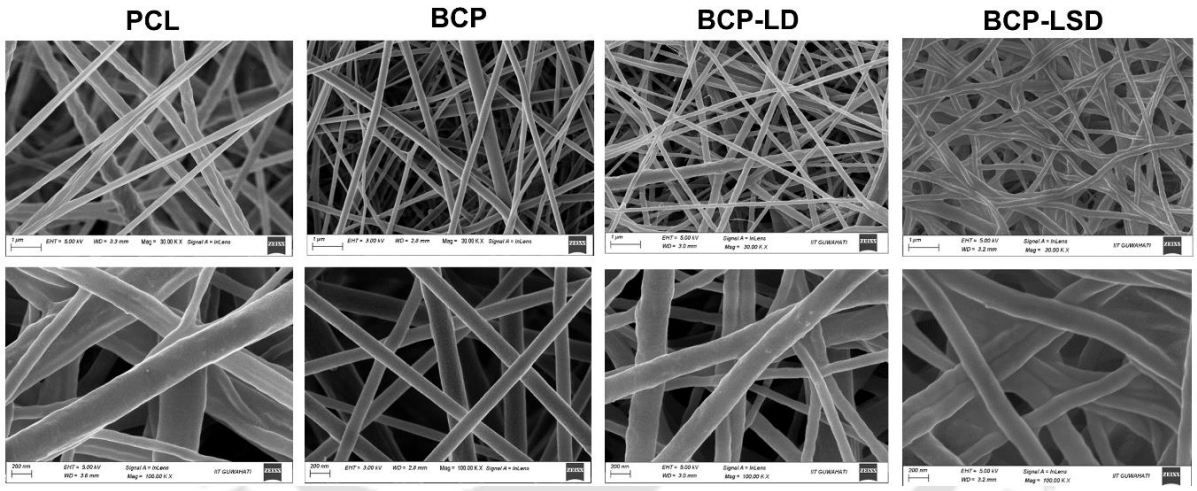

Figure 6.5. FESEM micrographs of neat PCL, BCP, BCP-LD and BCP-LSD nanofiber mats.

6.2.4. Wettability studies

The wettability of the scaffolds was recorded and shown in Figure 6.6 (a,b). The WCA of all the prepared scaffolds gradually decreased with time (10s to 60s) whereas neat PCL fibers exhibited a super-hydrophobic WCA of 139° even after 60s. With the incorporation of BC into the PCL fibers, there was a slight decrease (110° to 94° over 60s) in the WCA. Further, the addition of LID into the BCP nanofibers resulted in slight improvement in the wettability (83°) however this WCA value was not sufficient to utilize the fabricated material as a wound dressing material. The coating of AgSD-GA on the BCP-LD fibers resulted in a preferably low WCA (61°), therefore making it

a hydrophilic material suitable for wound dressing applications since wettability is a significant characteristic of a wound dressing material and it is directly connected to cell proliferation and adhesion. This decrease in WCA could be attributed to the hydrophilic nature of GA when attached to water molecules, as well as the increase in pore size of the nanofibrous scaffolds.

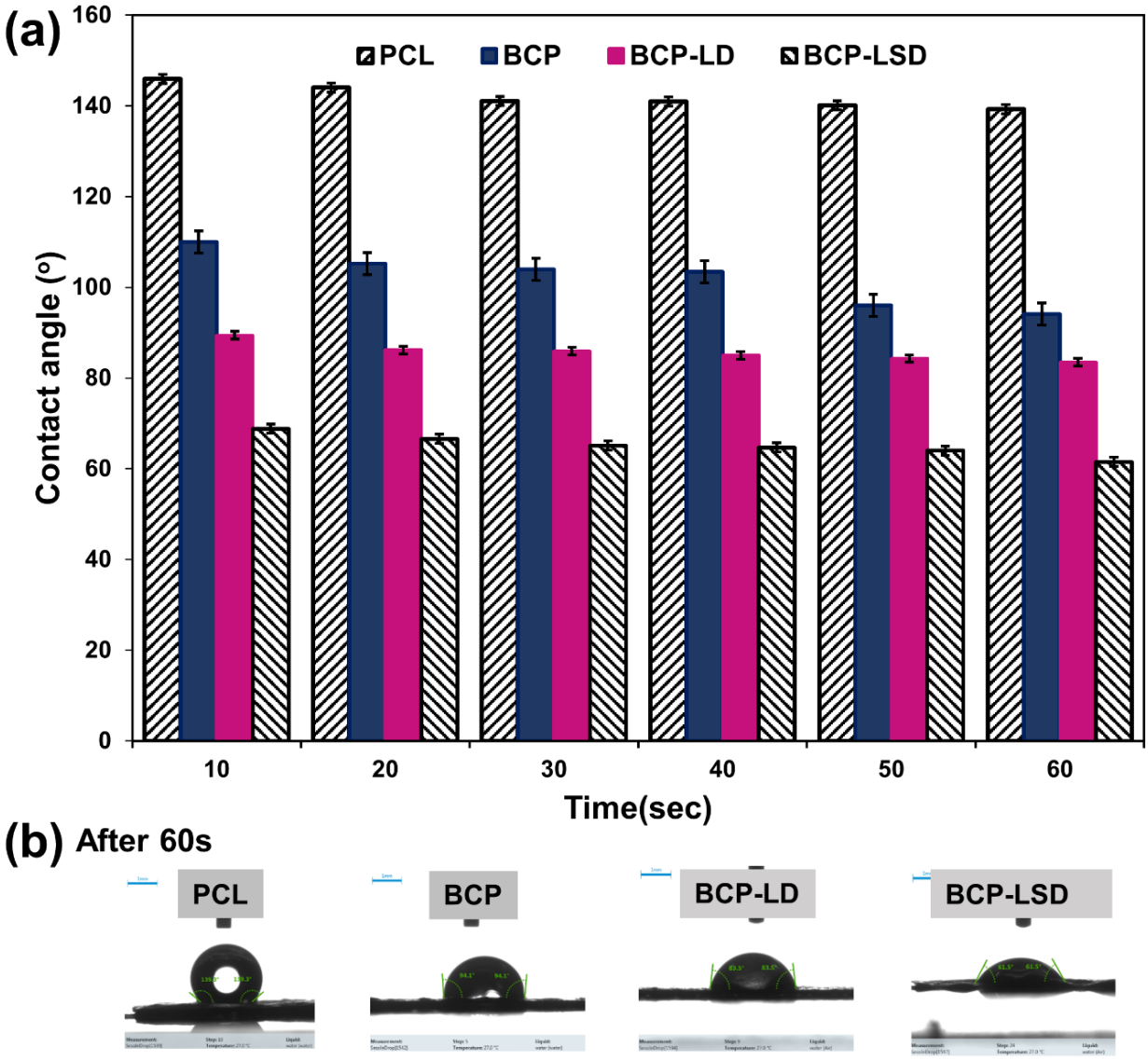

Figure 6.6. (a)Wettability plot of PCL, BCP, BCP-LD and BCP-LSD over 10-60sec. (b)Microscopic images of WCA of PCL, BCP, BCP-LD and BCP-LSD captured at 60 sec.

6.2.5. Water vapor permeability

The investigation of water vapor transmission through the nanofiber scaffolds was studied to understand the utility of the fabricated materials for wound dressing applications. The WVTR of the fiber samples including neat PCL, BCP, BCP-LD and BCP-LSD was monitored as 7306, 4212, 4899 and 3691 g/m^2 day, respectively as shown in Figure 8(a). Neat PCL exhibited a higher water vapor transmission as compared to the BC incorporated fibers, which could be due to the thick PCL fibers overall decreasing the porosity of the nanofiber mats. In general, all the fiber mats except neat PCL showed a WVTR value in the range for treating a wounded skin, i.e., 279-5138 g/m^2 day [160]. The water vapor transmission through BCP-LSD fiber scaffolds is slightly closer to the permissible WVTR value of 2500 g/m^2 day, which allows sufficient moisture and hydration to a wound [161].

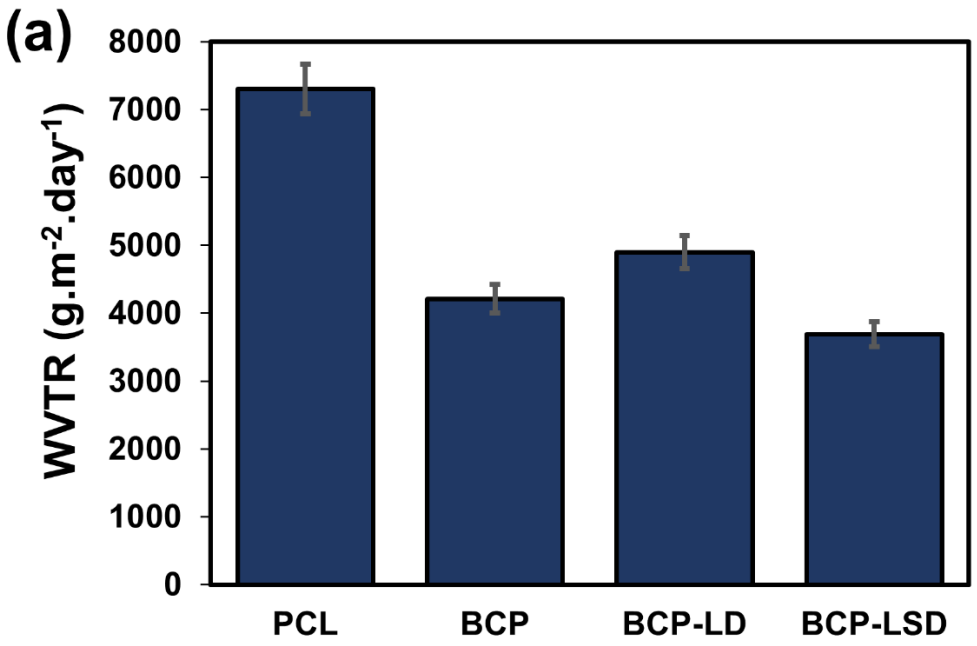

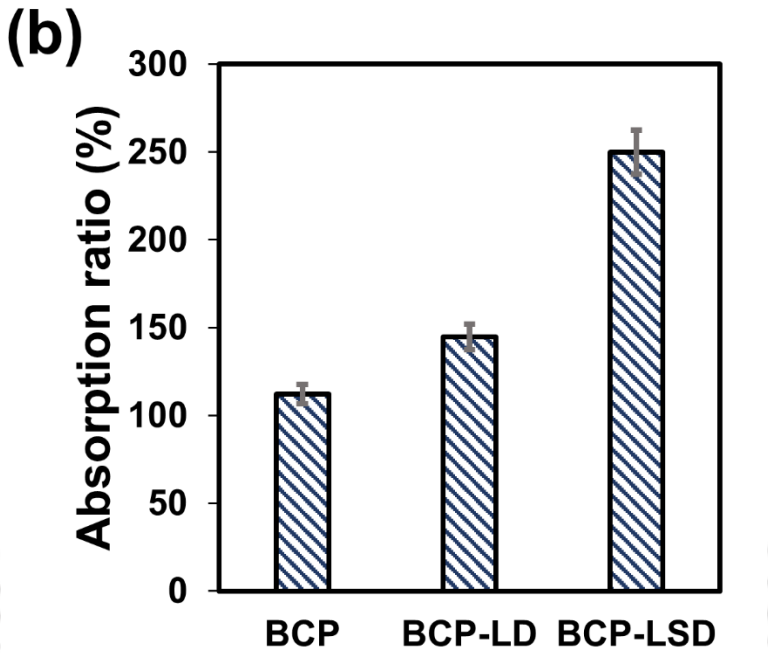

Figure 6.7. (a)Water vapor transmission rate of BCP, BCP-LD and BCP-LSD scaffolds, and (b) Swelling ratio of the nanofiber BCP, BCP-LD and BCP-LSD scaffolds.

Absorption is yet another important criterion to evaluate wound dressing materials [162]. Figure 6.7(b) shows the swelling behaviour of the BCP, BCP-LD and BCP-LSD scaffolds in PBS. It was observed that BCP-LSD has the highest swelling ratio of 250% as compared to BCP and BCP-LD with swelling ratio of 112-144%. The lower swelling percentage of neat BCP and BCP-LD scaffolds could be attributed to the hydrophobicity of PCL as well as the intact nanofibrous structure. The application of Ag-SD-GA coating on the BCP-LD scaffolds resulted in enhanced hydrophilicity of the BCP-LSD scaffolds and this observation is in accordance with wettability studies as indicated in Figure 6.6. Thus, the hydrophilic nature and good swelling behaviour of the BCP-LSD fibers will allow it to absorb the exudates from the wound site thereby maintaining a moist environment.

6.2.6. Antibacterial activity of the fabricated nanofiber scaffolds and their controlled release profile.

In this study, gram-negative and gram-positive bacteria, *E. coli* and *S. aureus*, were chosen for bacterial growth evaluation using colony-forming method, on agar plates containing small discs of the fabricated nanofibrous scaffolds at 37 ˚C. From Figure 6.8(a), it was clearly evident that the bacterial cells attached onto the BCP and BCP-LD samples without the appearance of inhibition

zone. This is because BCP nanofiber does not have an inherited antimicrobial activity towards the chosen bacteria. LID also did not inhibit any bacterial growth since it is resistant to *E. coli* and *S. aureus* and is only used as a pain-relieving agent in this study [163]. Thus, to incorporate antimicrobial effect on the fabricated BCP-LD nanofibrous scaffolds, a crosslinking solution of glutaraldehyde containing Ag-SD-GA was used to coat the nanofibers. The use of this crosslinker not only enhanced the antimicrobial properties of the scaffolds but also improved their wettability as shown in Figure 6.6. Thus, for sample BCP-LSD both *E. coli* and *S. aureus* exhibited a wider inhibition zone of 23 and 20 mm, respectively as shown in Figs. 6.7(a and b). The initial bacterial count of *E. coli* and *S. aureus* was calculated as 2×10^9 CFU/mL and 2×10^{10} CFU/mL, respectively. Thus, the use of electrospinning technique to fabricate nanofibers is highly beneficial due to the availability of ultrafine porous nanostructures [141] which enables easy attachment of drug particles and their controlled release.

6.2.7. In-vitro drug release study

The drug-release behaviour of the fabricated BCP-LSD scaffold in PBS (pH 7.4) was investigated and shown in Figure 6.8(c). The release of the drugs from the scaffold was evaluated by recording the absorbance values at λ_{max} = 241 nm (for Ag-SD) and λ_{max} = 263 nm (for LID) using UV-Visible spectroscopy. Both the drugs (LID and Ag-SD) encountered a rapid release of 29% and 28% into the system in first 30 min, followed by the controlled release of the remaining drug. The burst release effect in 30 min is expected to inhibit the bacterial infections and give some pain relief, immediately on application. Ag-SD release from the BCP-LSD scaffold showed a linear and gradual profile from 12 to 72 h with almost 100% release in 84 h, while LID was slowly and gradually released into the system in 108 h. The comparatively slow release of LID is expected to achieve a long-term pain relief action while Ag-SD works on inhibiting the microorganisms. Hence, the effectiveness of the fabricated scaffolds showed exceptional performance by inhibiting the cell generation with sustained and controlled release of the drugs.

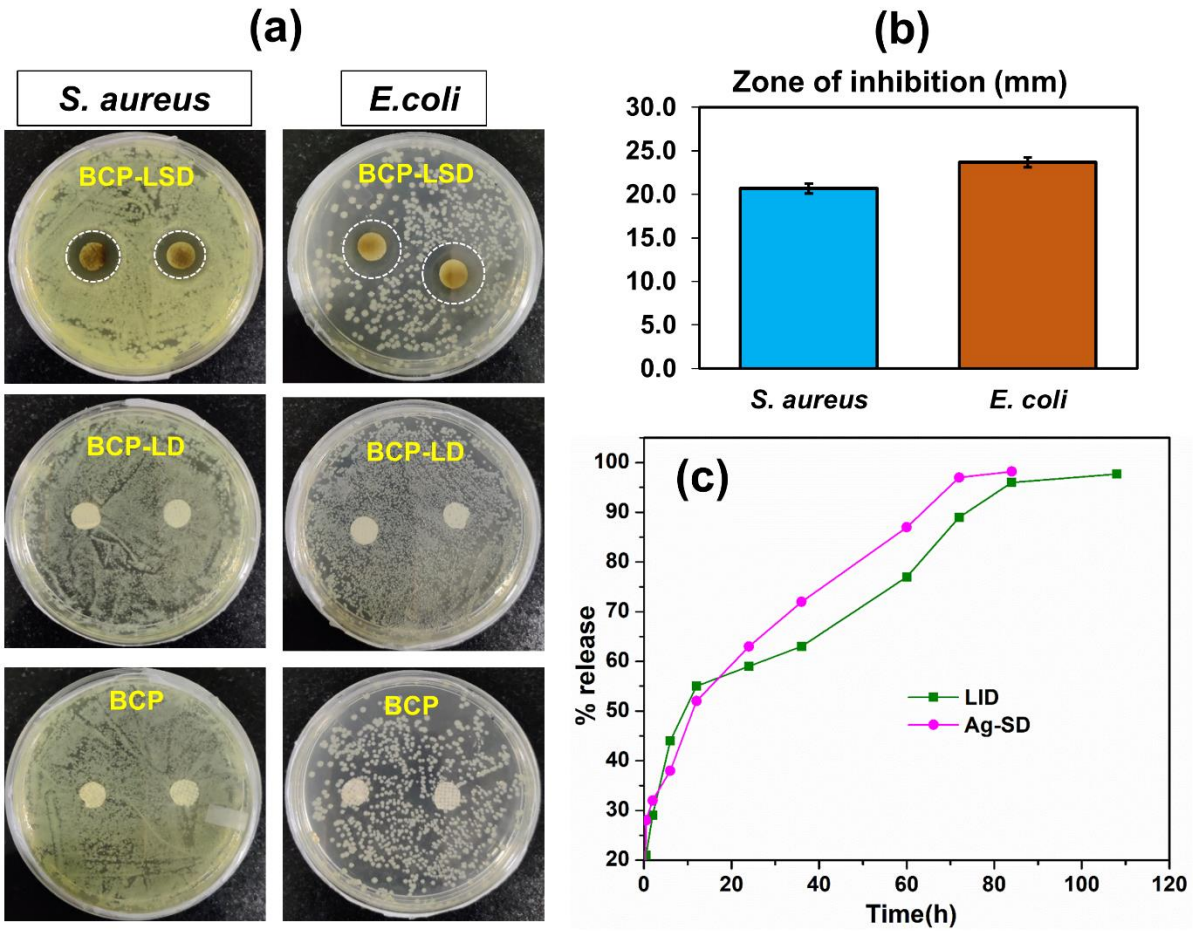

Figure 6.8. (a)Photographic images of BCP, BCP-LD and BCP-LSD discs showing antimicrobial activity against the chosen bacteria, (b) Zone of inhibition calculated in millimetres, and (c) Release behaviour from the BCP-LD and BCP-LSD scaffolds at pH 7.4.

6.2.8. Cytotoxicity and cell adhesion

The biocompatibility of the fabricated scaffolds was tested against baby hamster kidney cells using MTT assay as shown in Figure 6.9(c). A microscopic image of the prepared nanofiber scaffold is shown in Figure 6.9(a) to explain the cell adhesion properly. As reported in our earlier study [164], BCP has no toxicity against the BHK-21 cells which explains their biocompatible nature. Generally, an acceptable cell viability reduction of 15% is considered in wound dressing materials as per literature [165]. From Figure 6.9(c), it has been observed that the fabricated scaffolds PCL, BCP, BCP-LD and BCP-LSD exhibited a biocompatible behaviour allowing almost similar cell viability of 86%, 91%, 90% and 89%, respectively even after 72 h. Thus, the nanofiber morphology of the scaffolds has benefitted the enhancement of the cell proliferation on their surface.

The cytocompatibility of the fabricated scaffolds, BCP-LD and BCP-LSD with respect to the control for 24-72 h was investigated with a staining method using DAPI, where the living cells are highlighted in blue fluorescence as presented in Figure 6.9(b). It was noticeably evident that the stained cell nuclei adhered on to the nanofiber outline as well as inside the fiber layer of the electrospun mats shown in Figure 6.9(a). These results conclude that the fabricated scaffolds had no unfavourable impact on the cytocompatibility since cell attachment was clearly visible on their surface.

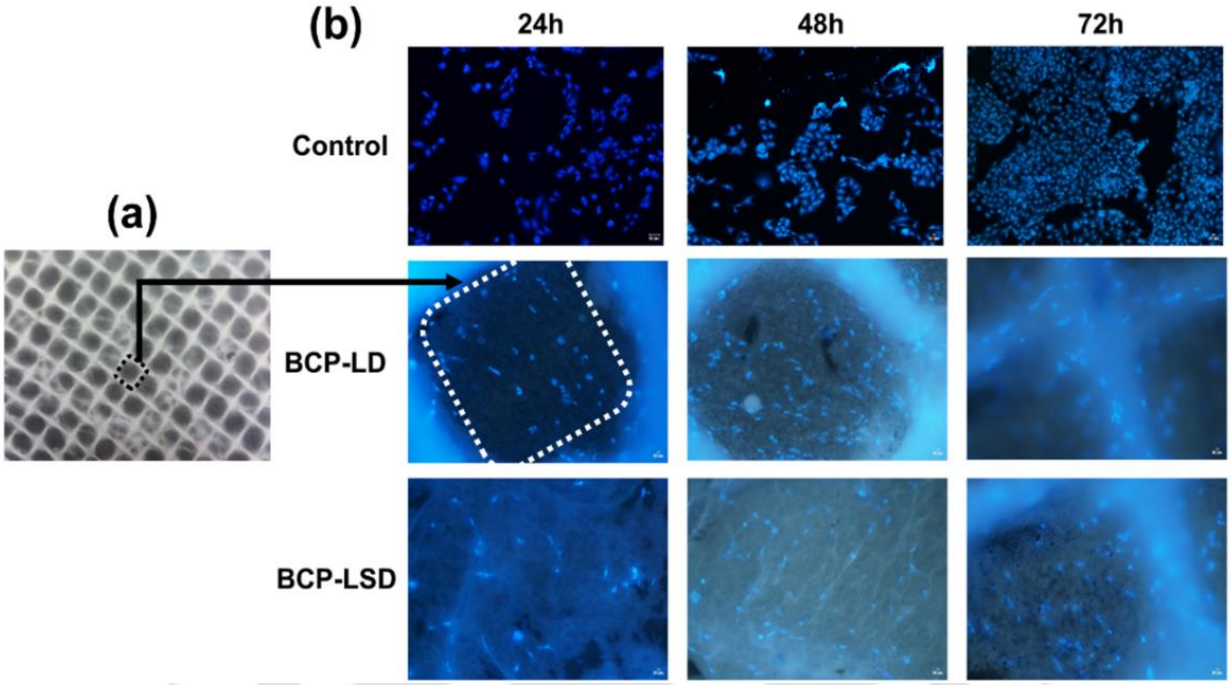

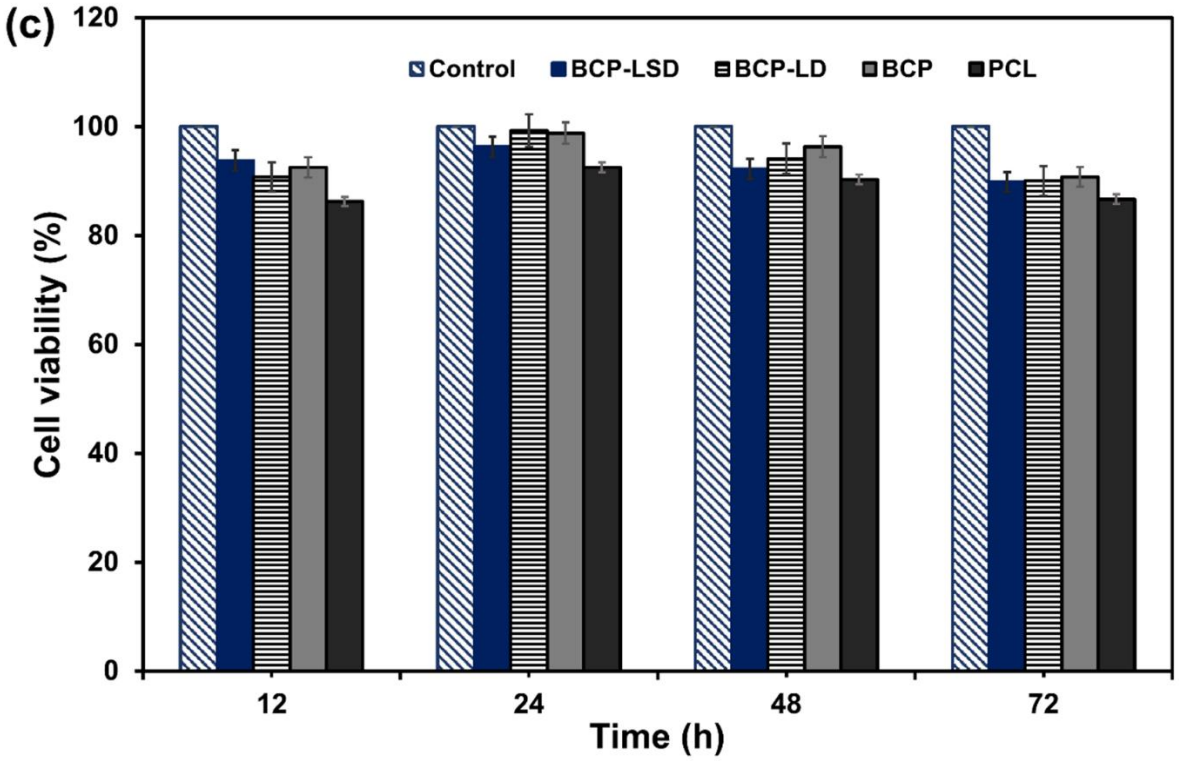

Figure 6.9. (a)Microscopic image of BCP-LSD scaffold, (b) BHK-21 cell attachment on the BCP-LD and BCP-LSD, stained with DAPI, and (c) Cell viability (%) of BHK-21 cells in contact with the fabricated scaffolds.

6.3. CONCLUSIONS

Electrospinning technique was very tactfully utilized to fabricate nanofibrous BCP scaffolds loaded with LID (1%) which was further coated with 0.5% Ag-SD solution. The developed scaffolds exhibited a uniform morphology with excellent biocompatibility and hydrophilicity. The cell adhesion studies showed that the nuclei of the stained cells spread evenly on the fiber surface as well as inside the fiber pores. The scaffolds also showed enhancement in physico-chemical and mechanical properties satisfying the wound dressing material criterion. The incorporation of LID and Ag-SD in the scaffolds resulted in the prompt release of both the drugs in first 30min, further following a sustained release trend with possible application as a pain-relieving, anti-microbial dressing. These results conclude that the fabricated BC based nanofibrous dressings make a potential candidate in wound dressing applications allowing adequate cell proliferation and biocompatibility.

Chapter 7

Studies on Fabrication of Immobilized Bacterial Cellulose Nanocrystals / Modified Gum Arabic Hydrogel

Motivation

Self-healing hydrogels are of particular interest in biomedical field due to their ability to repair structural alteration, and also act as carrier for drug delivery applications. Bacterial cellulose nanocrystals (BCNCs) are a class of biomaterial with high hydrophilicity due to the presence of abundant hydroxy groups, thus allowing their chemical modification as well as immobilization. Thus, considering the added advantage of BCNCs and HRP, the developed immobilized self-healing hydrogel could be utilized as a biosensor in biomedical applications.

Abstract

The production of cellulose nanomaterials from biomass opens an opportunity for the development and application of new materials in nanotechnology. In this chapter, the preparation of immobilized BCNC based hydrogels and their possible applications is summarized based on the results obtained from the analyses. Herein, gum arabic is chemically oxidized and used as a naturally derived nontoxic crosslinker to bind with the BCNCs. The formulated hydrogels exhibited good self-healing and improved mechanical properties, good porosity, which facilitated their application as promising biomaterials. The cross-linking was confirmed through characterization by FTIR spectroscopy, SEM morphology, thermal studies and water absorption capacity. Under optimal conditions, specific activity of HrP-immobilized BCNC hydrogel reached 106.6 Ug^{-1} min^{-1} (fresh) and 29.94 Ug^{-1} min^{-1} (after 60 days). The leakage from hydrogel was recorded after 6^{th} washing which showed an enzyme activity of 63.2 Ug^{-1} min^{-1}. These results show that the immobilization of HRP on modified BCNC hydrogel enhanced its appropriateness for a future use in various biotechnological and environmental applications.

Graphical Abstract

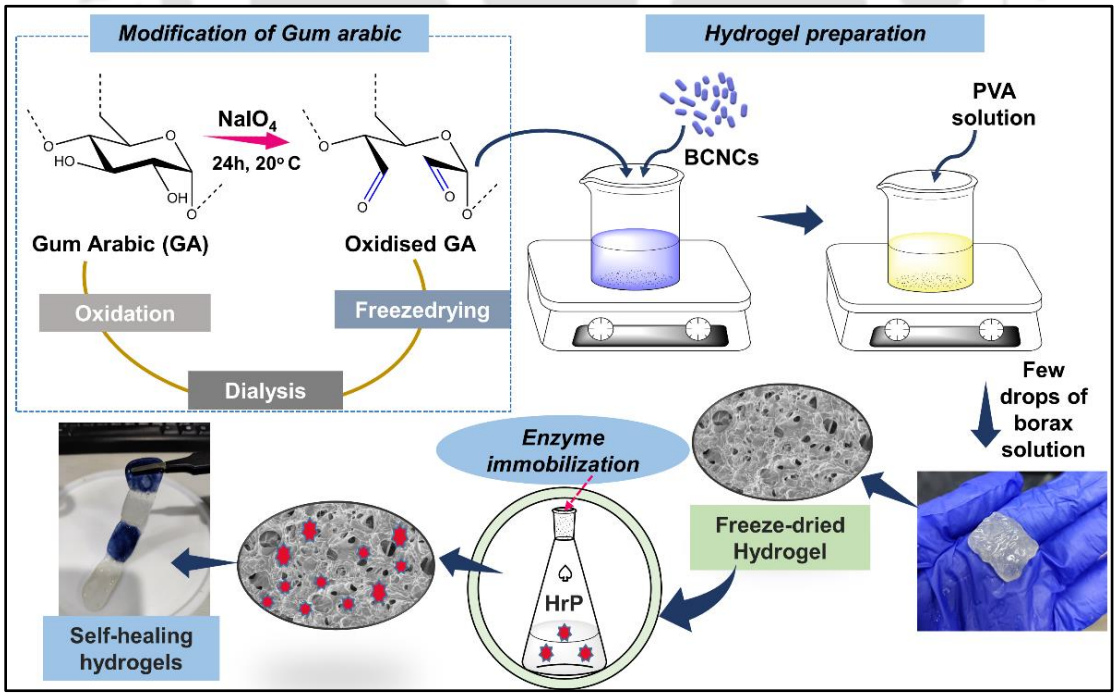

7.1. INTRODUCTION

Hydrogels are crosslinked three-dimensional network structures formed by the swelling of excess water by a polymer. Focus has been shifted to biopolymers and hydrogels as they open doors for many biotechnological applications, such as flexible sensors, drug delivery, etc. [166,167]. To prepare immobilized hydrogels, one of the most suitable enzymatic reactions is by catalytic activity of horseradish peroxide (HrP) [168,169]. Even though HrP has high selectivity, high activity and consistency over different treatment parameters, it has a few drawbacks like lower stability, low shelf life and it is also costlier [169,170]. Thus, to improve these drawbacks, enzymatic immobilization process is implemented in the presence of an environment-friendly carrier rather than harsh non-biodegradable carrier for HrP immobilization [169,171]. BC is a linear polymer with properties similar to a natural fiber having high water holding capacity and hence it can be considered the best suitable polymer for enzymatic immobilization [169,172,173]. But for enzymatic immobilization it is also necessary to break the amines of the proteins in the reaction and because of the presence of only hydroxy groups in BC it shows less reactivity. Thus, to overcome this issue, it is required to use a different polymer which can show high reactivity with amines of enzymatic proteins. Such a polymer is gum arabic (GA) which is a natural amphiphilic polysaccharide and literatures report the use of GA to prepare hydrogels but the hydrogels made solely with GA are gentle and brittle [174–176].

Hence, for the first time, incorporation of BCNCs in GA is hence proposed as a combination in this study to obtain a composite hydrogel. This research work reported that the produced hydrogels have superior self-healing properties along with increased mechanical strength and high porosity. With such improved characteristics, the fabricated modified HG-BCNC hydrogels can be utilized as biosensors, in biomedical devices/applications, and for various environmental and biotechnological purposes.

7.2. RESULTS AND DISCUSSIONS

7.2.1. Fabrication of modified Gum arabic based BCNC hydrogels.

In this chapter, the hydroxy groups present in the gum arabic structure are oxidised to its dialdehyde form using sodium(meta) periodate, and this process (Scheme 7.1) is considered advantageous as the excess periodate can be easily discarded through dialysis. The aldehyde group

of the modified GA then reacts with the hydroxy groups of BCNC forming acetal and hemiacetal bonds [177]. BCNC hydrogels were prepared by first dispersing the cellulose nanocrystals in the modified GA-PVA solution, followed by the addition of borax solution to form instantaneous crosslinked-hydrogels. Borax was used as a cross-linking agent as it can speed up the hydrogel formation in seconds by breaking down to boric acid and borate in an aqueous solution. Thus in our experiment, the borate present in the medium has undergone complexation with -OH groups of the BCNC-OGA mixture and resulted in instant gelation [178].

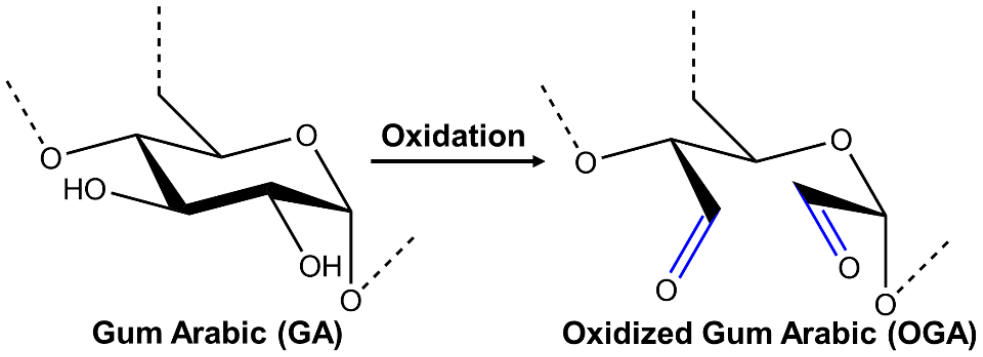

Scheme 7.1. Periodate oxidation of gum arabic, and the reaction breakdown of borax into boric acid and borate.

Figure 7.1 shows the surface morphology of the prepared hydrogels, and it was observed that OGA powder has a flaky appearance, while the fabricated hydrogels showed a porous structure. The average pore size of the HG, HG-BCNC(10%) and HG-BCNC(20%) hydrogels was found to be in the range of ±12.5 µm, ±3 µm and 8.6µm, respectively. From the FESEM micrograph and porosity of HG-BCNC(10%), it is understood that with the addition of BCNC in the HG hydrogel the pore size decreased. However, in HG-BCNC(20%) the pore size appears to again increase which could be due to the decrease in overall OGA concentration of the hydrogel [83]. The HG-BCNC(10%) hydrogel showed a uniform distribution of pores, forming a uniform and packed structure.

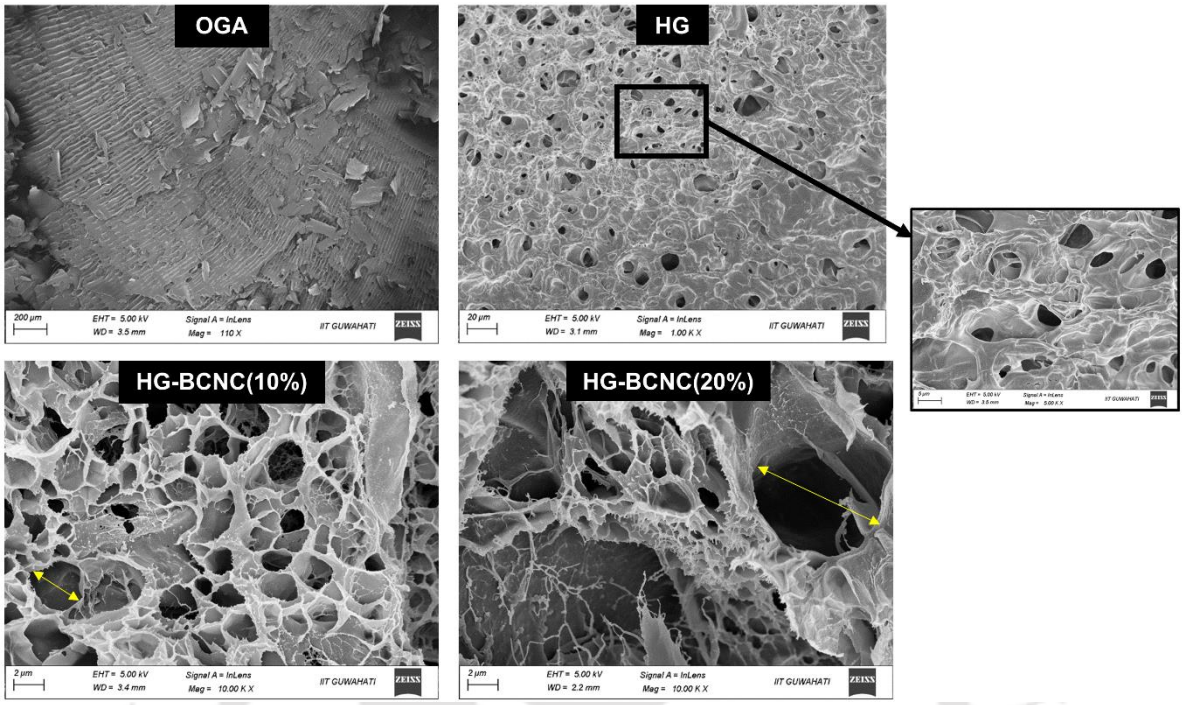

Figure 7.1. FESEM micrographs of OGA powder, HG, HG-BCNC(10%) and HG-BCNC(20%).

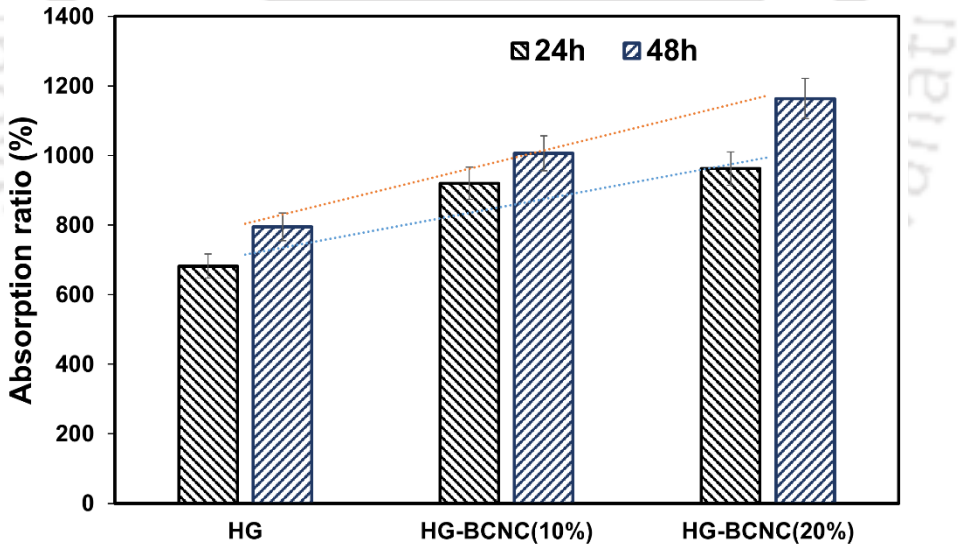

Figure 7.2. Water absorption plot of the prepared crosslinked hydrogels HG, HG-BCNC(10% and 20%) as a function of time.

The swelling ratio of the developed cross-linked hydrogels, HG, HG-BCNC(10%) and HG-BCNC(20%) was studied by soaking the hydrogels in distilled water. Figure 7.2 shows the swelling plot of the prepared hydrogels in 24h and 48h, and a lower swelling behavior was observed in the HG hydrogel as compared to the BCNC loaded hydrogels. The formation of a

highly cross-linked structure in the absence of BCNC could be the reason of this, as it may limit the polymer chain mobility and interaction with water molecules. In case of HG-BCNC (10% and 20%) hydrogels, the water-hydrogel interaction improved due to the availability of abundant -OH groups on the BCNC surface because of which more water was soaked into the hydrogel even after 24h and the saturation value was recorded at 48h.

7.2.2. Physico-chemical characterization of the fabricated hydrogels.

The structural formation of the hydrogels was confirmed by FT-IR spectroscopy as shown in Figure 7.3(a). The O-H, and asymmetric -C=O, -CH_2 stretching of GA was observed at 3298, 1599 and 2917 cm^{-1} respectively, while new peaks were observed in the OGA spectra corresponding to aldehyde -CO stretching and hemiacetal bond formation at 1731 and 890 cm^{-1}, respectively. The peaks observed at 1414 and 1021 cm^{-1} corresponds to the angular -CH bond deformation caused due to the skeletal movement of the GA carbon rings [179]. In the -IR spectra of HG-BCNC(20%), the peak at 1622 cm^{-1} corresponds to the C=O stretching vibration of the acetyl groups present in the PVA backbone. The addition of BCNC in the HG hydrogel can be attributed to the angular deformation of the C-H bonds at 1404 cm^{-1}. A sharp peak at 1019-1045 cm^{-1} corresponding to the O-C-O acetal group is observed in all the hydrogels [83].

The thermogravimetric profiles of GA, modified GA and hydrogels were studied by heating the samples from 30-700 $^{\circ}$C under inert atmosphere, and displayed in Figure 7.3 (b); where both GA and OGA had a first degradation step from 55-185 $^{\circ}$C of around 14% due to moisture attached to GA. HG and HG-BCNC(20%) also indicated a comparable loss of ~20% water vapor bonded to the GA in the first degradation from 57-222 $^{\circ}$C. A dramatic weight loss of ~65% was observed between 222-500 $^{\circ}$C, from the hydrogels which attributed to the dehydration and decomposition of the organic components. GA and OGA exhibited maximum degradation at 353-356 $^{\circ}$C while the hydrogels HG and HG-BCNC(20%) showed a maximum weight loss temperature till 500 $^{\circ}$C indicating the formation of highly cross-linked gels. The crosslinked structure of the hydrogel as well as the addition of BCNC restricted the chain mobility, thereby increasing the thermostability of the prepared hydrogels. Also, HG and HG-BCNC(20%) showed a very high ash content of 21 and 26% respectively, even after 700 $^{\circ}$C which could be linked with the carbonaceous residue breakdown leading to char oxidation whereas GA had only 4 % and OGA completely degraded at 700 $^{\circ}$C [164,180].

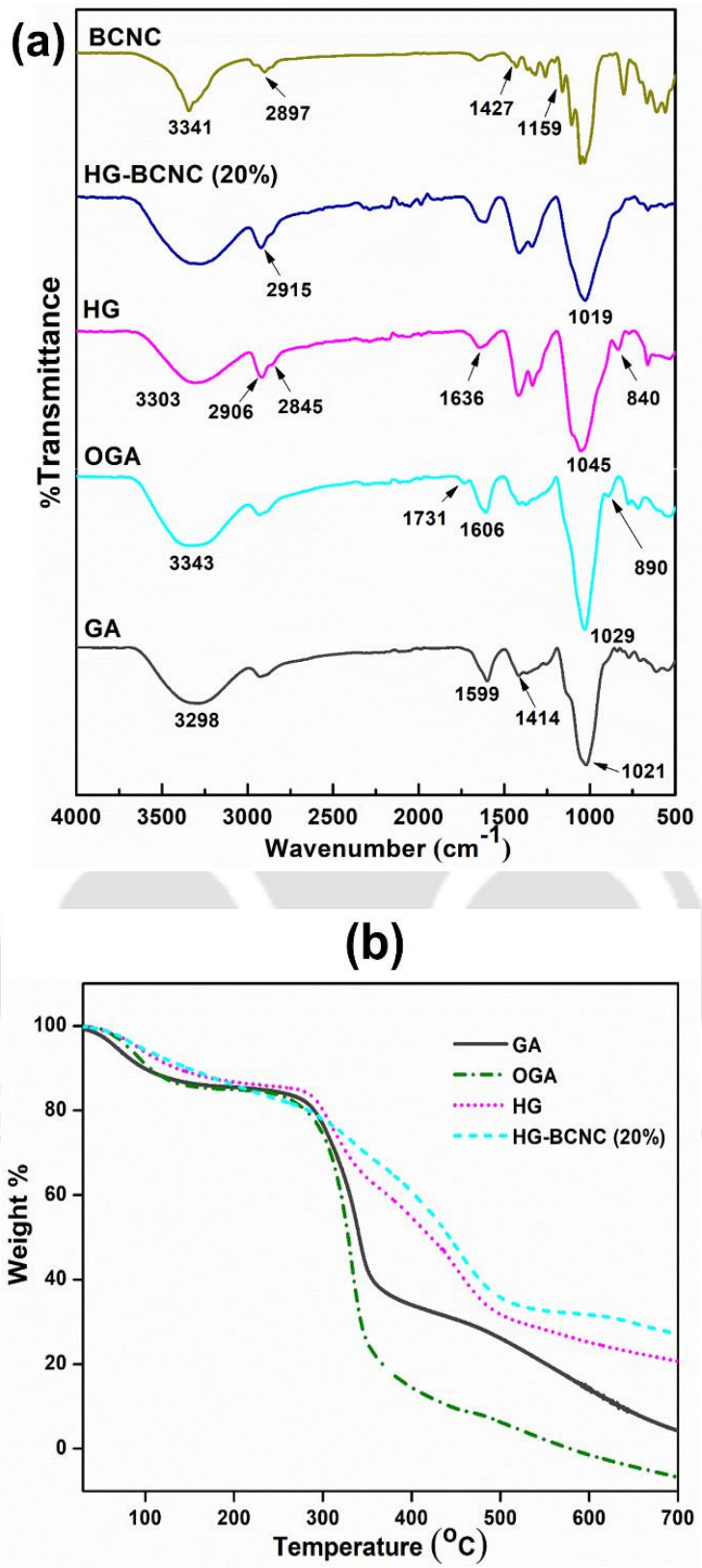

Figure 7.3. (a)FT-IR spectra of GA, OGA, HG, HG-BCNC(20%) and BCNC, (b) TGA thermograph comparison of GA, OGA, HG and HG-BCNC(20%).

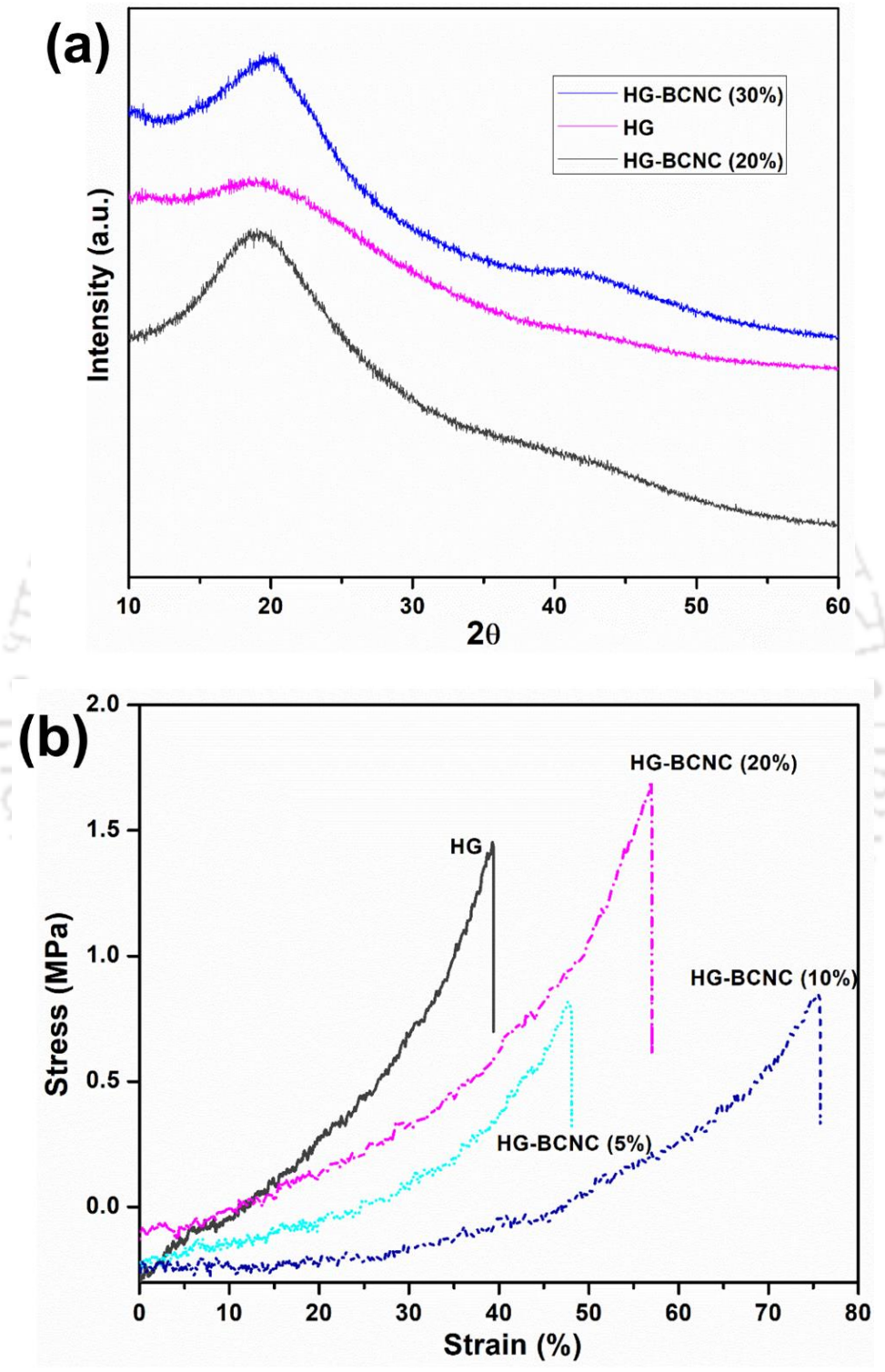

Figure 7.4. (a) XRD-patterns of GA and the crosslinked hydrogels, HG and HG-BCNC(20%), (b) Stress-strain graph of the fabricated crosslinked hydrogels.

The XRD patterns of the prepared hydrogels is shown in Figure 7.4 (a), HG hydrogel displayed a very small hump around 19.8° indicating amorphous nature of the crosslinked gel. However, the addition of crystalline BCNC during the hydrogel formation changed the XRD pattern of the hydrogels with the appearance of a distinct peak around 19.6° and a small hump at 42°. This change in the peak intensity is due to the crystallographic planes of 101 and 111, respectively [181] indicating the presence of BCNC in its structure as well as the presence of intermolecular H-bonding, which resulted in their semi-crystalline nature.

The mechanical properties of the prepared hydrogels were investigated at room temperature using compression test. From Figure 7.4(b), it has been observed that HG hydrogel displayed a tensile strength of 1.45 MPa and 40% elongation, and with the increase in BCNC concentration which indirectly decreased the OGA concentration; the percentage elongation increased. The increase in tensile strength (1.68MPa) of HG-BCNC(20%) could be associated with the presence of higher concentration of BCNC as well as better crosslinking of the hydrogel. However, the lower percent elongation (57%) of HG-BCNC(20%) as compared to HG-BCNC(10%) with 78% elongation could be linked with improved inter- and intra-molecular interactions between BCNC and OGA gel.

7.2.3. Immobilization of horseradish peroxidase on the fabricated BCNC hydrogels and their self-healing behaviour.

The immobilization of HRP on the fabricated hydrogel, HG-BCNC(20%) was done at a concentration of 0.1 mg/mL in PBS at pH 7.0. To compare the surface morphology, enzyme immobilization of BCNC was also carried out. In Figure 7.1, the porous morphology of HG-BCNC(20%) before immobilization has been already demonstrated. Figure 7.5 shows FESEM images of the hydrogel and BCNC surface after immobilization, and an increase in surface roughness of BCNC as well as hydrogel was observed due to the attachment of HRP on its surface and inside the porous structure. The use of glutaraldehyde to crosslink the HRP on the BCNC and gel surface could be a vital reason for this surface roughness. Also, the highly porous nature of hydrogel facilitated the enzyme loading density on its surface [182]. The appearance of bead-like substances on the surface confirms the immobilization of HRP onto the hydrogel.

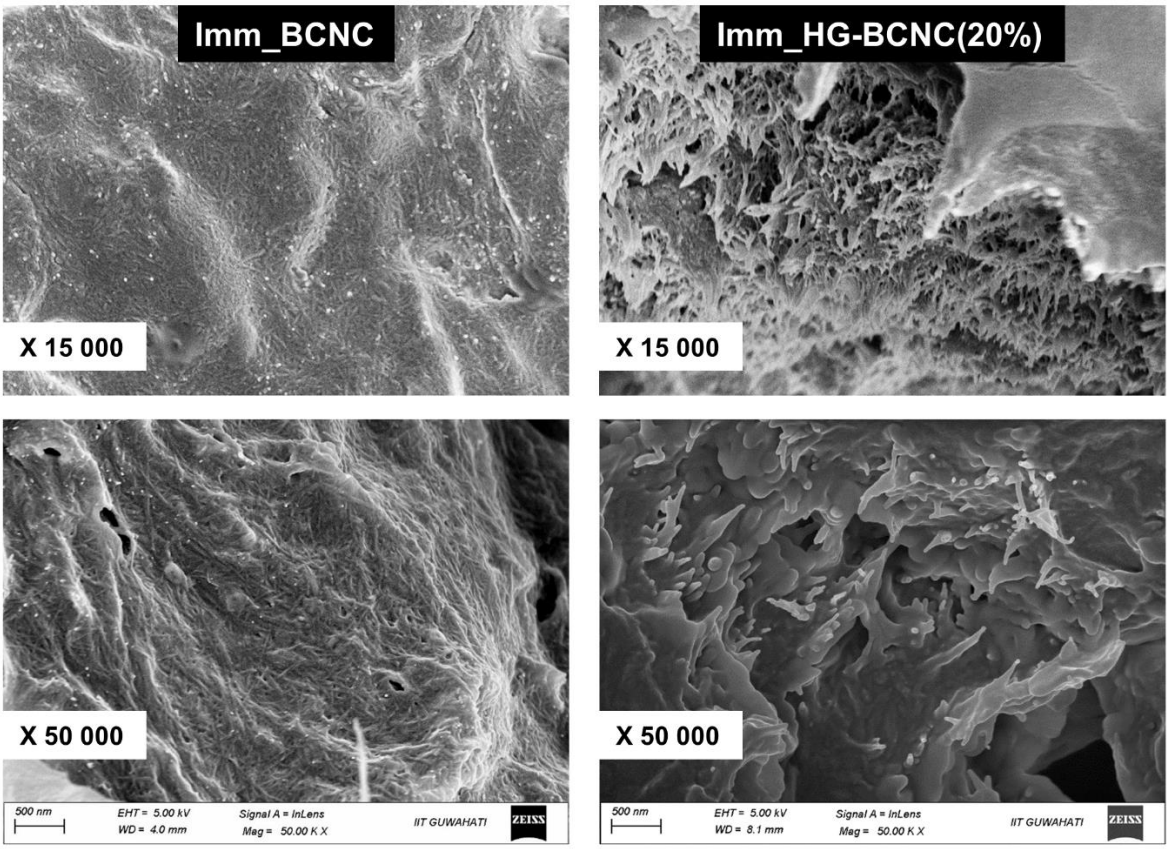

Figure. 7.5. FESEM images of immobilized BCNC and immobilized HG-BCNC(20%) under 15000 X and 50000 X magnification.

The sample preparation for the self-healing study was made by adding a small amount (less than 1mg) of aniline blue dye in the OGA-BCNC mixture before preparing the hydrogel. Hydrogels without dye were also made, and alternate coloured-uncoloured hydrogels were kept near each other, as shown in Figure 7.6 (b). After some time (20 sec), the fresh hydrogels attached to each other. Later they were again cut and placed together, as shown in Figure 7.6 (c), and in seconds, the cut hydrogels reformed into the previous shape confirming their self-healing nature. The prepared hydrogel was also pulled by hand, and it elongated up to 2 cm on each side from the actual size (2 cm) without breaking, as shown in Figure 7.6 (a).

7.2.4. Enzyme activity of immobilized horseradish peroxidase and their leakage test.

HRP decomposes hydrogen peroxide and generates an oxygen atom, which helps in the catalysis of ABTS to its oxidised form, i.e. the formation of ABTS radical dot+, indicating a green colour in the oxidised state. The activity of immobilized HRP was measured by monitoring the increase in oxidised ABTS and the rate of reaction was determined by the rate of formation of the green product in the cuvette at λ_{max} = 403 nm. The blank used as a reference became light green indicating the formation of some oxidised ABTS while the cuvette containing the immobilized enzyme changed to dark green colour after 20 min confirming successful encapsulation of HRP onto the hydrogel surface, shown in Figure 7.6(d). The dark green colour of the sample also indicates the presence of higher concentration of HRP.

Glutaraldehyde is used as a cross-linking agent for efficient binding of the enzyme on the material surface by covalent bonding, thus enhance the enzyme activity and reusability [169]. The optimized concentration of enzyme used in this study was 0.1 mg/mL. In this optimum condition, the immobilized hydrogel showed a specific activity of 106.6 Ug^{-1} min^{-1} for fresh sample and 29.94 Ug^{-1} min^{-1} for the same sample tested after 60 days. Also, the free HRP solution separated after collecting the immobilized hydrogel showed a specific activity of 92.3 Ug^{-1} $min^{-}1$ on the 1st day and 18.33 Ug^{-1} min^{-1} on the 60^{th} day. From the leakage test it was observed that the encapsulated HRP has strongly adhered onto the HG-BCNC(20%) surface, and even after 6^{th} time washing, the retained enzyme on the hydrogel surface showed a specific activity of 63.2 Ug^{-1} min^{-1} which is almost 60% of the fresh enzyme activity. Thus, from this study we can conclude that the fabricated BCNC based hydrogels are compatible with the HRP encapsulation on their surface. Hence, these hydrogels can act as support or template for effective enzyme immobilization.

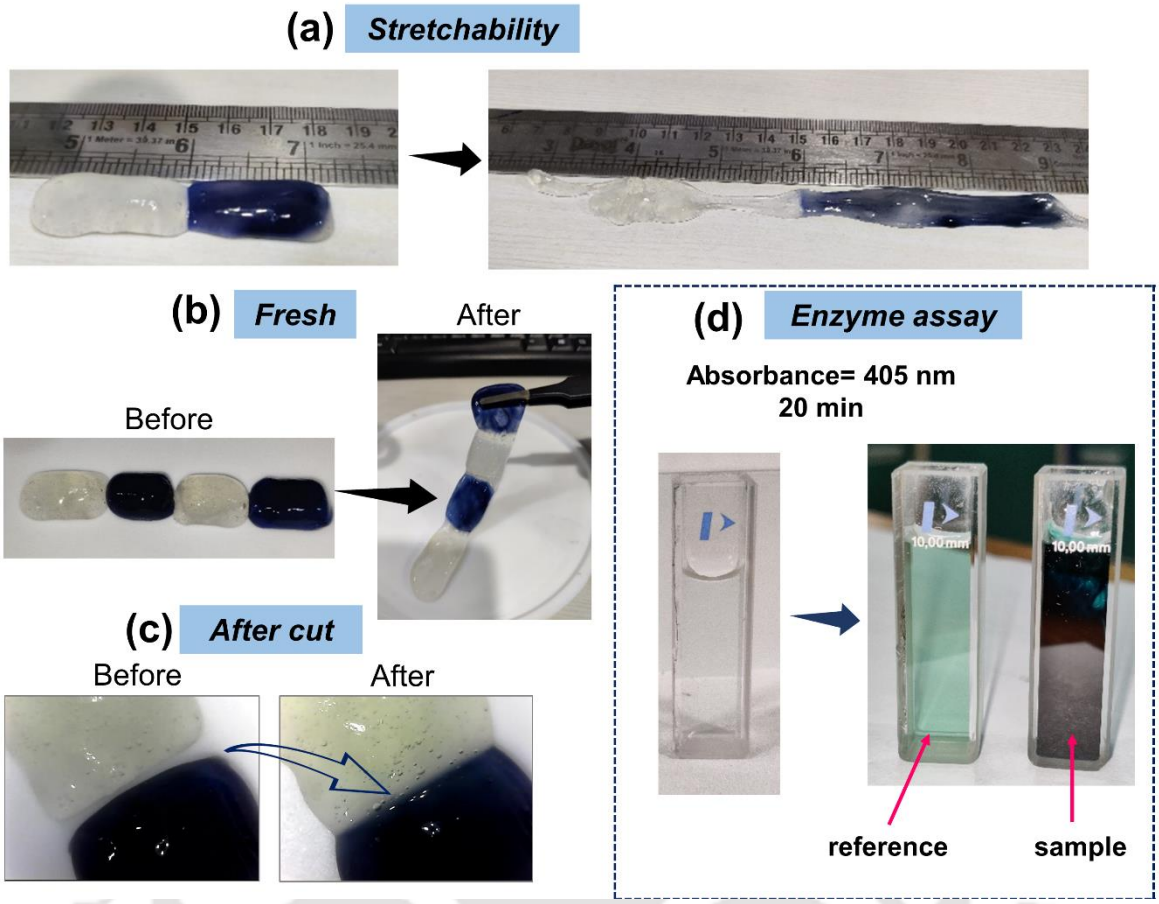

Figure 7.6. (a)Optical image showing high stretchability of the fabricated hydrogel, (b)Optical image showing the self-healing process, (c)Microscopic image of self-healing process, (d)Colorimetric enzyme assay indicating the presence of peroxidase in the sample.

7.3 CONCLUSIONS

In this study, we have reported the encapsulation of HRP on a BCNC loaded OGA hydrogel for the first time. The fabricated hydrogels showed good physico-chemical properties and excellent self-healing behaviour. The enzyme activity of the encapsulated HRP on the HG-BCNC(20%) surface and free HRP was investigated, and it was observed that the encapsulated HRP had higher specific activity than the free HRP. The leakage test of the immobilized HRP showed a strong affinity of HRP towards the gel surface even after 6^{th} wash. Thus the improved stability of the immobilized hydrogel along with their self-healing behaviour can be utilized to develop novel materials for application as biocatalyst or biosensors in biomedical field.

Chapter 8

Conclusions and Future Scope

This chapter discusses the major conclusions drawn based on the investigations carried out in this doctoral study. Also, this chapter provides useful recommendations for future work involving the utilization of these biomaterials and their application in relevant field.

8.1. CONCLUSIONS

In today's scenario, the environmental concerns related to the use of petroleum-based resources, in terms of waste management and disposal pose a serious threat to human society and the atmosphere. The use of biomass as a source not only will reduce the consumption of depleting petroleum resources but will also provide a greener and economic approach to obtain valuable biomaterials. Various strategies are formulated to produce efficient and sustainable bio-based material from biomass nowadays which could be recycled, reused, and utilized in food, packaging, textile and biomedical applications. Therefore, this dissertation work focuses on the utilization of biomass, *Gluconacetobacter xylinus* for the production of pure bacterial cellulose, and also aim in the exploration of their wide applications. Based on this, the major conclusions drawn are summarised below:

- The successful synthesis of bacterial cellulose has been interpreted by the physico-chemical characteristics. The ultrafine fibrous network of BC with excellent crystallinity (88%) and water absorption property has been characterised using spectroscopic and microscopic analyses. The highly pure, biocompatible and hydrophilic property of the synthesized BC was used as an advantageous criterion for their use in biomedical applications.
- Highly crystalline BCNCs with needle-like morphology were successfully extracted from BC using acid hydrolysis. The acid hydrolysis time was reduced and optimised as 2 h.
- The obtained biocompatible BC was successfully blended with PCL to fabricate antimicrobial wound dressing material by the impregnation of PCL into the BC matrix.

The resultant composites showed improved thermostability, wettability and excellent crystallinity (86%). The release profiles initially indicated a burst release (6 h) followed by controlled release of GEN (~42%) and SM (~58%) from the prepared scaffolds within 48 h. The in-vitro studies of the BC and BCP scaffolds against baby hamster kidney (BHK-21) cells revealed their cytocompatibility. These results interpret that the prepared drug-functionalized cellulosic scaffolds have a great potential as a wound dressing material in biomedical applications.

- BCNC templated heterogeneous ZrP catalyst was successfully synthesized and confirmed by FT-IR, XRD spectroscopy and microscopic analysis. The catalytic activity of synthesized BCNC_ZrP catalyst was examined in the conversion of furfural to HMF under different reaction conditions. The reusability of the synthesized catalyst was investigated for four runs, which resulted in comparable HMF yield. Thus, the BCNC-catalyzed hydroxymethylation reaction was successful in converting furfural to HMF giving a 28(mol%) HMF yield.
- Bacterial cellulose powder, and drug LID was successfully incorporated into PCL network using electrospinning process for the fabrication nanofibrous bandages. The developed scaffolds were then surface modified to prepare a wound dressing bandage. The prepared scaffolds exhibited excellent antimicrobial activity against *Escherichia coli* and *Staphylococcus aureus*. The drug release profiles initially indicated a 28% burst release (30 min) followed by controlled release of remaining Ag-SD in 84h and LID was released into the system in 108h with an initial burst release of 29% in 2h. Hence, these results interpret that the prepared drug-functionalized cellulosic scaffolds have a great potential as a wound dressing material in biomedical applications.
- Self-healing and stretchable hydrogels were successfully fabricated using modified Gum Arabic and BCNC. Further, the immobilization of the developed hydrogels were carried out using horseradish peroxidase enzyme. The cross-linking was confirmed through characterization by FTIR spectroscopy, SEM morphology, thermal studies. The specific enzyme activity reached 106.6 Umg^{-1} (fresh) and 29.94 Umg^{-1} (after 60 days). Thus, the immobilization of HRP on modified BCNC hydrogel enhanced its appropriateness for a future use in various biotechnological and environmental applications.

8.2 SCOPE OF FUTURE WORK

The studies carried out in this thesis can be presumed to lead to an inexpensive and sustainable approach that eliminates waste disposal and environmental concerns. This study presents a detailed investigation of the various possible applications of bacterial cellulose and its surface modification. However, there are several dimensions which may require further research exploration.

- In this study, conventional methodology was followed to synthesize BC which comprises of commercial glucose. Production of BC using different natural glucose source, such as fruit waste or components containing higher glucose content (sorghum juice, etc) can be studied. Mostly, biomass waste as glucose source can be utilized for the BC synthesis.
- A comparative analysis on the quality and quantity of bacterial cellulose can be studied using different reaction conditions.
- The statistical analysis of the bacterial growth curve can be studied.
- Optimization of BCNC production with varying reaction time and acid concentration can be studied based on their morphological and thermo-mechanical characteristics.
- In-vivo study of the electrospun nanofibrous bandages can be done to use them in practical wound healing applications.
- BCNC_ZrP was used as a catalyst in value-added chemical transformation in this study. Immobilization of this synthesized BCNC_ZrP catalyst can be done and further explored in chemical or biomedical applications as a biocatalyst.
- The mechanism of self-repair on molecular level as well as the mechanical property of the immobilized hydrogels can be investigated; and their application in biosensors can be explored.

REFERENCES

[1] W. Czaja, A. Krystynowicz, S. Bielecki, R.M. Brown, Microbial cellulose - The natural power to heal wounds, Biomaterials. 27 (2006) 145–151. https://doi.org/10.1016/j.biomaterials.2005.07.035.

[2] A. Pandit, R. Kumar, A Review on Production, Characterization and Application of Bacterial Cellulose and Its Biocomposites, J. Polym. Environ. (2021). https://doi.org/10.1007/s10924-021-02079-5.

[3] C.N. Choi, H.J. Song, M.J. Kim, M.H. Chang, S.J. Kim, Properties of bacterial cellulose produced in a pilot-scale spherical type bubble column bioreactor, Korean J. Chem. Eng. 26 (2009) 136–140. https://doi.org/10.1007/s11814-009-0021-1.

[4] S. Kaewnopparat, K. Sansernluk, D. Faroongsarng, Behavior of freezable bound water in the bacterial cellulose produced by Acetobacter xylinum: An approach using thermoporosimetry, AAPS PharmSciTech. 9 (2008) 701–707. https://doi.org/10.1208/s12249-008-9104-2.

[5] M. Ul-Islam, T. Khan, J.K. Park, Water holding and release properties of bacterial cellulose obtained by in situ and ex situ modification, Carbohydr. Polym. 88 (2012) 596–603. https://doi.org/10.1016/j.carbpol.2012.01.006.

[6] A.F.S. Costa, F.C.G. Almeida, G.M. Vinhas, L.A. Sarubbo, Production of bacterial cellulose by Gluconacetobacter hansenii using corn steep liquor as nutrient sources, Front. Microbiol. 8 (2017) 1–12. https://doi.org/10.3389/fmicb.2017.02027.

[7] D.A. Gregory, L. Tripathi, A.T.R. Fricker, E. Asare, I. Orlando, V. Raghavendran, I. Roy, Bacterial cellulose: A smart biomaterial with diverse applications, Mater. Sci. Eng. R Reports. 145 (2021) 100623. https://doi.org/10.1016/j.mser.2021.100623.

[8] F. Wahid, L.H. Huang, X.Q. Zhao, W.C. Li, Y.Y. Wang, S.R. Jia, C. Zhong, Bacterial cellulose and its potential for biomedical applications, Biotechnol. Adv. 53 (2021) 107856. https://doi.org/10.1016/j.biotechadv.2021.107856.

[9] L. Popa, M.V. Ghica, E.E. Tudoroiu, D.G. Ionescu, C.E. Dinu-Pîrvu, Bacterial Cellulose—

A Remarkable Polymer as a Source for Biomaterials Tailoring, Materials (Basel). 15 (2022). https://doi.org/10.3390/ma15031054.

[10] F. Esa, S.M. Tasirin, N.A. Rahman, Overview of Bacterial Cellulose Production and Application, Ital. Oral Surg. 2 (2014) 113–119. https://doi.org/10.1016/j.aaspro.2014.11.017.

[11] M.U. Islam, M.W. Ullah, S. Khan, N. Shah, J.K. Park, Strategies for cost-effective and enhanced production of bacterial cellulose, Int. J. Biol. Macromol. 102 (2017) 1166–1173. https://doi.org/10.1016/j.ijbiomac.2017.04.110.

[12] B. V. Mohite, B.K. Salunke, S. V. Patil, Enhanced production of bacterial cellulose by using gluconacetobacter hansenii NCIM 2529 strain under shaking conditions, Appl. Biochem. Biotechnol. 169 (2013) 1497–1511. https://doi.org/10.1007/s12010-013-0092-7.

[13] H.-J. Son, H.-G. Kim, K.-K. Kim, H.-S. Kim, Y.-G. Kim, S.-J. Lee, Increased production of bacterial cellulose by Acetobacter sp. V6 in synthetic media under shaking culture conditions, n.d.

[14] W. Czaja, D. Romanovicz, R.M. Brown, Structural investigations of microbial cellulose produced in stationary and agitated culture, n.d.

[15] A.F. Jozala, L.C. de Lencastre-Novaes, A.M. Lopes, V. de Carvalho Santos-Ebinuma, P.G. Mazzola, A. Pessoa-Jr, D. Grotto, M. Gerenutti, M.V. Chaud, Bacterial nanocellulose production and application: a 10-year overview, Appl. Microbiol. Biotechnol. 100 (2016) 2063–2072. https://doi.org/10.1007/s00253-015-7243-4.

[16] A.C. Rodrigues, A.I. Fontão, A. Coelho, M. Leal, F.A.G. Soares da Silva, Y. Wan, F. Dourado, M. Gama, Response surface statistical optimization of bacterial nanocellulose fermentation in static culture using a low-cost medium, N. Biotechnol. 49 (2019) 19–27. https://doi.org/10.1016/j.nbt.2018.12.002.

[17] K.C. Cheng, J.M. Catchmark, A. Demirci, Enhanced production of bacterial cellulose by using a biofilm reactor and its material property analysis, J. Biol. Eng. 3 (2009) 1–10. https://doi.org/10.1186/1754-1611-3-12.

[18] Z. Hussain, W. Sajjad, T. Khan, F. Wahid, Production of bacterial cellulose from industrial

wastes: a review, Cellulose. 26 (2019) 2895–2911. https://doi.org/10.1007/s10570-019-02307-1.

[19] M. Salari, M. Sowti Khiabani, R. Rezaei Mokarram, B. Ghanbarzadeh, H. Samadi Kafil, Preparation and characterization of cellulose nanocrystals from bacterial cellulose produced in sugar beet molasses and cheese whey media, Int. J. Biol. Macromol. 122 (2019) 280–288. https://doi.org/10.1016/j.ijbiomac.2018.10.136.

[20] W.W.Y. Voon, B.J. Muhialdin, N.L. Yusof, Y. Rukayadi, A.S. Meor Hussin, Bio-cellulose Production by Beijerinckia fluminensis WAUPM53 and Gluconacetobacter xylinus 0416 in Sago By-product Medium, Appl. Biochem. Biotechnol. 187 (2019) 211–220. https://doi.org/10.1007/s12010-018-2807-2.

[21] J. Ye, S. Zheng, Z. Zhang, F. Yang, K. Ma, Y. Feng, J. Zheng, D. Mao, X. Yang, Bacterial cellulose production by Acetobacter xylinum ATCC 23767 using tobacco waste extract as culture medium, Bioresour. Technol. 274 (2019) 518–524. https://doi.org/10.1016/j.biortech.2018.12.028.

[22] P. Marín, S.M. Martirani-Von Abercron, L. Urbina, D. Pacheco-Sánchez, M.A. Castañeda-Cataña, A. Retegi, A. Eceiza, S. Marqués, Bacterial nanocellulose production from naphthalene, Microb. Biotechnol. 12 (2019) 662–676. https://doi.org/10.1111/1751-7915.13399.

[23] S. Bae, Y. Sugano, M. Shoda, Improvement of Bacterial Cellulose Production by Addition of Agar in a Jar Fermentor, 2004.

[24] L.L. Zhou, D.P. Sun, L.Y. Hu, Y.W. Li, J.Z. Yang, Effect of addition of sodium alginate on bacterial cellulose production by Acetobacter xylinum, J. Ind. Microbiol. Biotechnol. 34 (2007) 483–489. https://doi.org/10.1007/s10295-007-0218-4.

[25] A.R.P. Figueiredo, A.J.D. Silvestre, C.P. Neto, C.S.R. Freire, In situ synthesis of bacterial cellulose / polycaprolactone blends for hot pressing nanocomposite films production, Carbohydr. Polym. 132 (2015) 400–408. https://doi.org/10.1016/j.carbpol.2015.06.001.

[26] O.M. Atta, S. Manan, M. Ul-Islam, A.A.Q. Ahmed, M.W. Ullah, G. Yang, Silver Decorated Bacterial Cellulose Nanocomposites as Antimicrobial Food Packaging Materials, ES Food

Agrofor. (2021) 12–26. https://doi.org/10.30919/esfaf590.

[27] S. Barbi, C. Taurino, S. La China, K. Anguluri, M. Gullo, M. Montorsi, Mechanical and structural properties of environmental green composites based on functionalized bacterial cellulose, Cellulose. 28 (2021) 1431–1442. https://doi.org/10.1007/s10570-020-03602-y.

[28] S. Taokaew, M. Phisalaphong, B. min Z. Newby, Modification of bacterial cellulose with organosilanes to improve attachment and spreading of human fibroblasts, Cellulose. 22 (2015) 2311–2324. https://doi.org/10.1007/s10570-015-0651-x.

[29] K.Y. Lee, J.J. Blaker, R. Murakami, J.Y.Y. Heng, A. Bismarck, Phase behavior of medium and high internal phase water-in-oil emulsions stabilized solely by hydrophobized bacterial cellulose nanofibrils, Langmuir. 30 (2014) 452–460. https://doi.org/10.1021/la4032514.

[30] H. Sai, R. Fu, L. Xing, J. Xiang, Z. Li, F. Li, T. Zhang, Surface modification of bacterial cellulose aerogels' web-like skeleton for oil/water separation, ACS Appl. Mater. Interfaces. 7 (2015) 7373–7381. https://doi.org/10.1021/acsami.5b00846.

[31] W. Shao, J. Wu, H. Liu, S. Ye, L. Jiang, X. Liu, Novel bioactive surface functionalization of bacterial cellulose membrane, Carbohydr. Polym. 178 (2017) 270–276. https://doi.org/10.1016/j.carbpol.2017.09.045.

[32] H. Luo, G. Xiong, Y. Huang, F. He, Y. Wang, Y. Wan, Preparation and characterization of a novel COL/BC composite for potential tissue engineering scaffolds, Mater. Chem. Phys. 110 (2008) 193–196. https://doi.org/10.1016/j.matchemphys.2008.01.040.

[33] C.R. Rambo, D.O.S. Recouvreux, C.A. Carminatti, A.K. Pitlovanciv, R. V. Antônio, L.M. Porto, Template assisted synthesis of porous nanofibrous cellulose membranes for tissue engineering, Mater. Sci. Eng. C. 28 (2008) 549–554. https://doi.org/10.1016/j.msec.2007.11.011.

[34] J. Li, Y. Wan, L. Li, H. Liang, J. Wang, Preparation and characterization of 2,3-dialdehyde bacterial cellulose for potential biodegradable tissue engineering scaffolds, Mater. Sci. Eng. C. 29 (2009) 1635–1642. https://doi.org/10.1016/j.msec.2009.01.006.

[35] Y. Hu, J.M. Catchmark, In vitro biodegradability and mechanical properties of bioabsorbable bacterial cellulose incorporating cellulases, Acta Biomater. 7 (2011) 2835–

2845. https://doi.org/10.1016/j.actbio.2011.03.028.

[36] Y. Hu, J.M. Catchmark, Integration of cellulases into bacterial cellulose: Toward bioabsorbable cellulose composites, J. Biomed. Mater. Res. - Part B Appl. Biomater. 97 B (2011) 114–123. https://doi.org/10.1002/jbm.b.31792.

[37] M. Rouabhia, J. Asselin, N. Tazi, Y. Messaddeq, D. Levinson, Z. Zhang, Production of biocompatible and antimicrobial bacterial cellulose polymers functionalized by RGDC grafting groups and gentamicin, ACS Appl. Mater. Interfaces. 6 (2014) 1439–1446. https://doi.org/10.1021/am4027983.

[38] A. Fatima, S. Yasir, M.S. Khan, S. Manan, M.W. Ullah, M. Ul-Islam, Plant extract-loaded bacterial cellulose composite membrane for potential biomedical applications, J. Bioresour. Bioprod. 6 (2021) 26–32. https://doi.org/10.1016/j.jobab.2020.11.002.

[39] Q. Shi, Y. Li, J. Sun, H. Zhang, L. Chen, B. Chen, H. Yang, Z. Wang, The osteogenesis of bacterial cellulose scaffold loaded with bone morphogenetic protein-2, Biomaterials. 33 (2012) 6644–6649. https://doi.org/10.1016/j.biomaterials.2012.05.071.

[40] J. George, Siddaramaiah, High performance edible nanocomposite films containing bacterial cellulose nanocrystals, Carbohydr. Polym. 87 (2012) 2031–2037. https://doi.org/10.1016/j.carbpol.2011.10.019.

[41] N.F. Vasconcelos, J.P.A. Feitosa, F.M.P. da Gama, J.P.S. Morais, F.K. Andrade, M. de S.M. de Souza Filho, M. de F. Rosa, Bacterial cellulose nanocrystals produced under different hydrolysis conditions: Properties and morphological features, Carbohydr. Polym. 155 (2017) 425–431. https://doi.org/10.1016/j.carbpol.2016.08.090.

[42] X. Kang, S. Kuga, C. Wang, Y. Zhao, M. Wu, Y. Huang, Green Preparation of Cellulose Nanocrystal and Its Application, ACS Sustain. Chem. Eng. 6 (2018) 2954–2960. https://doi.org/10.1021/acssuschemeng.7b02363.

[43] J. Tang, J. Sisler, N. Grishkewich, K.C. Tam, Functionalization of cellulose nanocrystals for advanced applications, J. Colloid Interface Sci. 494 (2017) 397–409. https://doi.org/10.1016/j.jcis.2017.01.077.

[44] V.S. Soeiro, L.L. Tundisi, L.C.L. Novaes, P.G. Mazzola, N. Aranha, D. Grotto, J.M.O.

Júnior, D. Komatsu, F.M.P. Gama, M. V. Chaud, A.F. Jozala, Production of bacterial cellulose nanocrystals via enzymatic hydrolysis and evaluation of their coating on alginate particles formed by ionotropic gelation, Carbohydr. Polym. Technol. Appl. 2 (2021). https://doi.org/10.1016/j.carpta.2021.100155.

[45] M. Rahimi Kord Sofla, R.J. Brown, T. Tsuzuki, T.J. Rainey, A comparison of cellulose nanocrystals and cellulose nanofibres extracted from bagasse using acid and ball milling methods, Adv. Nat. Sci. Nanosci. Nanotechnol. 7 (2016). https://doi.org/10.1088/2043-6262/7/3/035004.

[46] K. Arserim-uçar, F. Korel, L. Liu, K.L. Yam, Characterization of bacterial cellulose nanocrystals : E ff ect of acid treatments and neutralization, 336 (2021). https://doi.org/10.1016/j.foodchem.2020.127597.

[47] M. Salari, M. Sowti, R. Rezaei, B. Ghanbarzadeh, H. Samadi, International Journal of Biological Macromolecules Preparation and characterization of cellulose nanocrystals from bacterial cellulose produced in sugar beet molasses and cheese whey media, 122 (2019) 280–288. https://doi.org/10.1016/j.ijbiomac.2018.10.136.

[48] P. Singhsa, R. Narain, H. Manuspiya, Bacterial Cellulose Nanocrystals (BCNC) Preparation and Characterization from Three Bacterial Cellulose Sources and Development of Functionalized BCNCs as Nucleic Acid Delivery Systems, ACS Appl. Nano Mater. 1 (2018) 209–221. https://doi.org/10.1021/acsanm.7b00105.

[49] A. Hirai, O. Inui, F. Horii, M. Tsuji, Phase Separation Behavior in Aqueous Suspensions of Bacterial Cellulose Nanocrystals Prepared by Sulfuric Acid Treatment, (2009) 497–502.

[50] N.F. Vasconcelos, J.P.A. Feitosa, F.M.P. da Gama, J.P.S. Morais, F.K. Andrade, M. de S.M. de Souza Filho, M. de F. Rosa, Bacterial cellulose nanocrystals produced under different hydrolysis conditions: Properties and morphological features, Carbohydr. Polym. 155 (2017) 425–431. https://doi.org/10.1016/j.carbpol.2016.08.090.

[51] M. Roman, W.T. Winter, Effect of Sulfate Groups from Sulfuric Acid Hydrolysis on the Thermal Degradation Behavior of Bacterial Cellulose, Biomacromolecules 5(5) (2004) 1671–1677.

[52] D. Ciecha, Multifunctional Bacterial Cellulose / Chitosan Composite Materials for Medical Applications, 12 (2004) 69–72.

[53] T. Maneerung, S. Tokura, R. Rujiravanit, Impregnation of silver nanoparticles into bacterial cellulose for antimicrobial wound dressing, 72 (2008) 43–51. https://doi.org/10.1016/j.carbpol.2007.07.025.

[54] O. Saibuatong, M. Phisalaphong, Novo aloe vera – bacterial cellulose composite film from biosynthesis, Carbohydr. Polym. 79 (2010) 455–460. https://doi.org/10.1016/j.carbpol.2009.08.039.

[55] E. Altun, N. Ekren, S.E. Kuruca, O. Gunduz, Cell studies on Electrohydrodynamic (EHD)-3D-bioprinted Bacterial Cellulose\Polycaprolactone scaffolds for tissue engineering, Mater. Lett. 234 (2019) 163–167. https://doi.org/10.1016/j.matlet.2018.09.085.

[56] A.R.P. Figueiredo, A.J.D. Silvestre, C.P. Neto, C.S.R. Freire, In situ synthesis of bacterial cellulose/polycaprolactone blends for hot pressing nanocomposite films production, Carbohydr. Polym. 132 (2015) 400–408. https://doi.org/10.1016/j.carbpol.2015.06.001.

[57] H.S. Barud, S.J.L. Ribeiro, C.L.P. Carone, R. Ligabue, S. Einloft, P.V.S. Queiroz, A.P.B. Borges, V.D. Jahno, Optically transparent membrane based on bacterial cellulose/ polycaprolactone, Polimeros. 23 (2013) 135–138. https://doi.org/10.1590/S0104-14282013005000018.

[58] S. Gea, C.T. Reynolds, N. Roohpur, N. Soykeabkaew, Biodegradable Composites Based on Poly (-Caprolactone) and Bacterial Cellulose as a Reinforcing Agent, 4 (2010) 10–11. https://doi.org/10.1166/jbmb.2010.1108.

[59] C. Sharma, N.K. Bhardwaj, Bacterial nanocellulose: Present status, biomedical applications and future perspectives, Mater. Sci. Eng. C. 104 (2019) 109963. https://doi.org/10.1016/j.msec.2019.109963.

[60] J.D. Fontana, A.M. De Souza, C.K. Fontana, I.L. Torriani, J.C. Moreschi, B.J. Gallotti, S.J. De Souza, G.P. Narcisco, J.A. Bichara, L.F.X. Farah, Acetobacter cellulose pellicle as a temporary skin substitute, Appl. Biochem. Biotechnol. 24–25 (1990) 253–264. https://doi.org/10.1007/BF02920250.

[61] H.G. de Oliveira Barud, R.R. da Silva, H. da Silva Barud, A. Tercjak, J. Gutierrez, W.R. Lustri, O.B. de Oliveira, S.J.L. Ribeiro, A multipurpose natural and renewable polymer in medical applications: Bacterial cellulose, Carbohydr. Polym. 153 (2016) 406–420. https://doi.org/10.1016/j.carbpol.2016.07.059.

[62] Y. Xue, Z. Mou, H. Xiao, Nanocellulose as a sustainable biomass material: Structure, properties, present status and future prospects in biomedical applications, Nanoscale. 9 (2017) 14758–14781. https://doi.org/10.1039/c7nr04994c.

[63] M. Wasim, M. Mushtaq, S.U. Khan, A. Farooq, M.A. Naeem, M.R. Khan, A. Salam, Q. Wei, Development of bacterial cellulose nanocomposites: An overview of the synthesis of bacterial cellulose nanocomposites with metallic and metallic-oxide nanoparticles by different methods and techniques for biomedical applications, J. Ind. Text. 51 (2022) 1886S-1915S. https://doi.org/10.1177/1528083720977201.

[64] T. Aditya, J.P. Allain, C. Jaramillo, A.M. Restrepo, Surface Modification of Bacterial Cellulose for Biomedical Applications, Int. J. Mol. Sci. 23 (2022). https://doi.org/10.3390/ijms23020610.

[65] S. Jeremic, L. Djokic, V. Ajdačić, N. Božinović, V. Pavlovic, D.D. Manojlović, R. Babu, R. Senthamaraikannan, O. Rojas, I. Opsenica, J. Nikodinovic-Runic, Production of bacterial nanocellulose (BNC) and its application as a solid support in transition metal catalysed cross-coupling reactions, Int. J. Biol. Macromol. 129 (2019) 351–360. https://doi.org/10.1016/j.ijbiomac.2019.01.154.

[66] A. Khamkeaw, L. Phanthang, B. Jongsomjit, M. Phisalaphong, Activated carbon derived from bacterial cellulose and its use as catalyst support for ethanol conversion to ethylene, Catal. Commun. 129 (2019) 105750. https://doi.org/10.1016/j.catcom.2019.105750.

[67] T. Kamal, I. Ahmad, S.B. Khan, A.M. Asiri, Bacterial cellulose as support for biopolymer stabilized catalytic cobalt nanoparticles, Int. J. Biol. Macromol. 135 (2019) 1162–1170. https://doi.org/10.1016/j.ijbiomac.2019.05.057.

[68] L. Song, L. Shu, Y. Wang, X.F. Zhang, Z. Wang, Y. Feng, J. Yao, Metal nanoparticle-embedded bacterial cellulose aerogels via swelling-induced adsorption for nitrophenol

reduction, Int. J. Biol. Macromol. 143 (2020) 922–927. https://doi.org/10.1016/j.ijbiomac.2019.09.152.

[69] M. Pagliaro, R. Ciriminna, M. Yusuf, S. Eskandarinezhad, I. Ahmad Wani, M. Ghahremani, Z. Rezaei Nezhad, Application of nanocellulose composites in the environmental engineering: A review, J. Compos. Compd. 3 (2021) 114–128. https://doi.org/10.52547/jcc.3.2.5.

[70] O. Wichterle, D. Lím, Hydrophilic Gels for Biological Use, Nature. 185 (1960) 117–118. https://doi.org/10.1038/185117a0.

[71] E.M. Ahmed, Hydrogel: Preparation, characterization, and applications: A review, J. Adv. Res. 6 (2015) 105–121. https://doi.org/10.1016/j.jare.2013.07.006.

[72] D.A. Gyles, L.D. Castro, J.O.C. Silva, R.M. Ribeiro-Costa, A review of the designs and prominent biomedical advances of natural and synthetic hydrogel formulations, Eur. Polym. J. 88 (2017) 373–392. https://doi.org/10.1016/j.eurpolymj.2017.01.027.

[73] M. Chau, K.J. De France, B. Kopera, V.R. Machado, S. Rosenfeldt, L. Reyes, K.J.W. Chan, S. Förster, E.D. Cranston, T. Hoare, E. Kumacheva, Composite Hydrogels with Tunable Anisotropic Morphologies and Mechanical Properties, Chem. Mater. 28 (2016) 3406–3415. https://doi.org/10.1021/acs.chemmater.6b00792.

[74] T.R. Hoare, D.S. Kohane, Hydrogels in drug delivery: Progress and challenges, Polymer (Guildf). 49 (2008) 1993–2007. https://doi.org/10.1016/j.polymer.2008.01.027.

[75] J.W. McAllister, P.W. Schmidt, K.D. Dorfman, T.P. Lodge, F.S. Bates, Thermodynamics of Aqueous Methylcellulose Solutions, Macromolecules. 48 (2015) 7205–7215. https://doi.org/10.1021/acs.macromol.5b01544.

[76] J. Supramaniam, R. Adnan, N.H. Mohd Kaus, R. Bushra, Magnetic nanocellulose alginate hydrogel beads as potential drug delivery system, Int. J. Biol. Macromol. 118 (2018) 640–648. https://doi.org/10.1016/j.ijbiomac.2018.06.043.

[77] B.B. Mendes, M. Gómez-Florit, R.A. Pires, R.M.A. Domingues, R.L. Reis, M.E. Gomes, Human-based fibrillar nanocomposite hydrogels as bioinstructive matrices to tune stem cell behavior, Nanoscale. 10 (2018) 17388–17401. https://doi.org/10.1039/c8nr04273j.

[78] J.S. Gonzalez, L.N. Ludueña, A. Ponce, V.A. Alvarez, Poly(vinyl alcohol)/cellulose nanowhiskers nanocomposite hydrogels for potential wound dressings, Mater. Sci. Eng. C. 34 (2014) 54–61. https://doi.org/10.1016/j.msec.2013.10.006.

[79] P. Bhagabati, D. Hazarika, V. Katiyar, Tailor-made ultra-crystalline, high molecular weight poly(ε-caprolactone) films with improved oxygen gas barrier and optical properties: a facile and scalable approach, Int. J. Biol. Macromol. 124 (2019) 1040–1052. https://doi.org/10.1016/j.ijbiomac.2018.11.199.

[80] S. Bandyopadhyay, N. Saha, P. Saha, Characterization of Bacterial Cellulose Produced using Media Containing Waste Apple Juice, Appl. Biochem. Microbiol. 54 (2018) 649–657. https://doi.org/10.1134/S0003683818060042.

[81] S. Unal, S. Arslan, B. Karademir Yilmaz, D. Kazan, F.N. Oktar, O. Gunduz, Glioblastoma cell adhesion properties through bacterial cellulose nanocrystals in polycaprolactone/gelatin electrospun nanofibers, Carbohydr. Polym. 233 (2020). https://doi.org/10.1016/j.carbpol.2019.115820.

[82] J. Tuteja, S. Nishimura, K. Ebitani, Base-free chemoselective transfer hydrogenation of nitroarenes to anilines with formic acid as hydrogen source by a reusable heterogeneous Pd/ZrP catalyst, RSC Adv. 4 (2014) 38241–38249. https://doi.org/10.1039/c4ra06174h.

[83] A.H. Pandit, N. Mazumdar, K. Imtiyaz, M.M.A. Rizvi, S. Ahmad, Periodate-Modified Gum Arabic Cross-linked PVA Hydrogels: A Promising Approach toward Photoprotection and Sustained Delivery of Folic Acid, ACS Omega. 4 (2019) 16026–16036. https://doi.org/10.1021/acsomega.9b02137.

[84] P.R. Sarika, K. Cinthya, A. Jayakrishnan, P.R. Anilkumar, N.R. James, Modified gum arabic cross-linked gelatin scaffold for biomedical applications, Mater. Sci. Eng. C. 43 (2014) 272–279. https://doi.org/10.1016/j.msec.2014.06.042.

[85] B.W. Park, K.A. Ko, D.Y. Yoon, D.S. Kim, Enzyme activity assay for horseradish peroxidase encapsulated in peptide nanotubes, Enzyme Microb. Technol. 51 (2012) 81–85. https://doi.org/10.1016/j.enzmictec.2012.04.004.

[86] P. Chawla, B.E. Limited, I. Bajaj, Proizvodnja celuloze s pomo ć u mikroorganizama i

njezina primjena Microbial Cellulose : Fermentative Production and Applications, (2009).

[87] S. Ju, F. Zhang, J. Duan, J. Jiang, Characterization of bacterial cellulose composite films incorporated with bulk chitosan and chitosan nanoparticles: A comparative study, Carbohydr. Polym. 237 (2020) 116167. https://doi.org/10.1016/j.carbpol.2020.116167.

[88] R. Mayer, P. Ross, H. Weinhouse, D. Amikam, G. Volman, P. Ohana, R.D. Calhoont, H.C. Wongt, A.N.N.W. Emerickt, M. Benziman, Polypeptide composition of bacterial cyclic diguanylic acid-dependent cellulose synthase and the occurrence of immunologically crossreacting proteins in higher plants, 88 (1991) 5472–5476.

[89] J. Nam, Y. Hyun, S. Oh, J. Park, H. Jin, H. Won, Effect of cross-linkable bacterial cellulose nanocrystals on the physicochemical properties of silk sericin films, Polym. Test. 97 (2021) 107161. https://doi.org/10.1016/j.polymertesting.2021.107161.

[90] I. V. Novikov, M.A. Pigaleva, A. V. Naumkin, G.A. Badun, E.E. Levin, E.P. Kharitonova, T.I. Gromovykh, M.O. Gallyamov, Green approach for fabrication of bacterial cellulose-chitosan composites in the solutions of carbonic acid under high pressure CO2, Carbohydr. Polym. 258 (2021). https://doi.org/10.1016/j.carbpol.2021.117614.

[91] M.O. Aydogdu, E. Altun, J. Ahmed, O. Gunduz, M. Edirisinghe, Fiber forming capability of binary and ternary compositions in the polymer system: Bacterial cellulose-polycaprolactone-polylactic acid, Polymers (Basel). 11 (2019). https://doi.org/10.3390/polym11071148.

[92] W. Liu, H. Du, M. Zhang, K. Liu, H. Liu, H. Xie, X. Zhang, C. Si, Bacterial Cellulose-Based Composite Scaffolds for Biomedical Applications: A Review, ACS Sustain. Chem. Eng. 8 (2020) 7536–7562. https://doi.org/10.1021/acssuschemeng.0c00125.

[93] F. Wahid, X. Zhao, X. Zhao, X. Ma, N. Xue, X. Liu, F. Wang, S. Jia, C. Zhong, Fabrication of Bacterial Cellulose-Based Dressings for Promoting Infected Wound Healing, (2021). https://doi.org/10.1021/acsami.1c06986.

[94] G. Yang, J. Xie, F. Hong, Z. Cao, X. Yang, Antimicrobial activity of silver nanoparticle impregnated bacterial cellulose membrane: Effect of fermentation carbon sources of bacterial cellulose, Carbohydr. Polym. 87 (2012) 839–845.

https://doi.org/10.1016/j.carbpol.2011.08.079.

[95] M.C.I.M. Amin, A.G. Abadi, N. Ahmad, H. Katas, J.A. Jamal, Bacterial cellulose film coating as drug delivery system: Physicochemical, thermal and drug release properties, Sains Malaysiana. 41 (2012) 561–568.

[96] N. Eslahi, A. Mahmoodi, N. Mahmoudi, N. Zandi, A. Simchi, Processing and Properties of Nanofibrous Bacterial Cellulose-Containing Polymer Composites: A Review of Recent Advances for Biomedical Applications, Polym. Rev. 60 (2020) 144–170. https://doi.org/10.1080/15583724.2019.1663210.

[97] L.S. Nair, C.T. Laurencin, Biodegradable polymers as biomaterials, Prog. Polym. Sci. 32 (2007) 762–798. https://doi.org/10.1016/j.progpolymsci.2007.05.017.

[98] A. Prasad, B. Kandasubramanian, Fused deposition processing polycaprolactone of composites for biomedical applications, Polym. Technol. Mater. 58 (2019) 1365–1398. https://doi.org/10.1080/25740881.2018.1563117.

[99] M. Yamamoto, Y. Ikada, Y. Tabata, Controlled release of growth factors based on biodegradation of gelatin hydrogel, J. Biomater. Sci. Polym. Ed. 12 (2001) 77–88. https://doi.org/10.1163/156856201744461.

[100] Z. Muwaffak, A. Goyanes, V. Clark, A.W. Basit, S.T. Hilton, S. Gaisford, Patient-specific 3D scanned and 3D printed antimicrobial polycaprolactone wound dressings, Int. J. Pharm. 527 (2017) 161–170. https://doi.org/10.1016/j.ijpharm.2017.04.077.

[101] A. Bayoumi, M.T. Sarg, T.Y.A. Fahmy, N.F. Mohamed, W.K. El-Zawawy, The behavior of natural biomass materials as drug carriers in releasing loaded Gentamicin sulphate, Arab. J. Chem. 13 (2020) 8920–8934. https://doi.org/10.1016/j.arabjc.2020.10.018.

[102] E. Elizondo, S. Sala, E. Imbuluzqueta, D. González, M.J. Blanco-Prieto, C. Gamazo, N. Ventosa, J. Veciana, High loading of gentamicin in bioadhesive PVM/MA nanostructured microparticles using compressed carbon-dioxide, Pharm. Res. 28 (2011) 309–321. https://doi.org/10.1007/s11095-010-0248-x.

[103] E. Imbuluzqueta, E. Elizondo, C. Gamazo, E. Moreno-Calvo, J. Veciana, N. Ventosa, M.J. Blanco-Prieto, Novel bioactive hydrophobic gentamicin carriers for the treatment of

intracellular bacterial infections, Acta Biomater. 7 (2011) 1599–1608. https://doi.org/10.1016/j.actbio.2010.11.031.

[104] T. Sharma, A. Kumar, S.S. Shah, R.K. Bamezai, Analysis of interactions between streptomycin sulphate and aqueous food acids (L-ascorbic acid and citric acid): Physico-chemical and spectroscopic insights, J. Chem. Thermodyn. 151 (2020) 106207. https://doi.org/10.1016/j.jct.2020.106207.

[105] S. Sharma, K. Kumar, S. Chauhan, M.S. Chauhan, Conductometric and spectrophotometric studies of self-aggregation behavior of streptomycin sulphate in aqueous solution: Effect of electrolytes, J. Mol. Liq. 297 (2020) 111782. https://doi.org/10.1016/j.molliq.2019.111782.

[106] M. Singh, N. Schiavone, L. Papucci, P. Maan, J. Kaur, G. Singh, U. Nandi, D. Nosi, A. Tani, G.K. Khuller, M. Priya, R. Singh, I.P. Kaur, Streptomycin sulphate loaded solid lipid nanoparticles show enhanced uptake in macrophage, lower MIC in Mycobacterium and improved oral bioavailability, Eur. J. Pharm. Biopharm. 160 (2021) 100–124. https://doi.org/10.1016/j.ejpb.2021.01.009.

[107] Y. Jia, X. Wang, M. Huo, X. Zhai, F. Li, C. Zhong, Preparation and characterization of a novel bacterial cellulose / chitosan bio-hydrogel, 7 (2017) 1–8. https://doi.org/10.1177/1847980417707172.

[108] W.C. Lin, C.C. Lien, H.J. Yeh, C.M. Yu, S.H. Hsu, Bacterial cellulose and bacterial cellulose-chitosan membranes for wound dressing applications, Carbohydr. Polym. 94 (2013) 603–611. https://doi.org/10.1016/j.carbpol.2013.01.076.

[109] P. Kotcharat, P. Chuysinuan, T. Thanyacharoen, S. Techasakul, S. Ummartyotin, Development of bacterial cellulose and polycaprolactone (PCL) based composite for medical material, Sustain. Chem. Pharm. 20 (2021) 100404. https://doi.org/10.1016/j.scp.2021.100404.

[110] J.C. Meza-Contreras, R. Manriquez-Gonzalez, J.A. Gutiérrez-Ortega, Y. Gonzalez-Garcia, XRD and solid state 13C-NMR evaluation of the crystallinity enhancement of 13C-labeled bacterial cellulose biosynthesized by Komagataeibacter xylinus under different stimuli: A comparative strategy of analyses, Carbohydr. Res. 461 (2018) 51–59.

https://doi.org/10.1016/j.carres.2018.03.005.

[111] M. Wang, J. Li, G. Shi, G. Liu, A.J. Müller, D. Wang, Suppression of the Self-Nucleation Effect of Semicrystalline Polymers by Confinement, Macromolecules. 54 (2021) 3810–3821. https://doi.org/10.1021/acs.macromol.1c00485.

[112] S.C. Pinto, G. Gonçalves, S. Sandoval, A.M. López-Periago, A. Borras, C. Domingo, G. Tobias, I. Duarte, R. Vicente, P.A.A.P. Marques, Bacterial cellulose/graphene oxide aerogels with enhanced dimensional and thermal stability, Carbohydr. Polym. 230 (2020) 115598. https://doi.org/10.1016/j.carbpol.2019.115598.

[113] X. Wang, J. Tang, J. Huang, M. Hui, Production and characterization of bacterial cellulose membranes with hyaluronic acid and silk sericin, Colloids Surfaces B Biointerfaces. 195 (2020) 111273. https://doi.org/10.1016/j.colsurfb.2020.111273.

[114] R.L. Oliveira, J.G. Vieira, H.S. Barud, R.M.N. Assunção, G.R. Filho, S.J.L. Ribeiro, Y. Messadeqq, Synthesis and characterization of methylcellulose produced from bacterial cellulose under heterogeneous condition, J. Braz. Chem. Soc. 26 (2015) 1861–1870. https://doi.org/10.5935/0103-5053.20150163.

[115] B. Surma-Ślusarska, S. Presler, D. Danielewicz, Characteristics of bacterial cellulose obtained from Acetobacter Xylinum culture for application in papermaking, Fibres Text. East. Eur. 16 (2008) 108–111.

[116] A.N. Frone, D.M. Panaitescu, I. Chiulan, C.A. Nicolae, A. Casarica, A.R. Gabor, R. Trusca, C.M. Damian, V. Purcar, E. Alexandrescu, P.O. Stanescu, Surface treatment of bacterial cellulose in mild, eco-friendly conditions, Coatings. 8 (2018). https://doi.org/10.3390/coatings8060221.

[117] N. Chiaoprakobkij, T. Suwanmajo, N. Sanchavanakit, Curcumin-Loaded Bacterial Cellulose / Alginate / Gelatin, Mol. Imprinted Sensors. 25 (2020) 1–18.

[118] M. Milosevic, D.B. Stojanovic, V. Simic, M. Grkovic, M. Bjelovic, P.S. Uskokovic, M. Kojic, Preparation and modeling of three-layered PCL/PLGA/PCL fibrous scaffolds for prolonged drug release, Sci. Rep. 10 (2020) 1–12. https://doi.org/10.1038/s41598-020-68117-9.

[119] M. Sunde, M. Norström, The genetic background for streptomycin resistance in Escherichia coli influences the distribution of MICs, J. Antimicrob. Chemother. 56 (2005) 87–90. https://doi.org/10.1093/jac/dki150.

[120] C. Castro, R. Zuluaga, C. Álvarez, J.L. Putaux, G. Caro, O.J. Rojas, I. Mondragon, P. Gañán, Bacterial cellulose produced by a new acid-resistant strain of Gluconacetobacter genus, Carbohydr. Polym. 89 (2012) 1033–1037. https://doi.org/10.1016/j.carbpol.2012.03.045.

[121] C. Dwivedi, H. Pandey, A. Pandey, P. Ramteke, Fabrication and Assessment of Gentamicin Loaded Electrospun Nanofibrous Scaffolds as a Quick Wound Healing Dressing Material, Curr. Nanosci. 11 (2014) 222–228. https://doi.org/10.2174/15734137106661410032219 54.

[122] A.R. Unnithan, G. Gnanasekaran, Y. Sathishkumar, Y.S. Lee, C.S. Kim, Electrospun antibacterial polyurethane-cellulose acetate-zein composite mats for wound dressing, Carbohydr. Polym. 102 (2014) 884–892. https://doi.org/10.1016/j.carbpol.2013.10.070.

[123] B. Sun, F. Wei, W. Li, X. Xu, H. Zhang, M. Liu, J. Lin, B. Ma, C. Chen, D. Sun, Macroporous bacterial cellulose grafted by oligopeptides induces biomimetic mineralization via interfacial wettability, Colloids Surfaces B Biointerfaces. 183 (2019). https://doi.org/10.1016/j.colsurfb.2019.110457.

[124] G. Delepierre, O.M. Vanderfleet, E. Niinivaara, B. Zakani, E.D. Cranston, Benchmarking Cellulose Nanocrystals Part II: New Industrially Produced Materials, Langmuir. 37 (2021) 8393–8409. https://doi.org/10.1021/acs.langmuir.1c00550.

[125] G.K. Parshetti, M.S. Suryadharma, T.P.T. Pham, R. Mahmood, R. Balasubramanian, Heterogeneous catalyst-assisted thermochemical conversion of food waste biomass into 5-hydroxymethylfurfural, Bioresour. Technol. 178 (2015) 19–27. https://doi.org/10.1016/j.biortech.2014.10.066.

[126] H. Xie, X. Lai, H. Li, X. Zeng, Fabrication of ZrP nanosheet decorated macromolecular charring agent and its efficient synergism with ammonium polyphosphate in flame-retarding polypropylene, Compos. Part A Appl. Sci. Manuf. 105 (2018) 223–234. https://doi.org/10.1016/j.compositesa.2017.12.001.

[127] S. Nishimura, A. Shibata, K. Ebitani, Direct Hydroxymethylation of Furaldehydes with Aqueous Formaldehyde over a Reusable Sulfuric Functionalized Resin Catalyst, ACS Omega. 3 (2018) 5988–5993. https://doi.org/10.1021/acsomega.8b00120.

[128] J. Li, Y. Xu, M. Zhang, D. Wang, Determination of Furfural and 5-Hydroxymethylfurfural in Biomass Hydrolysate by High-Performance Liquid Chromatography, Energy and Fuels. 31 (2017) 13769–13774. https://doi.org/10.1021/acs.energyfuels.7b02827.

[129] B. Liu, Z. Zhang, Z. Kent, Microwave-assisted catalytic conversion of cellulose into 5-hydroxymethylfurfural in ionic liquids, Chem. Eng. J. 215–216 (2013) 517–521. https://doi.org/10.1016/j.cej.2012.11.019.

[130] B.K. Ozsel, D. Ozturk, B. Nis, One-pot hydrothermal conversion of different residues to value-added chemicals usıng new acidic carbonaceous catalyst, Bioresour. Technol. 289 (2019) 121627. https://doi.org/10.1016/j.biortech.2019.121627.

[131] Z. Miao, L. Xu, H. Song, H. Zhao, L. Chou, One-pot synthesis of ordered mesoporous zirconium oxophosphate with high thermostability and acidic properties, Catal. Sci. Technol. 3 (2013) 1942–1954. https://doi.org/10.1039/c3cy00085k.

[132] T. Parangi, B. Wani, U. Chudasama, A Comparative Study of Proton Transport Properties of Cerium (IV) and Thorium (IV) Phosphates, Electrochim. Acta. 148 (2014) 79–84. https://doi.org/10.1016/j.electacta.2014.10.032.

[133] A. Jain, A.M. Shore, S.C. Jonnalagadda, K. V. Ramanujachary, A. Mugweru, Conversion of fructose, glucose and sucrose to 5-hydroxymethyl-2-furfural over mesoporous zirconium phosphate catalyst, Appl. Catal. A Gen. 489 (2015) 72–76. https://doi.org/10.1016/j.apcata.2014.10.020.

[134] T.C. Huang, G.H. Lai, C.E. Li, M.H. Tsai, P.Y. Wan, Y.H. Chung, M.H. Lin, Advanced anti-corrosion coatings prepared from α-zirconium phosphate/polyurethane nanocomposites, RSC Adv. 7 (2017) 9908–9913. https://doi.org/10.1039/c6ra27588e.

[135] H. Motasadizadeh, S. Azizi, A. Shaabani, M.G. Sarvestani, R. Sedghi, R. Dinarvand, Development of PVA/Chitosan-g-Poly (N-vinyl imidazole)/TiO2/curcumin nanofibers as high-performance wound dressing, Carbohydr. Polym. 296 (2022) 119956.

https://doi.org/10.1016/j.carbpol.2022.119956.

[136] S. Yang, X. Li, P. Liu, M. Zhang, C. Wang, B. Zhang, Multifunctional Chitosan/Polycaprolactone Nanofiber Scaffolds with Varied Dual-Drug Release for Wound-Healing Applications, ACS Biomater. Sci. Eng. 6 (2020) 4666–4676. https://doi.org/10.1021/acsbiomaterials.0c00674.

[137] E. Rezvani Ghomi, S. Khalili, S. Nouri Khorasani, R. Esmaeely Neisiany, S. Ramakrishna, Wound dressings: Current advances and future directions, J. Appl. Polym. Sci. 136 (2019) 1–12. https://doi.org/10.1002/app.47738.

[138] G. Tao, R. Cai, Y. Wang, L. Liu, H. Zuo, P. Zhao, A. Umar, C. Mao, Q. Xia, H. He, Bioinspired design of AgNPs embedded silk sericin-based sponges for efficiently combating bacteria and promoting wound healing, Mater. Des. 180 (2019) 107940. https://doi.org/10.1016/j.matdes.2019.107940.

[139] D. Liang, B.S. Hsiao, B. Chu, Functional electrospun nanofibrous scaffolds for biomedical applications, Adv. Drug Deliv. Rev. 59 (2007) 1392–1412. https://doi.org/10.1016/j.addr.2007.04.021.

[140] K.Y. Lee, L. Jeong, Y.O. Kang, S.J. Lee, W.H. Park, Electrospinning of polysaccharides for regenerative medicine, Adv. Drug Deliv. Rev. 61 (2009) 1020–1032. https://doi.org/10.1016/j.addr.2009.07.006.

[141] J. Han, L. Xiong, X. Jiang, X. Yuan, Y. Zhao, D. Yang, Bio-functional electrospun nanomaterials: From topology design to biological applications, Prog. Polym. Sci. 91 (2019) 1–28. https://doi.org/10.1016/j.progpolymsci.2019.02.006.

[142] F. Zhou, C. Cui, S. Sun, S. Wu, S. Chen, J. Ma, C.M. Li, Electrospun ZnO-loaded chitosan/PCL bilayer membranes with spatially designed structure for accelerated wound healing, Carbohydr. Polym. 282 (2022) 119131. https://doi.org/10.1016/j.carbpol.2022.119131.

[143] C. Günday, S. Anand, H.B. Gencer, S. Munafò, L. Moroni, A. Fusco, G. Donnarumma, C. Ricci, P.C. Hatir, N.G. Türeli, A.E. Türeli, C. Mota, S. Danti, Ciprofloxacin-loaded polymeric nanoparticles incorporated electrospun fibers for drug delivery in tissue

engineering applications, Drug Deliv. Transl. Res. 10 (2020) 706–720. https://doi.org/10.1007/s13346-020-00736-1.

[144] M.T. Islam, R.M. Laing, C.A. Wilson, M. McConnell, M.A. Ali, Fabrication and characterization of 3-dimensional electrospun poly(vinyl alcohol)/keratin/chitosan nanofibrous scaffold, Carbohydr. Polym. 275 (2022) 118682. https://doi.org/10.1016/j.carbpol.2021.118682.

[145] F. Wahid, X.J. Zhao, X.Q. Zhao, X.F. Ma, N. Xue, X.Z. Liu, F.P. Wang, S.R. Jia, C. Zhong, Fabrication of Bacterial Cellulose-Based Dressings for Promoting Infected Wound Healing, ACS Appl. Mater. Interfaces. 13 (2021) 32716–32728. https://doi.org/10.1021/acsami.1c06986.

[146] S. Khan, M. Ul-Islam, M.W. Ullah, Y. Zhu, K.B. Narayanan, S.S. Han, J.K. Park, Fabrication strategies and biomedical applications of three-dimensional bacterial cellulose-based scaffolds: A review, Int. J. Biol. Macromol. 209 (2022) 9–30. https://doi.org/https://doi.org/10.1016/j.ijbiomac.2022.03.191.

[147] M.O. Aydogdu, E. Altun, M. Crabbe-Mann, F. Brako, F. Koc, G. Ozen, S.E. Kuruca, U. Edirisinghe, C.J. Luo, O. Gunduz, M. Edirisinghe, Cellular interactions with bacterial cellulose: Polycaprolactone nanofibrous scaffolds produced by a portable electrohydrodynamic gun for point-of-need wound dressing, Int. Wound J. 15 (2018) 789–797. https://doi.org/10.1111/iwj.12929.

[148] C. Zhijiang, X. Ping, H. Shiqi, Z. Cong, Soy protein nanoparticles modified bacterial cellulose electrospun nanofiber membrane scaffold by ultrasound-induced self-assembly technique: characterization and cytocompatibility, Cellulose. 26 (2019) 6133–6150. https://doi.org/10.1007/s10570-019-02513-x.

[149] B.J. Kim, H. Cheong, E. Choi, S. Yun, B. Choi, K. Park, I.S. Kim, D. Park, H.J. Cha, A ccelerated skin wound healing using electrospun nanofibrous mats blended with mussel adhesive protein and polycaprolactone, J. Biomed. Mater. Res. Part A. 105 (2017) 218–225.

[150] S. Saghazadeh, C. Rinoldi, M. Schot, S.S. Kashaf, F. Sharifi, E. Jalilian, K. Nuutila, G. Giatsidis, P. Mostafalu, H. Derakhshandeh, K. Yue, W. Swieszkowski, A. Memic, A.

Tamayol, A. Khademhosseini, Drug delivery systems and materials for wound healing applications, Adv. Drug Deliv. Rev. 127 (2018) 138–166. https://doi.org/https://doi.org/10.1016/j.addr.2018.04.008.

[151] K. Khoshnevisan, H. Maleki, H. Samadian, M. Doostan, M.R. Khorramizadeh, Antibacterial and antioxidant assessment of cellulose acetate/polycaprolactone nanofibrous mats impregnated with propolis, Int. J. Biol. Macromol. 140 (2019) 1260–1268. https://doi.org/https://doi.org/10.1016/j.ijbiomac.2019.08.207.

[152] Z. Moazzami Goudarzi, T. Behzad, L. Ghasemi-Mobarakeh, M. Kharaziha, M.S. Enayati, Structural and mechanical properties of fibrous poly (caprolactone)/gelatin nanocomposite incorporated with cellulose nanofibers, Polym. Bull. 77 (2020) 717–740. https://doi.org/10.1007/s00289-019-02756-5.

[153] S. Unal, S. Arslan, B. Karademir Yilmaz, D. Kazan, F.N. Oktar, O. Gunduz, Glioblastoma cell adhesion properties through bacterial cellulose nanocrystals in polycaprolactone/gelatin electrospun nanofibers, Carbohydr. Polym. 233 (2020) 115820. https://doi.org/10.1016/j.carbpol.2019.115820.

[154] A. Azarniya, E. Tamjid, N. Eslahi, A. Simchi, Modification of bacterial cellulose/keratin nanofibrous mats by a tragacanth gum-conjugated hydrogel for wound healing, Int. J. Biol. Macromol. 134 (2019) 280–289. https://doi.org/https://doi.org/10.1016/j.ijbiomac.2019.05.023.

[155] A. Fadakar Sarkandi, M. Montazer, M. Mahmoudi Rad, Oxygenated-bacterial-cellulose nanofibers with hydrogel, antimicrobial, and controlled oxygen release properties for rapid wound healing, J. Appl. Polym. Sci. 139 (2022) 51974.

[156] Y. Wan, S. Yang, J. Wang, D. Gan, M. Gama, Z. Yang, Y. Zhu, F. Yao, H. Luo, Scalable synthesis of robust and stretchable composite wound dressings by dispersing silver nanowires in continuous bacterial cellulose, Compos. Part B Eng. 199 (2020) 108259. https://doi.org/https://doi.org/10.1016/j.compositesb.2020.108259.

[157] R. Singh, P. Roopmani, M. Chauhan, S.M. Basu, W. Deeksha, M.D. Kazem, S. Hazra, E. Rajakumara, J. Giri, Silver sulfadiazine loaded core-shell airbrushed nanofibers for burn

wound healing application, Int. J. Pharm. 613 (2022) 121358. https://doi.org/10.1016/j.ijpharm.2021.121358.

[158] P. Kotcharat, P. Chuysinuan, T. Thanyacharoen, S. Techasakul, S. Ummartyotin, Enhanced Performance of Aloe vera-Incorporated Bacterial Cellulose/Polycaprolactone Composite Film for Wound Dressing Applications, J. Polym. Environ. (2021). https://doi.org/10.1007/s10924-021-02262-8.

[159] S. da S. Anacleto, M.M.C. Borges, H.L. de Oliveira, A.R. Vicente, E.C. de Figueiredo, M.A.L. de Oliveira, B.J.P. Borges, M.A. de Oliveira, W. de S. Borges, K.B. Borges, Evaluation of physicochemical properties as supporting information on quality control of raw materials and veterinary pharmaceutical formulations, J. Pharm. Anal. 8 (2018) 168–175. https://doi.org/10.1016/j.jpha.2018.01.001.

[160] J. Ahmed, M. Gultekinoglu, M. Edirisinghe, Bacterial cellulose micro-nano fibres for wound healing applications, Biotechnol. Adv. 41 (2020) 107549. https://doi.org/10.1016/j.biotechadv.2020.107549.

[161] M. Aljohani, J. Alkabli, M.M. Abualnaja, A.F. Alrefaei, S.J. Almehmadi, M.H.H. Mahmoud, N.M. El-Metwaly, Electrospun AgNPs-polylactate nanofibers and their antimicrobial applications, React. Funct. Polym. 167 (2021) 104999. https://doi.org/10.1016/j.reactfunctpolym.2021.104999.

[162] J. Tavakoli, Physico-mechanical, morphological and biomedical properties of a novel natural wound dressing material, J. Mech. Behav. Biomed. Mater. 65 (2017) 373–382. https://doi.org/10.1016/j.jmbbm.2016.09.008.

[163] K. Kaya, S. Rota, B. Doğan, G. Kökten, B. Günaydin, G. Bozdayi, Comparison of the antibacterial effects of two local anesthetics: Lidocaine and articaine, Turkish J. Med. Sci. 37 (2007) 7–10.

[164] M. Das, O. Zandraa, C. Mudenur, N. Saha, P. Sáha, B. Mandal, V. Katiyar, Composite Scaffolds Based on Bacterial Cellulose for Wound Dressing Application, ACS Appl. Bio Mater. 5 (2022) 3722–3733. https://doi.org/10.1021/acsabm.2c00226.

[165] S. Moreira, N.B. Silva, J. Almeida-Lima, H.A.O. Rocha, S.R.B. Medeiros, C. Alves, F.M.

Gama, BC nanofibres: In vitro study of genotoxicity and cell proliferation, Toxicol. Lett. 189 (2009) 235–241. https://doi.org/10.1016/j.toxlet.2009.06.849.

[166] J. Jian, Y. Xie, S. Gao, Y. Sun, C. Lai, J. Wang, C. Wang, F. Chu, D. Zhang, A skin-inspired biomimetic strategy to fabricate cellulose enhanced antibacterial hydrogels as strain sensors, Carbohydr. Polym. 294 (2022) 119760. https://doi.org/10.1016/j.carbpol.2022.119760.

[167] S. Jo, S. Park, Y. Oh, J. Hong, H.J. Kim, K.J. Kim, K.K. Oh, S.H. Lee, Development of Cellulose Hydrogel Microspheres for Lipase Immobilization, Biotechnol. Bioprocess Eng. 24 (2019) 145–154. https://doi.org/10.1007/s12257-018-0335-0.

[168] S. Wang, J. Xu, Q. Wang, X. Fan, Y. Yu, P. Wang, Y. Zhang, J. Yuan, A. Cavaco-Paulo, Preparation and rheological properties of starch-g-poly(butyl acrylate) catalyzed by horseradish peroxidase, Process Biochem. 59 (2017) 104–110. https://doi.org/10.1016/j.procbio.2017.01.014.

[169] B. Yu, H. Cheng, W. Zhuang, C.J. Zhu, J. Wu, H. Niu, D. Liu, Y. Chen, H. Ying, Stability and repeatability improvement of horseradish peroxidase by immobilization on amino-functionalized bacterial cellulose, Process Biochem. 79 (2019) 40–48. https://doi.org/10.1016/j.procbio.2018.12.024.

[170] M. Besharati Vineh, A.A. Saboury, A.A. Poostchi, A.M. Rashidi, K. Parivar, Stability and activity improvement of horseradish peroxidase by covalent immobilization on functionalized reduced graphene oxide and biodegradation of high phenol concentration, Int. J. Biol. Macromol. 106 (2018) 1314–1322. https://doi.org/10.1016/j.ijbiomac.2017.08.133.

[171] Q. Chang, H. Tang, Immobilization of horseradish peroxidase on NH2-modified magnetic Fe3O4/SiO2 particles and its application in removal of 2,4-dichlorophenol, Molecules. 19 (2014) 15768–15782. https://doi.org/10.3390/molecules191015768.

[172] M.L. Cacicedo, M.C. Castro, I. Servetas, L. Bosnea, K. Boura, P. Tsafrakidou, A. Dima, A. Terpou, A. Koutinas, G.R. Castro, Progress in bacterial cellulose matrices for biotechnological applications, Bioresour. Technol. 213 (2016) 172–180.

https://doi.org/10.1016/j.biortech.2016.02.071.

[173] G.F. Picheth, C.L. Pirich, M.R. Sierakowski, M.A. Woehl, C.N. Sakakibara, C.F. de Souza, A.A. Martin, R. da Silva, R.A. de Freitas, Bacterial cellulose in biomedical applications: A review, Int. J. Biol. Macromol. 104 (2017) 97–106. https://doi.org/10.1016/j.ijbiomac.2017.05.171.

[174] M. Li, H. Li, X. Li, H. Zhu, Z. Xu, L. Liu, J. Ma, M. Zhang, A Bioinspired Alginate-Gum Arabic Hydrogel with Micro-/Nanoscale Structures for Controlled Drug Release in Chronic Wound Healing, ACS Appl. Mater. Interfaces. 9 (2017) 22160–22175. https://doi.org/10.1021/acsami.7b04428.

[175] F.H. Tsai, Y. Kitamura, M. Kokawa, Effect of gum arabic-modified alginate on physicochemical properties, release kinetics, and storage stability of liquid-core hydrogel beads, Carbohydr. Polym. 174 (2017) 1069–1077. https://doi.org/10.1016/j.carbpol.2017.07.031.

[176] B. Singh, S. Sharma, A. Dhiman, Acacia gum polysaccharide based hydrogel wound dressings: Synthesis, characterization, drug delivery and biomedical properties, Carbohydr. Polym. 165 (2017) 294–303. https://doi.org/10.1016/j.carbpol.2017.02.039.

[177] S. Ondaral, O. Kurtuluş, G. Öztürk, M.E. Ergün, İ. Yakın, Aldehyde Starch Complexes: Adsorption on Cellulose Model Film and Performance as a Strength Additive for Papermaking, BioResources. 13 (2018) 4470–4483. https://doi.org/10.15376/BIORES.13.2.4470-4483.

[178] C. Shao, Y. Miyazaki, S. Matsuoka, K. Yoshimura, H. Sakashita, Complexation of borate with cross-linked polysaccharide anion exchanger: 11B NMR and adsorption properties studies, Macromolecules. 33 (2000) 19–25. https://doi.org/10.1021/ma991257o.

[179] M. Farooq, S. Sagbas, M. Sahiner, M. Siddiq, M. Turk, N. Aktas, N. Sahiner, Synthesis, characterization and modification of Gum Arabic microgels for hemocompatibility and antimicrobial studies, Carbohydr. Polym. 156 (2017) 380–389. https://doi.org/10.1016/j.carbpol.2016.09.052.

[180] T. Şişmanoɨlu, S. Karakuş, Ö. Birer, G.S.P. Soylu, A. Kolan, E. Tan, Ö. Ürk, G. Akdut, A.

Kilislioglu, Preparation and characterization of antibacterial Senegalia (Acacia) Senegal/iron-silica bio-nanocomposites, Appl. Surf. Sci. 354 (2015) 250–255. https://doi.org/10.1016/j.apsusc.2015.07.206.

[181] T.A.P. Hai, R. Sugimoto, Fabrication of multicolor fluorescent polyvinyl alcohol through surface modification with conjugated polymers by oxidative polymerization, Appl. Surf. Sci. 443 (2018) 1–10. https://doi.org/10.1016/j.apsusc.2018.02.200.

[182] L.Y. Jun, N.M. Mubarak, L.S. Yon, C.H. Bing, M. Khalid, P. Jagadish, E.C. Abdullah, Immobilization of Peroxidase on Functionalized MWCNTs-Buckypaper/Polyvinyl alcohol Nanocomposite Membrane, Sci. Rep. 9 (2019) 1–15. https://doi.org/10.1038/s41598-019-39621-4.

RESEARCH OUTPUT

Book Chapters

1) **M. Das**, B. Mandal, & V. Katiyar, (2020). Sustainable routes for synthesis of poly (ε-caprolactone): Prospects in chemical industries. In Advances in Sustainable Polymers (pp. 21-33). Springer, Singapore.
2) T. Ghosh, **M. Das**, & V. Katiyar. (2021). Starch-Based Nanostructured Materials in Edible Food Packaging. In Nanotechnology in Edible Food Packaging (pp. 139-164). Springer, Singapore.
3) T. Ghosh, M. Modu Aji, **M. Das**, & V. Katiyar. (2021). Biopolymer Nanocomposites in Edible Food Packaging: Opportunity and Applications. In Nanotechnology in Edible Food Packaging (pp. 233-257). Springer, Singapore.

Journal Publications

1) **M. Das**, O. Zandraa, C. Mudenur, N. Saha, P. Sáha, B. Mandal, V. Katiyar, (2022). "Composite Scaffolds Based on Bacterial Cellulose for Wound Dressing Application", *ACS Applied Bio Materials*, 5, 8, 3722–3733, https://doi.org/10.1021/acsabm.2c00226.
2) **M. Das**, B. Mandal, & V. Katiyar, (2020). "Environment-friendly synthesis of sustainable chitosan-based nonisocyanate polyurethane: a biobased polymeric film", *Journal of Applied Polymer Science*, 137(36), 49050.
3) **M. Das**, Narendren S., P. Shukla, B. Mandal, & V. Katiyar, Fabrication of electrospun bacterial cellulose/PCL nanofibrous wound dressing material. [*Communicated in Sustainable Chemistry and Pharmacy*]
4) **M. Das**, B. Mandal, & V. Katiyar, Green Preparation of Cellulose Nanocrystal and its Application in value-added chemical transformation. [*To be communicated*]
5) **M. Das**, B. Mandal, & V. Katiyar, Natural and Self-healing Immobilized Bacterial Cellulose Nanocrystals Hydrogel. [*To be communicated*]

Patents

1) V. Katiyar & **M. Das**, (2022). Process for preparation of nanocellulose supported heterogeneous catalyst for utilization in value-added chemical transformation [Application No.: 202331009555].
2) V. Katiyar & **M. Das**, (2022). Biodegradable electrospun bandage and a method of preparation thereof [Under Submission].

Conference Presentations

1) Munmi Das, Nabanita Saha, Petr Sáha, Bishnupada Mandal, Vimal Katiyar, Development of Sustainable Polymer Based Bionanocomposites as a Degradable Food Packaging Material, *International Symposium on Sustainable Polymers & National Symposium on Chemistry Education for Sustainable Engineering*, August 23-25, 2019, IIT Guwahati. [**ACS Best Poster Award]**
2) Munmi Das, Bishnupada Mandal, Vimal Katiyar, Effect of incorporation of Lignin on Green Polyurethane synthesized via Non-isocyanate route, *International Symposium on Advances in Sustainable Polymers, ASP-17*, January 8-11, 2018.

APPENDIX I: Front Pages of the Published Articles

ACS APPLIED BIO MATERIALS

www.acsabm.org Article

Composite Scaffolds Based on Bacterial Cellulose for Wound Dressing Application

Munmi Das, Oyunchimeg Zandraa, Chethana Mudenur, Nabanita Saha, Petr Sáha, Bishnupada Mandal, and Vimal Katiyar*

Cite This: *ACS Appl. Bio Mater.* 2022, 5, 3722−3733 Read Online

ACCESS | Metrics & More | Article Recommendations | Supporting Information

ABSTRACT: Wound dressing materials fabricated using biocompatible polymers have become quite relevant in medical applications, and one such material is bacterial cellulose (BC) with exceptional properties in terms of biocompatibility, high purity, crystallinity (~88%), and high water holding capacity. However, the lack of antibacterial activity slightly restricts its application as a wound dressing material. In this work, polycaprolactone (PCL) was first impregnated into the BC matrix to fabricate flexible bacterial cellulose-based PCL membranes (BCP), which was further functionalized with antibiotics gentamicin (GEN) and streptomycin (SM) separately, to form wound dressing composite scaffolds to aid infectious wound healing. Fourier transform infrared spectroscopy (FT-IR) results confirmed the presence of characteristic PCL and cellulose peaks in the composite scaffolds at 1720 cm^{-1}, 3400 cm^{-1}, and 2895 cm^{-1}, respectively, explaining the successful interaction of PCL with the BC matrix, which is further corroborated by scanning electron microscopy (SEM) images. X-ray diffraction (XRD) studies revealed the formation of highly crystalline BCP films (~86%). In vitro studies of the BC and BCP scaffolds against baby hamster kidney (BHK-21) cells revealed their cytocompatible nature; also the wettability studies indicated the hydrophilicity of the developed scaffolds, qualifying the main criterion in wound dressing applications. Energy dispersive X-ray analysis (EDX) of the drug loaded scaffolds showed the presence of sulfur in the composites. The prepared scaffolds also exhibited excellent antimicrobial activity against *Escherichia coli* and *Staphylococcus aureus*. The release profiles initially indicated a burst release (6 h) followed by controlled release of GEN (~42%) and SM (~58%) from the prepared scaffolds within 48 h. Hence, these results interpret that the prepared drug-functionalized cellulosic scaffolds have great potential as a wound dressing material in biomedical applications.

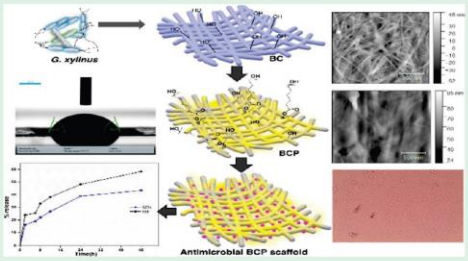

KEYWORDS: *bacterial cellulose, polycaprolactone, gentamicin, streptomycin, antimicrobial properties, biocompatibility, wound dressing*

1. INTRODUCTION

Skin, the human body's largest organ, plays a substantial role in protecting the body from pathological organisms by acting as a natural barrier, maintaining the body temperature, homeostatis, and dehydration.[1] However, these characteristics are disturbed whenever there is an injury or wound, leading to the invasion of bacteria through the site of injury. Thus, to repair these tissues, dressing materials are prepared. A proper wound dressing material should impart a moist environment, allow easy transport of gases, inhibit bacterial infections, should be nontoxic, nonallergenic, and promote heat insulation.[2] In the recent studies, bacterial cellulose (BC) has grabbed attention in the biomedical field due to its highly pure, biocompatible, nontoxic, and highly hydrophilic nature. These captivating properties make it a suitable contender in biomedical applications such as artificial skin, scaffolds, wound dressing materials, dental implants, and also in food packaging and paper industry.[3] BC is generally produced from *Acetobacter xylinum*, which is the most efficient BC producer as it can absorb several types of sugars leading to higher yields of cellulose at pH ≈ 3−7 and 25−30 °C temperature in liquid medium. BC is made up of ultrafine fiber network derived from well-arranged three-dimensional (3D) nanofibers, which results in the formation of hydrogel sheets with higher surface area and porosity.[4,5] As compared to plant-based cellulose, BC fibrils are very much smaller in diameter as well as length (about 100 times) with tailorable properties based on the composition of culture media, carbon source, and also on the producing organism used. BC also has certain promising

Received: March 14, 2022
Accepted: July 9, 2022
Published: July 19, 2022

https://doi.org/10.1021/acsabm.2c00226
ACS Appl. Bio Mater. 2022, 5, 3722−3733

Received: 29 August 2019 | Revised: 28 December 2019 | Accepted: 20 January 2020
DOI: 10.1002/app.49050

ARTICLE

Applied Polymer SCIENCE WILEY

Environment-friendly synthesis of sustainable chitosan-based nonisocyanate polyurethane: A biobased polymeric film

Munmi Das | **Bishnupada Mandal** | **Vimal Katiyar**

Department of Chemical Engineering, Indian Institute of Technology Guwahati, Guwahati, Assam, India

Correspondence
Vimal Katiyar, Department of Chemical Engineering, Indian Institute of Technology Guwahati, Assam 781039, India.
Email: vkatiyar@iitg.ac.in

Abstract

Sustainable, biobased nonisocyanate polyurethane (NIPU) films having excellent water absorption characteristics were synthesized by a green-chemistry approach, eliminating the use of any toxic component. An environment-friendly bulk polyaddition reaction was carried out between a natural amine-containing polysaccharide, chitosan, and carbonated soybean oil (CSBO) to prepare the NIPUs. Epoxidized soybean oil was reacted with carbon dioxide to obtain CSBO and the conversion was confirmed by Fourier transform infra-red and ^{1}H nuclear magnetic resonance spectroscopies. NIPUs synthesized via this method did not involve the use of any curing agent and the crosslinking density of the polymer could be varied by altering the amine content. NIPUs with higher chitosan content showed better thermal and chemical properties, and superior water absorption characteristics. FTIR studies confirmed the typical linkages of polyurethane and the swelling behavior justified its enhanced resistance to organic solvents. Karl Fischer titration study proved the excellent water-absorption capacity by absorbing ~90% moisture from toluene. These properties enable NIPUs to have diverse probable applications in the fields of chemical-resistant coating, sealant, and also as an inorganic plant growth substrate because of its high water holding capacity.

KEYWORDS
coatings, polycondensation, polyurethane

1 | INTRODUCTION

In the present day scenario, the perception of human society has been enlightened with the sparsity and fast depletion of petroleum-based resources, and an alertness has been generated to use renewable and biodegradable substitutes considering the environmental issues associated with the consumption of hazardous and toxic petroleum resources. Vegetable oils, a class of renewable triglycerides comprising of various fatty acids and unsaturation, has grabbed massive attention over the past decade because of its regenerative nature, abundance, low toxicity, and lower cost.[1] In addition to its environmental benefits, various alterations can be done with the vegetable oils to produce a diverse range of materials which could be further utilized to obtain various polymeric materials.[2] Soybean oil (SBO) is one of the most abundant and cheapest vegetable oils available in the oleochemical market. Over the past two decades, researchers have developed different ways to functionalize the C=C double bonds and ester groups present in the vegetable oils to produce sustainable materials.[3] Saremi et al.[4] have reported the production of epoxidized SBO (ESBO) from SBO using hydrogen peroxide as an oxidant, in the presence of formic acid at 50°C temperature and atmospheric pressure in 10 hr.

